NASA Contractor Report 189040

C° Continuity Elements by Hybrid Stress Method

David Sung-Soo Kang
Massachusetts Institute of Technology
Cambridge, Massachusetts

November 1991

Prepared for
Lewis Research Center
Under Grant NAG3–33

National Aeronautics and
Space Administration

C^0 CONTINUITY ELEMENTS

BY HYBRID STRESS METHOD

by

DAVID SUNG-SOO KANG
Massachusetts Institute of Technology
Department of Aeronautics and Astronautics
Cambridge, Massachusetts 02139

ABSTRACT

An intensive study of the assumed variable distribution necessary for the Assumed Displacement Formulation, the Hellinger-Reissner Formulation, and the Hu-Washizu Formulation is made in a unified manner. With emphasis on physical explanation, a systematic method for the Hybrid Stress element construction is outlined. The numerical examples employ four and eight node plane stress elements and eight and twenty node solid elements. Computation cost study indicates that the hybrid stress element derived using recently developed Uncoupled Stress Formulation is comparable in CPU time to the Assumed Displacement element. Overall, main emphasis is placed on providing a broader understanding of the Hybrid Stress Formulation.

TABLE OF CONTENTS

1. INTRODUCTION

The Finite Element Method is a numerical method with firmly established mathematical foundation. Popularized by the broad applicability, large finite element codes play a dominant role in the current structural analysis. Thus, in the past years, intense effort was applied to improve and optimize the finite element method.

The main thrust of this report is to present an explanation of the finite element method in the view of the theory coupled with computational algorythm. The functionals considered are that of the Hu-Washizu principle, π_{HW}, the Hellinger-Reissner principle, π_R, and the principle of minimum potential energy, π_P. By a direct comparison of these three functional, the role of the assumed field variables can be clarified. Furthermore, through a comparative evaluation, these theories will be approached in a unified manner.

The motivation came from earlier attempts for the explanation of the class of elements derived under hybrid stress method. Several months of numerical and literature research demanded more systematic method for the research into the hybrid stress elements. Using the latest development in the hybrid element research, a systematic method will be constructed step by step starting from the governing equations of elasticity.

2. GOVERNING EQUATIONS OF ELASTICITY

Since finite element methods in solid continuum operate on the governing equations of elasticity, several key observations must be emphasized before introducing the weak or the variational form of the equations. In this analysis, only the small displacement theory of elasticity will be considered. Also, the Rectangular Cartesian Coordinates will be employed for defining the three dimensional space.

STRESS

The condition for the stresses are obtained directly from the Newton's laws of motion pertaining to the bodies at rest, i.e. the force and moment equilibrium. Application of these laws on the stress yields the Equations of Equilibrium for stress.

$$\begin{aligned} \frac{\partial \sigma_x}{\partial x} + \frac{\partial \sigma_{xy}}{\partial y} + \frac{\partial \sigma_{xz}}{\partial z} + F_x &= 0 \\ \frac{\partial \sigma_{xy}}{\partial x} + \frac{\partial \sigma_y}{\partial y} + \frac{\partial \sigma_{yz}}{\partial z} + F_y &= 0 \\ \frac{\partial \sigma_{xz}}{\partial x} + \frac{\partial \sigma_{yz}}{\partial y} + \frac{\partial \sigma_z}{\partial z} + F_z &= 0 \end{aligned} \qquad (2.1)$$

In the matrix form,

$$\underset{\sim}{D}^T \underset{\sim}{\sigma} + \underset{\sim}{F} = 0$$

where,

$\underset{\sim}{\sigma}^T$ = Six stress components = $\{\sigma_x \sigma_y \sigma_z \sigma_{xy} \sigma_{yz} \sigma_{xz}\}$

$\underset{\sim}{F}$ = Body force components

$\underset{\sim}{D}$ = Matrix of differential operators

$$\underset{\sim}{D} = \begin{bmatrix} \frac{\partial}{\partial x} & 0 & 0 \\ 0 & \frac{\partial}{\partial y} & 0 \\ 0 & 0 & \frac{\partial}{\partial z} \\ \frac{\partial}{\partial y} & \frac{\partial}{\partial x} & 0 \\ 0 & \frac{\partial}{\partial z} & \frac{\partial}{\partial y} \\ \frac{\partial}{\partial z} & 0 & \frac{\partial}{\partial x} \end{bmatrix}$$

Thus, the chosen stress field must satisfy the pointwise homogeneous equilibrium dictated by the Newton's laws. This applies to the any functional whether it contains stress as explicit unknown functions or implicitly through the unknown displacement functions. Further discussion is reserved for later sections.

DISPLACEMENT

Since the class of elements presented require C^o continuity, the isoparametric formulation is the obvious choice. These elements will be later refered to as the C^o continuity elements. The procedure in obtaining the interpolation functions are well outlined in most finite element reference books, e.g. [2]. The notation used for the displacements are

$$\underset{\sim}{u} = \begin{Bmatrix} u \\ v \\ w \end{Bmatrix} \tag{2.2}$$

STRAINS

The strains are defined as

$$\varepsilon_x = \frac{\partial u}{\partial x} \qquad \varepsilon_y = \frac{\partial v}{\partial y} \qquad \varepsilon_z = \frac{\partial w}{\partial z} \tag{2.3}$$

$$\gamma_{xy} = \frac{\partial u}{\partial y} + \frac{\partial v}{\partial x} \qquad \gamma_{yz} = \frac{\partial v}{\partial z} + \frac{\partial w}{\partial y}$$

$$\gamma_{xz} = \frac{\partial u}{\partial z} + \frac{\partial w}{\partial x}$$

These six independent partial differential equations will be denoted as the Strain-Displacement Relations.

For the functionals, π_p and π_R, where displacements are included explicitly as unknowns in formulating the elasticity boundary value problem, no further conditions are necessary to ensure the existence of single-valued displacement. However, for π_{HW}, since the strains are also considered as independent unknowns, the compatibility conditions must be imposed on the strain-displacement relation to ensure that the unknown strains are indeed compatible with the unknown displacements.

The Compatibility Equations are

$$\frac{\partial^2 \varepsilon_x}{\partial y^2} + \frac{\partial^2 \varepsilon_y}{\partial x^2} - 2\frac{\partial^2 \varepsilon_{xy}}{\partial x \partial y} = 0$$

$$\frac{\partial^2 \varepsilon_y}{\partial z^2} + \frac{\partial^2 \varepsilon_z}{\partial y^2} - 2\frac{\partial^2 \varepsilon_{yz}}{\partial y \partial z} = 0$$

$$\frac{\partial^2 \varepsilon_z}{\partial x^2} + \frac{\partial^2 \varepsilon_x}{\partial z^2} - 2\frac{\partial^2 \varepsilon_{xz}}{\partial x \partial z} = 0 \qquad (2.4)$$

$$-\frac{\partial^2 \varepsilon_x}{\partial y \partial z} + \frac{\partial}{\partial x}\left(-\frac{\partial \varepsilon_{yz}}{\partial x} + \frac{\partial \varepsilon_{zx}}{\partial y} + \frac{\partial \varepsilon_{xy}}{\partial z}\right) = 0$$

$$-\frac{\partial^2 \varepsilon_y}{\partial x \partial z} + \frac{\partial}{\partial y}\left(\frac{\partial \varepsilon_{yz}}{\partial x} - \frac{\partial \varepsilon_{zx}}{\partial y} + \frac{\partial \varepsilon_{xy}}{\partial z}\right) = 0$$

$$-\frac{\partial^2 \varepsilon_z}{\partial x \partial y} + \frac{\partial}{\partial z}\left(\frac{\partial \varepsilon_{yz}}{\partial x} + \frac{\partial \varepsilon_{zx}}{\partial y} - \frac{\partial \varepsilon_{xy}}{\partial z}\right) = 0$$

These equations are known as the St.-Venant's compatibility equations. However the six equations do not represent six independent conditions. Yet the usual procedure is to include all six equations in the interior problem formulation, but to remember that they represent only three independent conditions [3].

Thus far, all the equations presented are completely independent of the relationship between stress and strain. They are applicable to any type of continuous body undergoing small displacement. However, to predict the behavior of a structure it is also necessary to know the components of stress as functions of the components of strain and vice versa. Through the Stress-Strain Relation the material properties of the body enter the problem. In the following development, the materials considered will be assumed to follow the generalized Hooke's law with 21 independent constants.

The stress-strain relation can be written in a matrix form as

$$\underset{\sim}{\sigma} = \underset{\sim}{C}\,\underset{\sim}{\varepsilon}$$

and (2.5)

$$\underset{\sim}{\varepsilon} = \underset{\sim}{S}\,\underset{\sim}{\sigma}$$

where,

$$\underset{\sim}{S} = \underset{\sim}{C}^{-1}$$

For this stage the most predominating factor must be

pointed out. This is simply that the stresses, the displacements, and the strains must satisfy these governing equations. When the approximate functions are used to solve these equations, the optimum choice of the assumed function is the one that satisfy each of these equations a priori to the highest polynomial order. This argument can be used to sort through all the admissible functions in formulating the best general finite element. Thus, whatever variational functional used to formulate the element, one must always refer back to the physics of the problem and not sink into the mathematical generality.

3. VARIATIONAL FUNCTIONALS

Without belaboring on the actual derivation of each functionals, the main references will be indicated and only the pertinent information for this discussion will be outlined. Presentation is organized to clearly indicate the a priori conditions and the stationary conditions which provide the Euler equation for each functional.

PRINCIPLE OF MINIMUM POTENTIAL ENERGY, $\Pi_p(\underset{\sim}{u})$

A priori conditions:

$$\left.\begin{aligned} \underset{\sim}{\varepsilon} &= \underset{\sim}{D}\,\underset{\sim}{u} \\ \underset{\sim}{\sigma} &= \underset{\sim}{C}\,\underset{\sim}{\varepsilon} \end{aligned}\right\} \text{ in } V \qquad \left.\begin{aligned} \underset{\sim}{u} &= \overline{\underset{\sim}{u}} \end{aligned}\right\} \text{ on } S_u \tag{3.1}$$

$$\Pi_p = \frac{1}{2}\int_V \underset{\sim}{\varepsilon}^T \underset{\sim}{C}\,\underset{\sim}{\varepsilon}\, dV - \int_V \overline{\underset{\sim}{F}}^T \underset{\sim}{u}\, dV - \int_{S_\sigma} \overline{\underset{\sim}{T}}^T \underset{\sim}{u}\, ds \tag{3.2}$$

The stationary condition, $\delta\Pi_p = 0$, yields

$$\begin{aligned} \underset{\sim}{D}^T\underset{\sim}{\sigma} + \overline{\underset{\sim}{F}} &= 0 \qquad \text{in } V \\ \underset{\sim}{T} &= \overline{\underset{\sim}{T}} \qquad \text{on } S_\sigma \end{aligned} \tag{3.3}$$

where,

$\underset{\sim}{\varepsilon}$ = Strain

$\underset{\sim}{\sigma}$ = Stress

$\underset{\sim}{C}$ = Stress-strain law

$\underset{\sim}{u}$ = Displacement

$\bar{\underset{\sim}{u}}$ = Prescribed displacements

$\bar{\underset{\sim}{T}}$ = Prescribed traction

$\bar{\underset{\sim}{F}}$ = Body force

V = Volume

S_u = Portion of surface where displacements are prescribed

S_σ = Portion of surface where stresses are prescribed

In π_p, the strain-displacement relation, stress-strain relation, and prescribed displacements are identically satisfied. However, the equilibrium condition and the prescribed tractions are only satisfied in a variational sense. By relaxing all three a priori conditions by using the Lagrange multiplier method, the generalized functional, π_{HW}, can be obtained.

HU-WASHIZU PRINCIPLE, $\pi_{HW}(\underset{\sim}{u}, \underset{\sim}{\sigma}, \underset{\sim}{\varepsilon})$

A priori conditions: NONE

$$\pi_{HW} = \int_V \left[\tfrac{1}{2}\underset{\sim}{\varepsilon}^T\underset{\sim}{C}\underset{\sim}{\varepsilon} - \bar{\underset{\sim}{F}}^T\underset{\sim}{u}\right] dV - \int_{S_\sigma} \bar{\underset{\sim}{T}}^T\underset{\sim}{u}\, dS - \int_V \underset{\sim}{\sigma}^T(\underset{\sim}{\varepsilon} - \underset{\sim}{D}\underset{\sim}{u})\, dV - \int_{S_u} \underset{\sim}{T}^T(\underset{\sim}{u} - \bar{\underset{\sim}{u}})\, ds \tag{3.4}$$

The stationary condition, $\delta\pi_{HW} = 0$, yields

$$\left.\begin{aligned} \underset{\sim}{\sigma} &= \underset{\sim}{C}\underset{\sim}{\varepsilon} \\ \underset{\sim}{D}^T\underset{\sim}{\sigma} + \bar{\underset{\sim}{F}} &= 0 \\ \underset{\sim}{\varepsilon} &= \underset{\sim}{D}\underset{\sim}{u} \end{aligned}\right\} \text{ in } V \tag{3.5}$$

$$\underset{\sim}{u} = \bar{\underset{\sim}{u}} \qquad \text{on } S_u$$

$$\underset{\sim}{T} = \underset{\sim}{\nu}\,\underset{\sim}{\sigma} = \bar{\underset{\sim}{T}} \qquad \text{on } S_\sigma$$

$$T_x = \nu_x \sigma_x + \nu_y \sigma_{xy} + \nu_z \sigma_{xz}$$

$$\vdots$$

$\nu_x = \cdots$ Directional Cosines

All governing equations are satisfied in a variational sense. Yet the price paid for the generalization is the two additional unknowns $\underset{\sim}{\varepsilon}$ and $\underset{\sim}{\sigma}$. The Hellinger-Reissner Principle can be easily obtained by introducing the stress-strain relation.

HELLINGER-REISSNER PRINCIPLE, $\Pi_R(\underset{\sim}{u}, \underset{\sim}{\sigma})$

A priori conditions:

$$\underset{\sim}{S}\,\underset{\sim}{\sigma} = \underset{\sim}{\varepsilon} \qquad \text{in } V \tag{3.6}$$

$$\Pi_R = \int_V \left[-\tfrac{1}{2}\,\underset{\sim}{\sigma}^T \underset{\sim}{S}\,\underset{\sim}{\sigma} + \underset{\sim}{\sigma}^T (\underset{\sim}{D}\,\underset{\sim}{u}) - \bar{\underset{\sim}{F}}^T \underset{\sim}{u} \right] dV - \int_{S_\sigma} \bar{\underset{\sim}{T}}^T \underset{\sim}{u}\, ds - \int_{S_u} \underset{\sim}{T}^T (\underset{\sim}{u} - \bar{\underset{\sim}{u}})\, ds \tag{3.7}$$

The stationary condition, $\delta \Pi_R = 0$, yields

$$\left.\begin{aligned} \underset{\sim}{S}\,\underset{\sim}{\sigma} &= \underset{\sim}{D}\,\underset{\sim}{u} \\ \underset{\sim}{D}^T \underset{\sim}{\sigma} + \bar{\underset{\sim}{F}} &= 0 \end{aligned}\right\} \quad \text{in } V \tag{3.8}$$

$$\underset{\sim}{T} = \overline{\underset{\sim}{T}} \qquad \text{on } S_\sigma$$

$$\underset{\sim}{u} = \overline{\underset{\sim}{u}} \qquad \text{on } S_u$$

By satisfying the equilibrium equations identically, π_R and π_{HW} can be shown to reduce to the Hybrid formulation via Principle of Complementary Energy [4]. Yet with availability of isoparametric formulation for C^o continuity elements, the Hybrid elements can be formulated using π_R or π_{HW} in more expedient manner.

In a recent publication by Pian and Chen [5], new formulation for hybrid elements provides a method to directly take advantage of the sparse nature of matrices involved in the construction of the hybrid elements. Briefly, the new formulation introduces an additional displacement field which act as a Lagrange multiplier on the homogeneous equilibrium equations. The major advantages will be described in the later sections. These new functionals will be refered to as the uncoupled stress versions.

UNCOUPLED STRESS VERSION OF π_R AND π_{HW}

The element displacement $\underset{\sim}{u}$ is divided into two separate parts.

$$\underset{\sim}{u} = \underset{\sim}{u}_s + \underset{\sim}{u}_\lambda \qquad (3.9)$$

$\underset{\sim}{u}_s$ is the usual compatible displacement in terms of the

nodal displacements. $\underset{\sim}{u}_\lambda$ is the additional internal displacement which acts as the Lagrange multiplier for the homogeneous equilibrium. When this form of displacement is implemented into the π_R and π_{HW}, Equations (3.7) and (3.4), with body force and prescribed traction terms dropped, the resulting equations are

$$\pi_R = \int_V \left[-\frac{1}{2} \underset{\sim}{\sigma}^T \underset{\sim}{\underset{\sim}{S}} \underset{\sim}{\sigma} + \underset{\sim}{\sigma}^T (\underset{\sim}{\underset{\sim}{D}} \underset{\sim}{u}_s) - (\underset{\sim}{\underset{\sim}{b}}^T \underset{\sim}{\sigma})^T \underset{\sim}{u}_\lambda \right] dV \qquad (3.10)$$

$$\pi_{HW} = \int_V \left[\frac{1}{2} \underset{\sim}{\varepsilon}^T \underset{\sim}{\underset{\sim}{C}} \underset{\sim}{\varepsilon} - \underset{\sim}{\sigma}^T \underset{\sim}{\varepsilon} + \underset{\sim}{\sigma}^T (\underset{\sim}{\underset{\sim}{D}} \underset{\sim}{u}_s) + \underset{\sim}{\sigma}^T (\underset{\sim}{\underset{\sim}{D}} \underset{\sim}{u}_\lambda) \right] dV \qquad (3.11)$$

As a remark on notation, since the hybrid formulation can be obtained via π_R or π_{HW} in both coupled and uncoupled stress versions, π_H will be used to refer to the general hybrid element case where the stresses are constrained to be in equilibrium.

4. FIELD VARIABLES and STATEMENT of EQUIVALENCE

The first question that must be answered in any finite element development is whether the method converges. The mathematical proof for the convergence of π_p and π_H are given in the References [6] and [7]. Yet these proofs only justify the use of the finite element method and not whether it is feasible for engineering application. The demanding requirement is the rate of convergence.

The two modes of convergence are the h-convergence, the diameter of the largest element, h-max, approaches zero, and the p-convergence, the minumum order of the polynomial basis functions, p-min, approaches infinity. The comparison of the rate of convergence between these two modes for π_p is covered by Bubuska and Szabo [8]. The results given in this article should be clarified in the view of general purpose elements. First, most structural problems only require low order polynomial. Thus the lower order elements can be employed for most practical engineering problems. Secondly the special purpose elements and other methods such as the reduced integration techniques should be considered. The main reason for the discussion of this article is to point out that before the general purpose elements can be constructed, better unified understanding of the special purpose elements and various other techniques is

necessary. As the solution of the problem by finite element method becomes more complex, as exemplified in crack and composite material analysis, the analyst judgement and experience will not be adequate in determining the accuracy of the solution.

Another important point that must be defined involves the past attempts to improve elements based upon π_p . The first workable attempt was presented by Wilson [9] with his incompatible displacement models. Recognizing the deficiency in the isoparametric displacement elements, he introduced the bending modes into the element displacement field. Other trials that falls into this catagory can be exemplified by the introduction of $1/r$ singularity by distorting the nodes. The second catagory can be classified into the scheme of reduced integration technique. This technique works well to prevent locking in the generalized shell element as well as other applications. The major point that most researchers in finite element method ignored is the fact that both Wilson's incompatible element and the reduced integration technique result in identical stiffness matrix as the hybrid formulation. This bold clue that hybrid formulation can reveal the way to develop the optimal element has been casually dismissed in view of computational cost in a premature fashion.

With this emphasis clearly made, a close examination of the finite element method in a unified manner can be

made. First the field variable for each functional will be listed.

$\pi_P(\underset{\sim}{u})$ displacement

$\pi_R(\underset{\sim}{u},\underset{\sim}{\sigma})$ displacement, stress

$\pi_{HW}(\underset{\sim}{u},\underset{\sim}{\sigma},\underset{\sim}{\varepsilon})$ displacement, stress, strain

The Statement of Equivalence describes that when the displacement modes from π_P yields the stress and strain modes for π_R and π_{HW}, the three functionals are equivalent or identical. To illustrate, take the simplest case of linear displacement modes. Since this yields constant stress and strain modes, if $\underset{\sim}{\sigma}$ and $\underset{\sim}{\varepsilon}$ contains the constant modes, the three functionals are equivalent up to a constant stress and strain. The argument directly leads to the order of equivalence.

From the consequence of above statement, using the inductive reasoning, any class of problems that have constant stress of strain will yield the exact solution using any of the above functionals. Using the Statement of Equivalence as a benchmark, the examination of each functionals separately may be continued. As a warning, the mechanics of construction of the desirable field variables are left for the later section and should not enter here as a consideration. This is justifiable since for clarification purposes, ideal cases may be presented.

-- $\Pi_P(\underset{\sim}{u})$ --

A priori conditions (3.1) imply that the choice of $\underset{\sim}{u}$ automatically determines $\underset{\sim}{\varepsilon}$ and $\underset{\sim}{\sigma}$. Under isoparametric formulation, there is no flexibility on the choice of $\underset{\sim}{u}$. Therefore, further discussion on $\underset{\sim}{u}$ is not necessary.

Recall, from the section 2, that the governing equations are the equilibrium equations (2.1), the strain-displacement relation (2.3), and the stress-strain relation (2.5). Equations (2.3) and (2.5) are automatically satisfied under the isoparametric formulation. However, the equilibrium equations (2.1) applied to the stress components obtained from the displacement modes is not satisfied. Furthermore, the stress modes are artificially coupled. Artificial in a sense that one stress component coupling into another in a way not possible under equilibrium considerations. The undesirable trait appears as locking for the bending problem. The solution to bypass this problem is to assume separate $\underset{\sim}{u}$ and $\underset{\sim}{\sigma}$ with $\underset{\sim}{\sigma}$ satisfying equilibrium, thereby satisfying all of the governing equations.

-- $\Pi_R(\underset{\sim}{u}, \underset{\sim}{\sigma})$ --

Under the governing equations the forces, $\underset{\sim}{\sigma}$, and the deflections, $\underset{\sim}{u}$, couple only through the stress-strain relations. By choosing $\underset{\sim}{u}$ and $\underset{\sim}{\sigma}$ independently, all three governing equations can be satisfied a priori. Therefore,

with $\underset{\sim}{u}$ obtained through isoparametric formulation and $\underset{\sim}{\sigma}$ chosen correctly, an optimal general finite element can be constructed.

In selecting the stress field, two articles provide means to overcome the preliminary roadblocks. A method to bypass the zero-energy deformation modes due to the rank deficiency in the stiffness matrix is outlined by Pian and Chen[10]. Their method simply matches a stress mode for each possible strain mode in order to force non-zero strain energy. This method is easy to apply and provide effective means to detect and eliminate the troublesome zero-energy deformation modes.

The second article, by Tong and Pian [7], on the convergence of the finite element method based on assumed stress and displacement distribution, outlines the procedure to gage the accuracy of such an element. In order to obtain progressively better accuracy, both the stress and the displacement approximations must be improved properly and simultaneously. In another words, the largest error, whether the error is from the $\underset{\sim}{u}$ or $\underset{\sim}{\sigma}$, is the error of the finite element approximation.

-- $\Pi_{HW}(\underset{\sim}{u}, \underset{\sim}{\sigma}, \underset{\sim}{\xi})$--

The Hu-Washizu principle is a generalized functional which allows full flexibility on the choice of the assumed field variables. This is called "generalized" since no a

priori assumption is made and thus the governing equations of elasticity are satisfied as Euler equations of the functional. Even with the full flexibility, the choice of the assumed field variables follow the same constraints as indicated for π_R . Although using π_{HW} to obtain a hybrid element seem a "round-about" way, the reason will be apparent under computational efficiency dealing with anisotropic material.

ROLE OF THE LAGRANGE MULTIPLIER

In the finite element method, the Lagrange multiplier relaxes the corresponding governing equation. Thus, the resulting functional becomes more flexible for the implementation of the desired element properties. From the view of understanding the mechanics of the finite element method, the Lagrange multiplier decouples the role of the assumed variables. From the view of computational algorythm, the Lagrange multiplier introduces flexibility needed to reduce computational cost. By decoupling the assumed variables, algorythms can be implemented to take full advantage of the sparse nature of the necessary matrices for element generation.

Even with added flexibility, emphasis must be made on a simple knowledge that for a given well posed boundary condition, the governing equations of elasticity has a

unique solution. Thus restriction depends on whether the element is general purpose or special purpose element.

5. GENERAL PURPOSE FINITE ELEMENTS

The key to constructing the general purpose finite element is the actual understanding of each element in both mathematical and physical sense. In the early stages of hybrid element research, Irons provided a strong physical insight in the process of the development of an assumed stress version of the Wilson's incompatible 8-node isoparametric brick element [11]. He obtained the correct stress parameters by simply choosing the modes that describes physical states of the classic problems. For example, the pure bending modes should be included in the stress field, whereas other terms that contribute to the spurious strain energy should be excluded. As Irons pointed out, the isoparametric element prevents the need for engineering insight. Both the researchers and analysts must recognize the limitations of each element which is clearly provided in the development process of hybrid/mixed formulations. The closed minded approach of using the simplest functional, Π_p, and ignoring the rest will hinder the progress. Recognize that the construction of isoparametric element is simple because the steps allow no flexibility and thus faced with its full limitations.

Falling back on the Statement of Equivalence, any desired element characteristics, when proven to exist in Π_p formulation can be reproduced in the other functionals. Since the Wilson's incompatible element and

the reduced integration scheme can produce pure bending modes, these desired characteristics can be reproduced using π_R or π_{HW}. The difference lies in the algorythm used for the construction of each element.

Thus far since only the C^0 continuity elements were considered, the time is ripe for the discussion of the elements requiring C^1 continuity as later referred to as C^1 continuity elements. Since the original application of the hybrid formulation was intended for the C^1 continuity elements using the modified complementary energy principle [12], this discussion inevitably follows.

First recall that the primary reason for the derivation of the beam, plate, and shell theories were to simplify the analysis in order to obtain an analytical solution. Each theory is based upon the assumption that one or more dimensions of the problem collapses. To illustrate, the governing equations can be non-dimensionalized using a characteristic dimensions of the problem. As one of the dimensions collapses, for example the thickness, the equations can be expanded into a perturbation series. Thus, the structural theories are basically the leading order, or the zeroeth order, equation of the governing partial differential equations. As the perturbation parameter increases, the accuracy of the leading order equation diminishes. In order to improve the range of validity of the approximation, later works introduced the transverse shear effect as

exemplified by the Mindlin plate theory. Although the attempt will not be made here, the transverse shear effect probably is the first order correction of the perturbation expansion.

The price paid for the simplification made by the structural theory is the requirement for C^1 continuity in the finite element analysis. Even to this day the agreement whether this price is justified in the finite element analysis has not been reached. However, the degenerated plate and shell element is gaining popularity for the practical applications. Note that the degenerated element class only require C^0 continuity for the displacements.

In the article by Bathe and Bolourchi [13], an extensive coverage of the degenerated plate and shell element using π_p formulation has been made. The numerical examples given indicated that the best solution is obtained by using the selective, or reduced, integration technique. Thus by using the hybrid formulation the results obtained through reduced integration can be identically reproduced.

The major advantage of the C^1 continuity elements is the ability to represent the bending behavior. If the C^0 continuity element can represent the bending behavior, then the general purpose finite element can indeed be constructed. The line of research along this path using π_p formulation has been hindered through the difficulty

arising with the locking problem. Since locking is caused by artificial coupling that is inherent in the isoparametric assumed displacement formulation, the problem can be easily remedied by the use of the hybrid formulation. Furthermore, the bending modes can be implemented even in the linear hybrid elements. Then the only limitation on using a solid element to model, for example, the thin plate behavior is the numerical stability. By using high enough decimal precision this limitation can be avoided.

6. SYMMETRY AND RELAXATION

As numerically demonstrated by Pian, Chen, and Kang [14], the symmetry condition is an important criterion that must be considered in obtaining the assumed field variable distribution. This is physically consistant since the finite element should be symmetric in all three directions. For example, when choosing the stress modes, bending behavior in all three coordinates should be represented. This criterion is invaluable tool for the solid element construction.

Before the relaxation condition can be described, a better understanding of the zero-energy deformation mode (ZEDM) is in order. Although mathematically ZEDM is a rank deficiency beyond the rigid body modes in the stiffness matrix and its prevention outlined in the reference [10], more physical explanation is necessary. In the case of solid elements, each node contains three independent displacements, u, v, and w, to describe all possible motions of the node. With all the element nodes moving in conjunction, all possible deflection modes can be determined. For most of these deflection modes physical significance can be attached such as pure tension, shear, or bending. For the rest, no such physical association can be made. Granted each material point has three degrees of freedom, but that point cannot be considered as an isolated particle in free space. A

continuum collection of material particles has additional physical deformation restrictions. The modes with no physical association arise strictly through the mathematical modeling process.

Whether the deflection mode has a physical significance or not, the corresponding non-orthogonal stress mode must be provided in order to prevent ZEDM. Non-orthogonality of the modes guarantee non-zero strain energy. Therefore by identification of all the deflection modes, ZEDM's can be easily eliminated.

As a classic example of the duality principle, a parallel analogy is presented by Loikkanen [15] using the stress modes. In the article, he nicknamed the "nonsense" stresses refering to the stress modes with no physical association. However, for the purposes of generalization for the higher order elements, the use of deflection modes will be more convenient since through the isoparametric formulation the deflection modes are given and the stress modes yet to be determined. Note that any non-orthogonal stress mode can be used even though the lowest order mode is preferred for the numerical integration considerations. Figure 6.1 pictorially summarizes the above discussion. For continuum problems, a complex combination of forces required to excite such an element deflection within a mesh arises only for the occasion when the mesh is much too coarse.

From here on, the "nonsense" stress mode refers to

any stress mode with only general non-orthogonality restrictions used in conjunction with the deflection modes with no physical association. With this in mind the relaxation condition can be simply stated. For the "nonsense" stress mode and the corresponding deflection mode, the governing equations can be relaxed without loss of accuracy of the element. In the practical application of the above statement, in π_A the equilibrium condition can be relaxed for the "nonsense" stress modes and in π_{HW} the stress-strain relation can also be relaxed. Surprisingly large computational costs can be saved by using the relaxation condition. In addition, more accurate solution can be achieved by eliminating all the supporting terms necessary to keep these "nonsense" stress modes in equilibrium.

7. FINITE ELEMENT METHOD

For the finite element method presented below, only a single element domain is under consideration for each of the functionals.

7.1 PRINCIPLE OF MINIMUM POTENTIAL ENERGY, π_p ($\underset{\sim}{u}$)

In using the principle of minimum potential energy to formulate the element stiffness matrix the following functional π_p for an element should be stationary,

$$\pi_p = \frac{1}{2}\int_v \underset{\sim}{\varepsilon}^T \underset{\sim}{C}\,\underset{\sim}{\varepsilon}\, dV - \int_v \underset{\sim}{\bar{F}}^T \underset{\sim}{u}\, dV - \int_{S_\sigma} \underset{\sim}{\bar{T}}^T \underset{\sim}{u}\, dS \qquad (3.2)$$

In the matrix form,

$$\pi_p = \frac{1}{2}\,\underset{\sim}{\delta}^T \underset{\sim}{K}\,\underset{\sim}{\delta} - \underset{\sim}{Q}^T \underset{\sim}{\delta} \qquad (7.1)$$

where

$\underset{\sim}{K}$ = Stiffness matrix

$\underset{\sim}{\delta}$ = Nodal displacement

$\underset{\sim}{Q}$ = Load matrix

Furthermore,

$$\underset{\sim}{K} = \int_v \underset{\sim}{B}^T \underset{\sim}{C}\,\underset{\sim}{B}\, dV \qquad (7.2)$$

$$\underset{\sim}{Q} = \int_v \underset{\sim}{N}^T \underset{\sim}{\bar{F}}\, dV + \int_{S_\sigma} \underset{\sim}{N}^T \underset{\sim}{\bar{T}}\, dS$$

The relations used above are

$$\underset{\sim}{u} = \underset{\sim}{N}\,\underset{\sim}{q} \tag{7.3}$$

$$\underset{\sim}{\varepsilon} = \underset{\sim}{D}\,\underset{\sim}{u} = (\underset{\sim}{D}\,\underset{\sim}{N})\,\underset{\sim}{q} = \underset{\sim}{B}\,\underset{\sim}{q}$$

where

$\underset{\sim}{N}$ = Interpolation matrix

$\underset{\sim}{D}$ = Derivative matrix

$\underset{\sim}{B}$ = Strain-displacement matrix

7.2 HELLINGER-REISSNER PRINCIPLE, $\pi_R(\underset{\sim}{u}, \underset{\sim}{\sigma})$

For the Hellinger-Reissner principle, the following functional π_R for an element should be stationary,

$$\pi_R = \int_V \left[-\frac{1}{2} \underset{\sim}{\sigma}^T \underset{\sim}{S} \underset{\sim}{\sigma} + \underset{\sim}{\sigma}^T (\underset{\sim}{D}\underset{\sim}{u}) - \underset{\sim}{\bar{F}}^T \underset{\sim}{u} \right] dV - \int_{S_\sigma} \underset{\sim}{\bar{T}}^T \underset{\sim}{u} \, ds - \int_{S_u} \underset{\sim}{T}^T (\underset{\sim}{u} - \underset{\sim}{\bar{u}}) \, ds \tag{3.7}$$

In the matrix form, assuming $\underset{\sim}{u} = \underset{\sim}{\bar{u}}$ on S_u ,

$$\pi_R = \frac{1}{2} \underset{\sim}{\beta}^T \underset{\sim}{H} \underset{\sim}{\beta} - \underset{\sim}{\beta}^T \underset{\sim}{G} \underset{\sim}{g} - \underset{\sim}{Q}^T \underset{\sim}{g} \tag{7.4}$$

where

$$\begin{aligned} \underset{\sim}{\sigma} &= \underset{\sim}{P} \underset{\sim}{\beta} \\ \underset{\sim}{u} &= \underset{\sim}{N} \underset{\sim}{g} \end{aligned} \tag{7.5}$$

and

$$\begin{aligned} \underset{\sim}{H} &= \int_V \underset{\sim}{P}^T \underset{\sim}{S} \underset{\sim}{P} \, dV \\ \underset{\sim}{G} &= \int_V \underset{\sim}{P}^T \underset{\sim}{B} \, dV \\ \underset{\sim}{Q} &= \int_V \underset{\sim}{N}^T \underset{\sim}{\bar{F}} \, dV + \int_{S_\sigma} \underset{\sim}{N}^T \underset{\sim}{\bar{T}} \, ds \end{aligned} \tag{7.6}$$

The matrix, $\underset{\sim}{P}$, contains the internal stress modes and $\underset{\sim}{\beta}$ is the corresponding unknown coefficients. In order to obtain the standard stiffness matrix form, use the stationary condition on Equation (7.4) with respect to $\underset{\sim}{\beta}$.

$$\frac{\partial \pi_R}{\partial \underset{\sim}{\beta}} = \underset{\sim}{H}\,\underset{\sim}{\beta} - \underset{\sim}{G}\,\underset{\sim}{g} = 0 \qquad (7.7)$$

or

$$\underset{\sim}{\beta} = \underset{\sim}{H}^{-1}\,\underset{\sim}{G}\,\underset{\sim}{g}$$

Substituting back into Equation (7.4) yields the familiar form

$$\pi_R = \tfrac{1}{2}\,\underset{\sim}{g}^T\,\underset{\sim}{K}\,\underset{\sim}{g} - \underset{\sim}{Q}^T\,\underset{\sim}{g} \qquad (7.8)$$

where,

$$\underset{\sim}{K} = \underset{\sim}{G}^T\,\underset{\sim}{H}^{-1}\,\underset{\sim}{G} \qquad (7.9)$$

In order to obtain the stiffness matrix, Equation (7.9), $\underset{\sim}{H}$ matrix must be inverted. The order of $\underset{\sim}{H}$ matrix is the number of stress parameters, β's, used for the element development. The condition for the existence of the solution for β's is given in the reference [7]. Let m equal to the number of β's, k equal to the number of element degrees of freedom, and 1 equal to the number of rigid body modes. Then this condition is simply that $m \geq k-1$. Therefore, since the order of the $\underset{\sim}{H}$ matrix is (m*m), the minimum possible m is k-1. Since the number of algebraic steps required for the inversion is on the order of m^3, the computational cost for generating the stiffness matrix can be significantly more than that for the π_p element stiffness matrix.

7.3 HU-WASHIZU PRINCIPLE, $\pi_{HW}(\underset{\sim}{u}, \underset{\sim}{\sigma}, \underset{\sim}{\varepsilon})$

For the Hu-Washizu principle, following functional π_{HW} should be stationary,

$$\pi_{HW} = \int_V \left[\tfrac{1}{2} \underset{\sim}{\varepsilon}^T \underset{\sim}{C} \underset{\sim}{\varepsilon} - \underset{\sim}{\bar{F}}^T \underset{\sim}{u} \right] dV - \int_{S_\sigma} \underset{\sim}{\bar{T}}^T \underset{\sim}{u} \, ds \qquad (3.4)$$

$$- \int_V \underset{\sim}{\sigma}^T (\underset{\sim}{\varepsilon} - \underset{\sim}{D} \underset{\sim}{u}) \, dV - \int_{S_u} \underset{\sim}{T}^T (\underset{\sim}{u} - \underset{\sim}{\bar{u}}) \, ds$$

In the matrix form, assuming $\underset{\sim}{u} = \underset{\sim}{\bar{u}}$ on S_u,

$$\pi_{HW} = \tfrac{1}{2} \underset{\sim}{\alpha}^T \underset{\sim}{J} \underset{\sim}{\alpha} - \underset{\sim}{\beta}^T \underset{\sim}{H} \underset{\sim}{\alpha} + \underset{\sim}{\beta}^T \underset{\sim}{G} \underset{\sim}{q} - \underset{\sim}{Q}^T \underset{\sim}{q} \qquad (7.10)$$

where

$$\begin{aligned} \underset{\sim}{\sigma} &= \underset{\sim}{P} \underset{\sim}{\beta} \\ \underset{\sim}{\varepsilon} &= \underset{\sim}{P} \underset{\sim}{\alpha} \\ \underset{\sim}{u} &= \underset{\sim}{N} \underset{\sim}{q} \end{aligned} \qquad (7.11)$$

and

$$\begin{aligned} \underset{\sim}{H} &= \int_V \underset{\sim}{P}^T \underset{\sim}{P} \, dV \\ \underset{\sim}{J} &= \int_V \underset{\sim}{P}^T \underset{\sim}{C} \underset{\sim}{P} \, dV \\ \underset{\sim}{G} &= \int_V \underset{\sim}{P}^T \underset{\sim}{B} \, dV \\ \underset{\sim}{Q} &= \int_V \underset{\sim}{N}^T \underset{\sim}{\bar{F}} \, dV + \int_{S_\sigma} \underset{\sim}{N}^T \underset{\sim}{\bar{T}} \, ds \end{aligned} \qquad (7.12)$$

With the assumption that the material behaves according to the generalized Hooke's law, the use of same modes for both stress and strain is consistent since strain is a linear combination of stress and vice versa. However the major deficiency in using π_{HW} formulation in this form is that both the stress equilibrium condition and the stress-strain relation cannot be enforced a priori for the physically significant modes.

Using the stationary condition with respect to $\underset{\sim}{\alpha}$ and $\underset{\sim}{\beta}$,

$$\frac{\partial \pi_{HW}}{\partial \underset{\sim}{\alpha}} = \underset{\sim}{J}\,\underset{\sim}{\alpha} - \underset{\sim}{H}\,\underset{\sim}{\beta} = 0$$

$$\frac{\partial \pi_{HW}}{\partial \underset{\sim}{\beta}} = -\underset{\sim}{H}\,\underset{\sim}{\alpha} + \underset{\sim}{G}\,\underset{\sim}{g} = 0 \qquad (7.13)$$

or

$$\underset{\sim}{\alpha} = \underset{\sim}{H}^{-1}\,\underset{\sim}{G}\,\underset{\sim}{g}$$

$$\underset{\sim}{\beta} = \underset{\sim}{H}^{-1}\,\underset{\sim}{J}\,\underset{\sim}{\alpha} = \underset{\sim}{H}^{-1}\,\underset{\sim}{J}\,\underset{\sim}{H}^{-1}\,\underset{\sim}{G}\,\underset{\sim}{g} \qquad (7.14)$$

Substituting back into Equation (7.10) yields

$$\pi_{HW} = \frac{1}{2}\,\underset{\sim}{g}^{T}\,\underset{\sim}{K}\,\underset{\sim}{g} - \underset{\sim}{Q}^{T}\,\underset{\sim}{g} \qquad (7.15)$$

where

$$\underset{\sim}{K} = \underset{\sim}{G}^{T}\,\underset{\sim}{H}^{-1}\,\underset{\sim}{J}\,\underset{\sim}{H}^{-1}\,\underset{\sim}{G} \qquad (7.16)$$

7.4 UNCOUPLED STRESS VERSION OF Π_R AND Π_{HW}

As given by Pian and Chen[5] uncoupled stress version of Π_R with additional Lagrange multipliers $\underset{\sim}{u}_\lambda$ is

$$\Pi_R = \int_V \left[-\tfrac{1}{2} \underset{\sim}{\sigma}^T \underset{\sim}{S} \underset{\sim}{\sigma} + \underset{\sim}{\sigma}^T (\underset{\sim}{D} \underset{\sim}{u}_\beta) - (\underset{\sim}{D}^T \underset{\sim}{\sigma})^T \underset{\sim}{u}_\lambda \right] dV \qquad (3.10)$$

In the matrix form,

$$\Pi_R = -\tfrac{1}{2} \underset{\sim}{\beta}^T \underset{\sim}{H} \underset{\sim}{\beta} + \underset{\sim}{\beta}^T \underset{\sim}{G} \underset{\sim}{q} - \underset{\sim}{\beta}^T \underset{\sim}{R} \underset{\sim}{\lambda} \qquad (7.17)$$

where

$$\begin{aligned} \underset{\sim}{\sigma} &= \underset{\sim}{P} \underset{\sim}{\beta} \\ \underset{\sim}{u} &= \underset{\sim}{u}_\beta + \underset{\sim}{u}_\lambda \\ \underset{\sim}{u}_\beta &= \underset{\sim}{N} \underset{\sim}{q} \\ \underset{\sim}{u}_\lambda &= \underset{\sim}{M} \underset{\sim}{\lambda} \\ \underset{\sim}{D}^T \underset{\sim}{\sigma} &= \underset{\sim}{E} \underset{\sim}{\beta} \end{aligned} \qquad (7.18)$$

$\underset{\sim}{D}^T$ = Homogeneous equilibrium operator

and

$$\begin{aligned} \underset{\sim}{H} &= \int_V \underset{\sim}{P}^T \underset{\sim}{S} \underset{\sim}{P} \, dV \\ \underset{\sim}{G} &= \int_V \underset{\sim}{P}^T \underset{\sim}{B} \, dV \\ \underset{\sim}{R} &= \int_V \underset{\sim}{E}^T \underset{\sim}{M} \, dV \end{aligned} \qquad (7.19)$$

Using the stationary condition with respect to $\underset{\sim}{\beta}$ and $\underset{\sim}{\lambda}$,

$$\frac{\partial \pi_R}{\partial \underset{\sim}{\beta}} = -\underset{\sim}{H}\underset{\sim}{\beta} + \underset{\sim}{G}\underset{\sim}{g} - \underset{\sim}{R}\underset{\sim}{\lambda} = 0$$

$$\frac{\partial \pi_R}{\partial \underset{\sim}{\lambda}} = -\underset{\sim}{R}^T\underset{\sim}{\beta} = 0 \qquad (7.20)$$

or

$$\underset{\sim}{\beta} = \underset{\sim}{H}^{-1}(\underset{\sim}{G}\underset{\sim}{g} - \underset{\sim}{R}\underset{\sim}{\lambda}) \qquad (7.21)$$

$$\underset{\sim}{\lambda} = (\underset{\sim}{R}^T\underset{\sim}{H}^{-1}\underset{\sim}{R})^{-1}\underset{\sim}{R}^T\underset{\sim}{H}^{-1}\underset{\sim}{G}\underset{\sim}{g}$$

Combining,

$$\underset{\sim}{\beta} = \underset{\sim}{H}^{-1}\bar{\underset{\sim}{G}}\underset{\sim}{g} \qquad (7.22)$$

where

$$\bar{\underset{\sim}{G}} = \underset{\sim}{G} - \underset{\sim}{R}(\underset{\sim}{R}^T\underset{\sim}{H}^{-1}\underset{\sim}{R})^{-1}\underset{\sim}{R}^T\underset{\sim}{H}^{-1}\underset{\sim}{G} \qquad (7.23)$$

The resulting stiffness matrix is

$$\underset{\sim}{K} = \bar{\underset{\sim}{G}}^T\underset{\sim}{H}^{-1}\bar{\underset{\sim}{G}} \qquad (7.24)$$

Although at a first glance the uncoupled stress version of π_R seems overly complex, this functional elegantly takes a full advantage of the sparse nature of each matrices. Observe that the necessary bulk matrix multiplication, Equation (7.23), is performed only once. With an appropriate choice of $\underset{\sim}{u}_\lambda$, this formulation becomes identical to the standard π_R, Equation (3.7). More careful examination of the mechanics of the element

construction is worthwhile at this point.

Since the equilibrium condition is imposed through the use of the Lagrange multiplier $\underset{\sim}{u}_\lambda$, the stress components are uncoupled.

$$\underset{\sim}{\sigma} = \begin{Bmatrix} \sigma_x \\ \sigma_y \\ \sigma_z \\ \sigma_{xy} \\ \sigma_{yz} \\ \sigma_{xz} \end{Bmatrix} = \begin{bmatrix} \underset{\sim}{P}_1 & & & & & \\ & \underset{\sim}{P}_2 & & & \underset{\sim}{0} & \\ & & \underset{\sim}{P}_3 & & & \\ & & & \underset{\sim}{P}_4 & & \\ & \underset{\sim}{0} & & & \underset{\sim}{P}_5 & \\ & & & & & \underset{\sim}{P}_6 \end{bmatrix} \begin{Bmatrix} \underset{\sim}{\beta}_1 \\ \underset{\sim}{\beta}_2 \\ \underset{\sim}{\beta}_3 \\ \underset{\sim}{\beta}_4 \\ \underset{\sim}{\beta}_5 \\ \underset{\sim}{\beta}_6 \end{Bmatrix} \qquad (7.25)$$

For the reasons of computational efficiency, Π_R should be only used for the isotropic material. For the anisotropic material, the uncoupled Π_{HW} will be much more efficient.

From the Equations (7.24) and (7.23), to generate the stiffness matrix $\underset{\sim}{H}$ and $(\underset{\sim}{R}^T \underset{\sim}{H}^{-1} \underset{\sim}{R})$ matrices must be inverted. First examine the $\underset{\sim}{H}$ matrix for the isotropic material.

Define

$$\underset{\sim}{\overline{P}}_i = \int_V \underset{\sim}{P}_i^T \underset{\sim}{P}_i \, dV \qquad (7.26)$$

After algebraic manipulation, from Equation (7.19)

$$\underset{\sim}{H}^{-1} = \frac{E}{1-\nu^2}\begin{bmatrix} \bar{\underset{\sim}{P}}_1^{-1} & \nu\bar{\underset{\sim}{P}}_1^{-1} & \nu\bar{\underset{\sim}{P}}_1^{-1} & & & \\ & \bar{\underset{\sim}{P}}_1^{-1} & \nu\bar{\underset{\sim}{P}}_1^{-1} & & \underset{\sim}{0} & \\ & & \bar{\underset{\sim}{P}}_1^{-1} & & & \\ & \text{Sym.} & & \frac{1-\nu}{2}\bar{\underset{\sim}{P}}_4^{-1} & & \\ & & & & \frac{1-\nu}{2}\bar{\underset{\sim}{P}}_5^{-1} & \\ & & & & & \frac{1-\nu}{2}\bar{\underset{\sim}{P}}_6^{-1} \end{bmatrix} \qquad (7.27)$$

assuming

$$\underset{\sim}{P}_1 = \underset{\sim}{P}_2 = \underset{\sim}{P}_3$$

Thus the order of inversion is drastically reduced. The choice of setting $\underset{\sim}{P}_1 = \underset{\sim}{P}_2 = \underset{\sim}{P}_3$ instead of equating all six $\underset{\sim}{P}_i$ is induced by the necessary inversion of $(\underset{\sim}{R}^T \underset{\sim}{H}^{-1} \underset{\sim}{R})$ matrix. The order of $(\underset{\sim}{R}^T \underset{\sim}{H}^{-1} \underset{\sim}{R})$ matrix is determined by the required number of λ's, Equation (7.18), to impose equilibrium condition. The number of λ's required can be determined by imposing equilibrium on the stress components and counting the number of constraints on the β's. Therefore the tradeoff is that if all six $\underset{\sim}{P}_i$'s are equated, the number of λ's will increase drastically.

The reduction of the inversion order of $\underset{\sim}{H}$ matrix solves the question of the high computational cost using hybrid elements. An additional flexibility in the uncoupled stress formulation provides more versatile element. When the element is skewed the displacement modes becomes correspondingly skewed in the rectangular Cartesian coordinates. In order to exactly match these

skewed modes, the assumed stress modes should also be defined in the natural coodinate system. The uncoupled stress formulation provide this flexibility.

In order to establish the mechanics to assume the stress modes in the natural coordinates, further explanation of the $\underset{\sim}{R}$ matrix, Equation (7.19), is needed. The stationary condition, Equation (7.20), and the Equation (7.19) provide two possible ways to obtain the $\underset{\sim}{R}$ matrix.

$$\underset{\sim}{R} = \int_V \underset{\sim}{E}^T \underset{\sim}{M} \, dV \qquad (7.19)$$

$$\underset{\sim}{R}^T \underset{\sim}{\beta} = 0 \qquad (7.20)$$

Using Equation (7.20) the constraints on the β's obtained through the homogeneous equilibrium equations can be directly imposed if the stresses are defined in the rectangular Cartesian coordinates. The $\underset{\sim}{R}$ matrix in this case simply zero or couple the appropriate β's. By assuming $\underset{\sim}{\sigma}$ and $\underset{\sim}{u}_\lambda$ modes in natural coordinates and using Equation (7.19), similar type of constraints can be imposed.

For the Hu-Washizu formulation,

$$\pi_{HW} = \int_V \left[\tfrac{1}{2} \underset{\sim}{\varepsilon}^T \underset{\sim}{C} \underset{\sim}{\varepsilon} - \underset{\sim}{\sigma}^T \underset{\sim}{\varepsilon} + \underset{\sim}{\sigma}^T (\underset{\sim}{D} \underset{\sim}{u}_\beta) + \underset{\sim}{\sigma}^T (\underset{\sim}{D} \underset{\sim}{u}_\lambda) \right] dV \qquad (3.11)$$

In the matrix form,

$$\Pi_{HW} = \frac{1}{2} \underset{\sim}{\alpha}^T \underset{\sim}{J} \underset{\sim}{\alpha} - \underset{\sim}{\beta}^T \underset{\sim}{\bar{H}} \underset{\sim}{\alpha} + \underset{\sim}{\beta}^T \underset{\sim}{G} \underset{\sim}{g} - \underset{\sim}{\beta}^T \underset{\sim}{R} \underset{\sim}{\lambda} \tag{7.28}$$

where

$$\begin{aligned} \underset{\sim}{\sigma} &= \underset{\sim}{P} \underset{\sim}{\beta} \\ \underset{\sim}{\varepsilon} &= \underset{\sim}{P} \underset{\sim}{\alpha} \\ \underset{\sim}{u} &= \underset{\sim}{u}_g + \underset{\sim}{u}_\lambda \\ \underset{\sim}{u}_g &= \underset{\sim}{N} \underset{\sim}{g} \\ \underset{\sim}{u}_\lambda &= \underset{\sim}{M} \underset{\sim}{\lambda} \\ \underset{\sim}{D}^T \underset{\sim}{\sigma} &= \underset{\sim}{E} \underset{\sim}{\beta} \end{aligned} \tag{7.29}$$

and

$$\begin{aligned} \underset{\sim}{\bar{H}} &= \int_V \underset{\sim}{P}^T \underset{\sim}{P} \, dV \\ \underset{\sim}{J} &= \int_V \underset{\sim}{P}^T \underset{\sim}{C} \underset{\sim}{P} \, dV \\ \underset{\sim}{G} &= \int_V \underset{\sim}{P}^T \underset{\sim}{B} \, dV \\ \underset{\sim}{R} &= \int_V \underset{\sim}{E}^T \underset{\sim}{M} \, dV \end{aligned} \tag{7.30}$$

Using the stationary condition,

$$\begin{aligned} \frac{\partial \Pi_{HW}}{\partial \underset{\sim}{\beta}} &= -\underset{\sim}{\bar{H}} \underset{\sim}{\alpha} + \underset{\sim}{G} \underset{\sim}{g} - \underset{\sim}{R} \underset{\sim}{\lambda} = 0 \\ \frac{\partial \Pi_{HW}}{\partial \underset{\sim}{\alpha}} &= \underset{\sim}{J} \underset{\sim}{\alpha} - \underset{\sim}{\bar{H}} \underset{\sim}{\beta} = 0 \end{aligned} \tag{7.31}$$

$$\frac{\partial \pi_{HW}}{\partial \underset{\sim}{\lambda}} = - \underset{\sim}{R}^T \underset{\sim}{\beta} = 0$$

or

$$\begin{aligned} \underset{\sim}{\alpha} &= \bar{\underset{\sim}{H}}^{-1} [\underset{\sim}{G} \underset{\sim}{g} - \underset{\sim}{R} \underset{\sim}{\lambda}] \\ \underset{\sim}{\beta} &= \bar{\underset{\sim}{H}}^{-1} \underset{\sim}{J} \underset{\sim}{\alpha} \\ \underset{\sim}{\lambda} &= (\underset{\sim}{R}^T \bar{\underset{\sim}{H}}^{-1} \underset{\sim}{J} \bar{\underset{\sim}{H}}^{-1} \underset{\sim}{R})^{-1} \underset{\sim}{R}^T \bar{\underset{\sim}{H}}^{-1} \underset{\sim}{J} \bar{\underset{\sim}{H}}^{-1} \underset{\sim}{g} \end{aligned} \tag{7.32}$$

Define,

$$\underset{\sim}{W} = \bar{\underset{\sim}{H}}^{-1} \underset{\sim}{J} \bar{\underset{\sim}{H}}^{-1} \tag{7.33}$$

$$\bar{\underset{\sim}{G}} = \underset{\sim}{G} - \underset{\sim}{R} (\underset{\sim}{R}^T \underset{\sim}{W} \underset{\sim}{R})^{-1} \underset{\sim}{R}^T \underset{\sim}{W} \underset{\sim}{G} \tag{7.34}$$

The resulting stiffness matrix is

$$\underset{\sim}{K} = \bar{\underset{\sim}{G}}^T \underset{\sim}{W} \bar{\underset{\sim}{G}} \tag{7.35}$$

Since the Hu-Washizu formulation relaxes the stress-strain relation, further constraints on the choice of the $\underset{\sim}{P}$ matrix must be established. These constraints arise due to the assumption that

$$\begin{aligned} \underset{\sim}{\sigma} &= \underset{\sim}{P} \underset{\sim}{\beta} \\ \underset{\sim}{\varepsilon} &= \underset{\sim}{P} \underset{\sim}{\alpha} \end{aligned} \tag{7.29}$$

Define $\underset{\sim}{P}$ as

$$\underset{\sim}{P} = \begin{bmatrix} \underset{\sim}{P}_1 & & & & & \\ & \underset{\sim}{P}_2 & & & \underset{\sim}{0} & \\ & & \underset{\sim}{P}_3 & & & \\ & & & \underset{\sim}{P}_4 & & \\ & \underset{\sim}{0} & & & \underset{\sim}{P}_5 & \\ & & & & & \underset{\sim}{P}_6 \end{bmatrix} \tag{7.36}$$

For the anisotropic material law, in order to obtain

$$\underset{\sim}{\sigma} = \underset{\sim}{C}\,\underset{\sim}{\varepsilon} \tag{2.5}$$

exactly, the $\underset{\sim}{P}$ matrix has to be chosen such that

$$\underset{\sim}{P}_1 = \underset{\sim}{P}_2 = \underset{\sim}{P}_3 = \underset{\sim}{P}_4 = \underset{\sim}{P}_5 = \underset{\sim}{P}_6$$

For the orthotropic case, only $\underset{\sim}{P}_1, \underset{\sim}{P}_2, \underset{\sim}{P}_3$ must be equal to each other. To satisfy the pointwise equilibrium, the procedure used for Π_R also applies to this functional.

When the matrices required to generate the stiffness matrix for the uncoupled stress Π_R and Π_{HW}, the equivalence condition for the two functionals are observed to be

$$\underset{\sim}{W} = \underset{\sim}{\bar{H}}^{-1}\,\underset{\sim}{J}\,\underset{\sim}{\bar{H}}^{-1} = \underset{\sim}{H}^{-1} \tag{7.37}$$

At this point, the purpose in exploring the Hu-Washizu principle can be easily demonstrated. The most significant difference between the finite element formulation using Π_R and Π_{HW} arises for the anisotropic material. To illustrate, for a 20-node solid element, the minimum number of β's is 54. In order to satisfy the

requirement that all $\underset{\sim}{P}_i$ are equal, 120 β's (full cubic) are required. To apply equilibrium and reduce this to 54 β's, 66 λ's are necessary. Thus the order of $(\underset{\sim}{R}^T \underset{\sim}{H}^{-1} \underset{\sim}{R})^{-1}$ required for the stiffness matrix is 66. This defeats the purpose of using the uncoupled stress approach.

In the Hu-Washizu formulation, the stress-strain relation can be relaxed for the "nonsense" stress terms analogous to relaxed equilibrium condition for π_R. Thus, the stress-strain parameters $\underset{\sim}{P}_i$ can be assumed to be only identical up to a chosen order. Furthermore, different $\underset{\sim}{P}_i$'s can be used since $\underset{\sim}{\bar{H}}$ is in a diagonal form.

$$\underset{\sim}{\bar{H}}^{-1} = \begin{bmatrix} \underset{\sim}{\bar{P}}_{11}^{-1} & & & & & \underset{\sim}{0} \\ & \underset{\sim}{\bar{P}}_{22}^{-1} & & & & \\ & & \underset{\sim}{\bar{P}}_{33}^{-1} & & & \\ & & & \underset{\sim}{\bar{P}}_{44}^{-1} & & \\ \underset{\sim}{0} & & & & \underset{\sim}{\bar{P}}_{55}^{-1} & \\ & & & & & \underset{\sim}{\bar{P}}_{66}^{-1} \end{bmatrix} \qquad (7.38)$$

where

$$\underset{\sim}{\bar{P}}_{ii} = \int_V \underset{\sim}{P}_i^T \underset{\sim}{P}_i \, dV \qquad (i \text{ not summed}) \qquad (7.39)$$

By also relaxing equilibrium for the "nonsense" stress terms, the total number of β's required can be greatly reduced. A numerical example is provided in the later section.

8. ELEMENTS

8.1 4-NODE LINEAR PLANE ELEMENTS

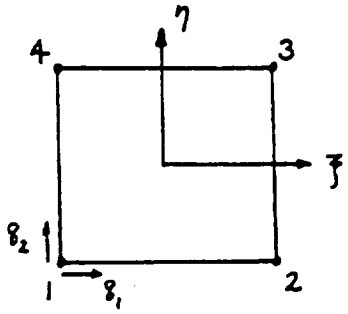

ISOPARAMETRIC ASSUMED DISPLACEMENT ELEMENT

Interpolation functions for 4-node plane elements are

$$\underset{\sim}{u} = \underset{\sim}{N}\,\underset{\sim}{\delta} \tag{8.1}$$

$$N_i = \frac{1}{4}(1+\xi_i\xi)(1+\eta_i\eta) \qquad i = 1,2,3,4$$

By expanding the interpolation functions N_i, the displacement modes can be obtained. The coefficients of each mode is denoted α_i.

$$\begin{aligned} u &= \alpha_1 + \alpha_2\xi + \alpha_3\eta + \alpha_4\xi\eta \\ v &= \alpha_5 + \alpha_6\xi + \alpha_7\eta + \alpha_8\xi\eta \end{aligned} \tag{8.2}$$

Without loss of generality, since isoparametric mapping has one-to-one correspondence, consider a rectangular element with x and y correspond to ξ and η, respectively. Using the strain-displacement relation, the

strain modes corresponding to Equation (8.2) are

$$\begin{aligned} \varepsilon_x &= \alpha_2 + \alpha_4 y \\ \varepsilon_y &= \alpha_7 + \alpha_8 x \\ \gamma_{xy} &= (\alpha_3 + \alpha_6) + \alpha_4 x + \alpha_8 y \end{aligned} \tag{8.3}$$

Isolating each strain modes,

$$\left.\begin{aligned} \varepsilon_x &= \alpha_2 \\ \varepsilon_y &= \alpha_7 \end{aligned}\right\} \text{ELONGATION} \tag{8.4}$$

$$\left.\gamma_{xy} = \alpha_3 + \alpha_6\right\} \text{DISTORTION} \tag{8.5}$$

$$\begin{aligned} \varepsilon_x &= \alpha_4 y & \varepsilon_x &= 0 \\ \varepsilon_y &= 0 & \varepsilon_y &= \alpha_8 x \\ \gamma_{xy} &= \alpha_4 x & \gamma_{xy} &= \alpha_8 y \end{aligned} \tag{8.6}$$

The two modes indicated in Equation (8.6) demonstrate the artificial coupling inherent in the isoparametric formulation. This coupling nature is the reason why π_p elements handles the pure bending poorly. In pure bending the shear term approaches zero as the thickness diminishes. The two modes in Equation (8.6) with the same coefficient must increment both normal and shear strains simultaneously.

WILSON'S INCOMPATIBLE ELEMENT

Wilson's incompatible displacement fields for 4-node plane element are

$$u = \alpha_1 + \alpha_2\xi + \alpha_3\eta + \alpha_4\xi\eta + \lambda_1(1-\xi^2) + \lambda_2(1-\eta^2)$$
$$v = \alpha_5 + \alpha_6\xi + \alpha_7\eta + \alpha_8\xi\eta + \lambda_3(1-\xi^2) + \lambda_4(1-\eta^2) \quad (8.7)$$

The four additional terms are the incompatible displacement terms to represent the bending behavior. The analysis of this element follows the same procedure.

$$\varepsilon_x = \alpha_2 + \alpha_4 y - 2\lambda_1 x$$
$$\varepsilon_y = \alpha_7 + \alpha_8 x - 2\lambda_4 y \quad (8.8)$$
$$\gamma_{xy} = (\alpha_3 + \alpha_6) + \alpha_4 x + \alpha_8 y - 2\lambda_2 y - 2\lambda_3 x$$

By redefining the coefficients in Equation (8.8) as

$$\Lambda_1 = \alpha_4 - 2\lambda_3 \quad (8.9)$$
$$\Lambda_2 = \alpha_8 - 2\lambda_2$$

the strain modes can be isolated. Upon substitution,

$$\varepsilon_x = \alpha_2 + \Lambda_1 y + 2\lambda_3 y - 2\lambda_1 x$$
$$\varepsilon_y = \alpha_7 + \Lambda_2 x + 2\lambda_2 x - 2\lambda_4 y \quad (8.10)$$
$$\gamma_{xy} = (\alpha_3 + \alpha_6) + \Lambda_1 x + \Lambda_2 y$$

Although the bending behavior is retained in the Wilson's incompatible element by the added λ_3 and λ_2 modes, the element fails the patch test unless the shape of the element is rectangular[11].

HYBRID ELEMENT

A demonstration of constructing the uncoupled stress π_R and π_{HW} elements is left for more general solid element discussion. For the plane elements, only the hybrid elements constructed using the standard π_R are illustrated.

To eliminate the zero-energy deformation modes, the strain modes obtained from the displacement modes, Equation (8.3), provides a convenient method. Each strain mode must be matched with stress mode to form non-zero energy. The technique is to first eliminate artificial coupling by using additional β's in the matching process. Thus Equation (8.3) forms

$$\begin{aligned} \sigma_x &= \beta_1 + \beta_4 y \\ \sigma_y &= \beta_2 + \beta_5 x \\ \sigma_{xy} &= \beta_3 + \beta_6 x + \beta_7 y \end{aligned} \qquad (8.11)$$

Other modes, such as $\sigma_x = x$ and $\sigma_y = y$, are not considered since they introduce additional error. Since these modes are not present in the strain modes, they interact with all the non-orthogonal terms in the element energy integral and thus introducing artificial coupling error. To illustrate, if the mode $\sigma_x = \beta_8 x$ is included equilibrium condition requires that $\sigma_{xy} = -\beta_8 y$. The coupling arise when $\sigma_{xy} = -\beta_8 y$ interact with α_4 mode in Equation (8.3). Thus the shear again couple into the bending behavior.

Applying the equilibrium condition on Equation (8.11) yields the optimal assumed stress modes.

$$\beta_7 = 0$$
$$\beta_6 = 0$$

$$\sigma_x = \beta_1 + \beta_4 y \qquad (8.12)$$
$$\sigma_y = \beta_2 + \beta_5 x$$
$$\sigma_{xy} = \beta_3$$

Since these stress modes are not invariant with respect to the reference coordinates, local axes should be used. Forcing invariance through the use of complete polynomial[16] diminishes the true advantage of the hybrid formulation for the general purpose elements.

At this stage the reason why the selective integration technique and the Wilson's incompatible element reduce to hybrid element for the rectangular geometry is clear. In the selective integration technique, by using lower order integration for γ_{xy} in Equation (8.3), the shear strain reduces to $\gamma_{xy} = \alpha_3 + \alpha_6$, thereby retaining the pure bending behavior. Also for the Wilson's element in rectangular geometry, the contributions from λ_3 and λ_2 support the pure bending behavior exactly. Furthermore, since unique solution exists for the governing equations of elasticity, the stiffness matrix must be identical for all these cases.

8.2 8-NODE QUADRATIC PLANE ELEMENTS

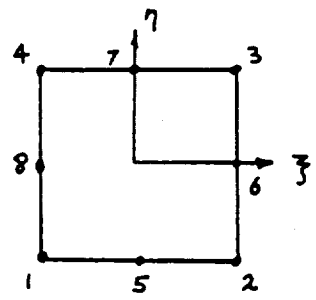

ISOPARAMETRIC ASSUMED DISPLACEMENT ELEMENT

For the 8-node plane element,

$$\underset{\sim}{u} = \underset{\sim}{N}\,\underset{\sim}{\delta} \tag{8.13}$$

$$N_i = \tfrac{1}{4}(1+\xi_i\xi)(1+\eta_i\eta)(\xi_i\xi+\eta_i\eta-1) \qquad i=1,2,3,4$$

$$= \tfrac{1}{2}(1-\xi^2)(1+\eta_i\eta) \qquad i=5,7$$

$$= \tfrac{1}{2}(1-\eta^2)(1+\xi_i\xi) \qquad i=6,8$$

The displacement modes are

$$u = \alpha_1 + \alpha_2\xi + \alpha_3\eta + \alpha_4\xi\eta + \alpha_5\xi^2 + \alpha_6\eta^2 + \alpha_7\xi^2\eta + \alpha_8\xi\eta^2 \tag{8.14}$$

$$v = \alpha_9 + \alpha_{10}\xi + \alpha_{11}\eta + \alpha_{12}\xi\eta + \alpha_{13}\xi^2 + \alpha_{14}\eta^2 + \alpha_{15}\xi^2\eta + \alpha_{16}\xi\eta^2$$

The strain modes,

$$\varepsilon_x = \alpha_2 + \alpha_4 y + 2\alpha_5 x + 2\alpha_7 xy + \alpha_8 y^2 \tag{8.15}$$

$$\varepsilon_y = \alpha_{11} + \alpha_{12} x + 2\alpha_{14} y + \alpha_{15} x^2 + 2\alpha_{16} xy$$

$$\gamma_{xy} = (\alpha_3 + \alpha_{10}) + (\alpha_4 + 2\alpha_{13})\, x + (\alpha_{12} + 2\alpha_6)\, y + (2\alpha_8 + 2\alpha_{15})\, xy + \alpha_7 x^2 + \alpha_{16} y^2$$

From here on the purpose for the isolation of the strain modes is to systematically construct the hybrid elements.

HYBRID ELEMENT

Following the procedure described previously for the linear elements, return to Equation (8.15) and eliminate artificial coupling and redundancy.

$$\begin{aligned} \sigma_x &= \beta_1 + \beta_4 x + \beta_7 y + \beta_{10} xy + \beta_{13} y^2 \\ \sigma_y &= \beta_2 + \beta_5 x + \beta_8 y + \beta_{11} xy + \beta_{14} x^2 \\ \sigma_{xy} &= \beta_3 + \beta_6 x + \beta_9 y + \beta_{12} xy + \beta_{15} x^2 + \beta_{16} y^2 \end{aligned} \qquad (8.16)$$

The equilibrium equation yields following constraints on the β's

$$\begin{aligned} \beta_4 + \beta_9 &= 0 \\ \beta_8 + \beta_6 &= 0 \\ \beta_{12} &= 0 \\ \beta_{10} + 2\beta_{16} &= 0 \\ \beta_{11} + 2\beta_{15} &= 0 \end{aligned} \qquad (8.17)$$

Applying the constraints and shifting the coefficient numbers yields following stress modes.

$$
\begin{aligned}
\sigma_x &= \beta_1 + \beta_4 x + \beta_6 y + \beta_8 xy + \beta_{10} y^2 \\
\sigma_y &= \beta_2 + \beta_5 x + \beta_7 y + \beta_9 xy + \beta_{11} x^2 \\
\sigma_{xy} &= \beta_3 - \beta_4 y - \beta_7 x - \tfrac{1}{2}\beta_8 y^2 - \tfrac{1}{2}\beta_9 x^2
\end{aligned}
\qquad (8.18)
$$

Since a minimum of 13 β's are required to obtain unique solution and thus eliminate the zero-energy deformation modes, two extra stress modes have to be included in the Equation (8.18). Furthermore, for the general purpose element, the two extra modes serve no purpose other than the elimination of zero-energy deformation modes. As before, the two modes are classified as the "nonsense" stress modes. With this in mind, all constraints imposed by the governing equations can be relaxed for the "nonsense" stress modes without loss of accuracy.

Two possible candidates, in view of numerical integration and application of uncoupled stress formulation, are

$$
\begin{aligned}
\sigma_x &= \beta_{12}\, xy^2 \\
\sigma_y &= \beta_{13}\, x^2 y
\end{aligned}
\qquad (8.18a)
$$

These modes interact with $\varepsilon_x = x$ and $\varepsilon_y = y$ to form non-zero energy. For more in depth coverage refer to the reference[10].

8.3 8-NODE LINEAR SOLID ELEMENTS

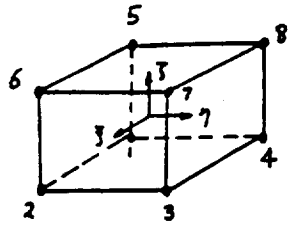

ISOPARAMETRIC ASSUMED DISPLACEMENT ELEMENT

For the 8-node solid element,

$$\underset{\sim}{u} = \underset{\sim}{N}\,\underset{\sim}{\delta} \tag{8.19}$$

$$N_i = \tfrac{1}{8}(1+\xi_i\xi)(1+\eta_i\eta)(1+\zeta_i\zeta) \qquad i = 1,2,\ldots,8$$

The displacement modes are

$$\begin{aligned} u &= \alpha_1 + \alpha_2\xi + \alpha_3\eta + \alpha_4\zeta + \alpha_5\xi\eta + \alpha_6\eta\zeta + \alpha_7\xi\zeta + \alpha_8\xi\eta\zeta \\ v &= \alpha_9 + \alpha_{10}\xi + \alpha_{11}\eta + \alpha_{12}\zeta + \alpha_{13}\xi\eta + \alpha_{14}\eta\zeta + \alpha_{15}\xi\zeta + \alpha_{16}\xi\eta\zeta \\ w &= \alpha_{17} + \alpha_{18}\xi + \alpha_{19}\eta + \alpha_{20}\zeta + \alpha_{21}\xi\eta + \alpha_{22}\eta\zeta + \alpha_{23}\xi\zeta + \alpha_{24}\xi\eta\zeta \end{aligned} \tag{8.19a}$$

The strain modes,

$$\begin{aligned} \varepsilon_x &= \alpha_2 + \alpha_5 y + \alpha_7 z + \alpha_8 yz \\ \varepsilon_y &= \alpha_{11} + \alpha_{13} x + \alpha_{14} z + \alpha_{16} xz \\ \varepsilon_z &= \alpha_{20} + \alpha_{22} y + \alpha_{23} x + \alpha_{24} xy \end{aligned} \tag{8.20}$$

$$\gamma_{xy} = (\alpha_3 + \alpha_{10}) + \alpha_5 x + \alpha_{13} y + (\alpha_6 + \alpha_{15}) z + \alpha_8 xz + \alpha_{16} yz$$

$$\gamma_{yz} = (\alpha_{12} + \alpha_{19}) + (\alpha_{15} + \alpha_{21}) x + \alpha_{14} y + \alpha_{22} z + \alpha_{16} xy + \alpha_{24} xz$$

$$\gamma_{xz} = (\alpha_4 + \alpha_{18}) + \alpha_7 x + (\alpha_6 + \alpha_{21}) y + \alpha_{23} z + \alpha_8 xy + \alpha_{24} yz$$

HYBRID ELEMENT

First eliminate the artificial coupling in the equation (8.20).

$$\begin{aligned}
\sigma_x &= \beta_1 + \beta_7 y + \beta_{10} z + \beta_{19} yz \\
\sigma_y &= \beta_2 + \beta_8 x + \beta_{11} z + \beta_{20} xz \\
\sigma_z &= \beta_3 + \beta_9 x + \beta_{12} y + \beta_{21} xy \\
\sigma_{xy} &= \beta_4 + \beta_{13} x + \beta_{16} y + \beta_{22} xz + \beta_{25} yz + \beta_{28} z \\
\sigma_{yz} &= \beta_5 + \beta_{14} y + \beta_{17} z + \beta_{23} xy + \beta_{26} xz + \beta_{29} x \\
\sigma_{xz} &= \beta_6 + \beta_{15} x + \beta_{18} z + \beta_{24} xy + \beta_{27} yz + \beta_{30} y
\end{aligned} \qquad (8.21)$$

From equilibrium,

$$\begin{aligned}
&\beta_{16} + \beta_{18} = 0 \\
&\beta_{13} + \beta_{17} = 0 \\
&\beta_{15} + \beta_{14} = 0 \\
&\beta_{22} = \beta_{23} = \beta_{24} = \beta_{25} = \beta_{26} = \beta_{27} = 0
\end{aligned} \qquad (8.22)$$

Applying these constraints,

$$
\begin{aligned}
\sigma_x &= \beta_1 + \beta_7 y + \beta_{10} z + \beta_{16} yz \\
\sigma_y &= \beta_2 + \beta_8 x + \beta_{11} z + \beta_{17} xz \\
\sigma_z &= \beta_3 + \beta_9 x + \beta_{12} y + \beta_{18} xy
\end{aligned}
\qquad (8.23)
$$

$$
\begin{aligned}
\sigma_{xy} &= \beta_4 + \beta_{13} z + \beta_{19} y + \beta_{20} x \\
\sigma_{yz} &= \beta_5 + \beta_{14} x - \beta_{20} z + \beta_{21} y \\
\sigma_{xz} &= \beta_6 + \beta_{15} y - \beta_{19} z - \beta_{21} x
\end{aligned}
$$

From the three dimensionality of the element construction, an additional step must be performed before arriving at the final stress modes. By comparing the Equation (8.23) with the Equation (8.20), the modes β_{19}, β_{20}, and β_{21} above are not represented as a possible deformation under the isoparametric formulation. Thus, these three additional β's must be set to zero. Note that through the process of eliminating the artificial coupling in the Equation (8.21), additional possible modes under equilibrium are introduced. These β's do not contribute in accordance with the deformation modes and thus should be left out.

The resulting stress modes are

$$
\begin{aligned}
\sigma_x &= \beta_1 + \beta_7 y + \beta_{10} z + \beta_{16} yz \\
\sigma_y &= \beta_2 + \beta_8 x + \beta_{11} z + \beta_{17} xz \\
\sigma_z &= \beta_3 + \beta_9 x + \beta_{12} y + \beta_{18} xy
\end{aligned}
\qquad (8.24)
$$

$$\sigma_{xy} = \beta_4 + \beta_{13} z$$

$$\sigma_{yz} = \beta_5 + \beta_{14} x$$

$$\sigma_{xz} = \beta_6 + \beta_{15} y$$

Recall from the Section 6 and the Figure 6.1 that β_{16}, β_{17}, and β_{18} are "nonsense" stress modes and the governing equations can be relaxed for these terms.

UNCOUPLED STRESS HYBRID ELEMENT

$$-\Pi_R -$$

In order to achieve fully equivalent element as the previous hybrid element with stress assumption in Equation (8.24) following uncoupled stress assumption must be used for computationally efficient element with isotropic material property.

$$\begin{aligned}
\sigma_x &= \beta_1 + \beta_2 x + \beta_3 y + \beta_4 z + \beta_5 xy + \beta_6 yz + \beta_7 xz \\
\sigma_y &= \beta_8 + \beta_9 x + \beta_{10} y + \beta_{11} z + \beta_{12} xy + \beta_{13} yz + \beta_{14} xz \\
\sigma_z &= \beta_{15} + \beta_{16} x + \beta_{17} y + \beta_{19} z + \beta_{21} xy + \beta_{22} yz + \beta_{23} xz \\
\sigma_{xy} &= \beta_{22} + \beta_{23} z \\
\sigma_{yz} &= \beta_{24} + \beta_{25} x \\
\sigma_{xz} &= \beta_{26} + \beta_{27} y
\end{aligned} \qquad (8.25)$$

Proper β's can be eliminated or coupled directly by choosing the $\underset{\sim}{R}$ matrix according to

$$\underset{\sim}{R}^T \underset{\sim}{\beta} = 0 \tag{7.20}$$

The order of $\underset{\sim}{R}$ matrix for the above stress assumption is number of β's by 9. Thus additional inversion of (9x9) matrix ($\underset{\sim}{R}^T \underset{\sim}{H}^{-1} \underset{\sim}{R}$) will be required.

In the natural coordinate system of the element, the stress assumption corresponding to Equation (8.25) is

$$\begin{aligned}
\sigma_x &= \beta_1 + \beta_2\xi + \beta_3\eta + \beta_4\zeta + \beta_5\xi\eta + \beta_6\eta\zeta + \beta_7\xi\zeta \\
\sigma_y &= \beta_8 + \beta_9\xi + \beta_{10}\eta + \beta_{11}\zeta + \beta_{12}\xi\eta + \beta_{13}\eta\zeta + \beta_{14}\xi\zeta \\
\sigma_z &= \beta_{15} + \beta_{16}\xi + \beta_{17}\eta + \beta_{18}\zeta + \beta_{19}\xi\eta + \beta_{20}\eta\zeta + \beta_{21}\xi\zeta \\
\sigma_{xy} &= \beta_{22} + \beta_{23}\zeta \\
\sigma_{yz} &= \beta_{24} + \beta_{25}\xi \\
\sigma_{xz} &= \beta_{26} + \beta_{27}\eta
\end{aligned} \tag{8.26}$$

with $\underset{\sim}{u}_\lambda$ as

$$\begin{aligned}
u_\lambda &= \lambda_1 + \lambda_2\eta + \lambda_3\zeta \\
v_\lambda &= \lambda_4 + \lambda_5\xi + \lambda_6\zeta \\
w_\lambda &= \lambda_7 + \lambda_8\xi + \lambda_9\eta
\end{aligned} \tag{8.27}$$

Note that if the element is rectangular, above stress assumption reduces equivalently to Equation (8.33) since the Jacobian is constant.

A large reduction in computional cost can be induced by recognizing that the quadratic terms are the "nonsense" stress modes and serve only to suppress the zero-energy deformation modes. With this in mind a resulting stress

assumption arrived is given below.

$$\begin{aligned}
\sigma_x &= \beta_1 + \beta_2 \xi + \beta_3 \eta + \beta_4 \zeta + \beta_5 (\xi\eta + \eta\zeta + \xi\zeta) \\
\sigma_y &= \beta_6 + \beta_7 \xi + \beta_8 \eta + \beta_9 \zeta + \beta_{10} (\xi\eta + \eta\zeta + \xi\zeta) \\
\sigma_z &= \beta_{11} + \beta_{12} \xi + \beta_{13} \eta + \beta_{14} \zeta + \beta_{15} (\xi\eta + \eta\zeta + \xi\zeta) \\
\sigma_{xy} &= \beta_{16} + \beta_{17} \zeta \\
\sigma_{yz} &= \beta_{18} + \beta_{19} \xi \\
\sigma_{xz} &= \beta_{20} + \beta_{21} \eta
\end{aligned} \tag{8.28}$$

With

$$\begin{aligned}
u_\lambda &= \lambda_1 \\
v_\lambda &= \lambda_2 \\
w_\lambda &= \lambda_3
\end{aligned} \tag{8.29}$$

Thus the order of $(\underset{\sim}{R}^T \underset{\sim}{H}^{-1} \underset{\sim}{R})$ is reduced to (3×3) and the order of other matrices necessary for the stiffness matrix generation have been correspondingly reduced.

— Π_{HW} —

Recall that for the anisotropic material law, in order for

$$\underset{\sim}{\sigma} = \underset{\sim}{C}\,\underset{\sim}{\varepsilon} \tag{2.5}$$

the constraints on $\underset{\sim}{\sigma}$ and $\underset{\sim}{\varepsilon}$ are

$$\begin{aligned}
\underset{\sim}{\sigma} &= \underset{\sim}{P}\,\underset{\sim}{\beta} \\
\underset{\sim}{\varepsilon} &= \underset{\sim}{P}\,\underset{\sim}{\alpha}
\end{aligned} \tag{7.29}$$

$$\underset{\sim}{P}_1 = \underset{\sim}{P}_2 = \underset{\sim}{P}_3 = \underset{\sim}{P}_4 = \underset{\sim}{P}_5 = \underset{\sim}{P}_6 \tag{7.36a}$$

A promising choice under this constraint for the stress assumption is

$$
\begin{aligned}
\sigma_x &= \beta_1 + \beta_2 \xi + \beta_3 \eta + \beta_4 \zeta + \beta_5 (\xi\eta + \eta\zeta + \xi\zeta) \\
\sigma_y &= \beta_6 + \beta_7 \xi + \beta_8 \eta + \beta_9 \zeta + \beta_{10} (\xi\eta + \eta\zeta + \xi\zeta) \\
\sigma_z &= \beta_{11} + \beta_{12} \xi + \beta_{13} \eta + \beta_{14} \zeta + \beta_{15} (\xi\eta + \eta\zeta + \xi\zeta) \\
\sigma_{xy} &= \beta_{16} + \beta_{17} \xi + \beta_{18} \eta + \beta_{19} \zeta + \beta_{20} (\xi\eta + \eta\zeta + \xi\zeta) \\
\sigma_{yz} &= \beta_{21} + \beta_{22} \xi + \beta_{23} \eta + \beta_{24} \zeta + \beta_{25} (\xi\eta + \eta\zeta + \xi\zeta) \\
\sigma_{xz} &= \beta_{26} + \beta_{27} \xi + \beta_{28} \eta + \beta_{29} \zeta + \beta_{30} (\xi\eta + \eta\zeta + \xi\zeta)
\end{aligned}
\tag{8.30}
$$

However, since the stress distribution in Equation (8.30) may be too rigid, additional relaxation of the governing equations may be necessary.

8.4 20-NODE QUADRATIC SOLID ELEMENTS

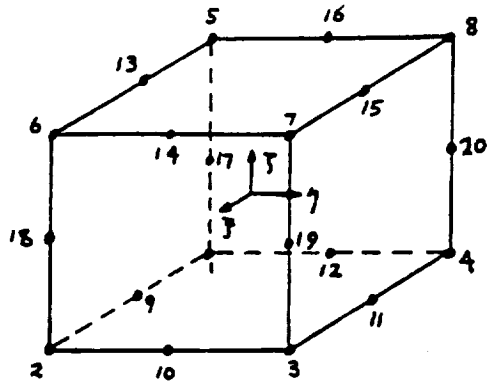

ISOPARAMETRIC ASSUMED DISPLACEMENT ELEMENT

For 20-node solid elements,

$$\underset{\sim}{u} = \underset{\sim}{N}\,\underset{\sim}{q} \tag{8.31}$$

$$N_i = \tfrac{1}{8}(1+\xi_i\xi)(1+\eta_i\eta)(1+\zeta_i\zeta)(\xi_i\xi+\eta_i\eta+\zeta_i\zeta-2) \qquad i=1,2,\cdots,8$$

$$= \tfrac{1}{4}(1-\xi^2)(1+\eta_i\eta)(1+\zeta_i\zeta) \qquad i=9,11,13,15$$

$$= \tfrac{1}{4}(1-\eta^2)(1+\xi_i\xi)(1+\zeta_i\zeta) \qquad i=10,12,14,16$$

$$= \tfrac{1}{4}(1-\zeta^2)(1+\xi_i\xi)(1+\eta_i\eta) \qquad i=17,18,19,20$$

The displacement modes are

$$u = \alpha_1 + \alpha_2\xi + \alpha_3\eta + \alpha_4\zeta + \alpha_5\xi\eta + \alpha_6\eta\zeta + \alpha_7\xi\zeta + \alpha_8\xi^2 + \alpha_9\eta^2 + \alpha_{10}\zeta^2$$
$$+ \alpha_{11}\xi^2\eta + \alpha_{12}\xi^2\zeta + \alpha_{13}\eta^2\zeta + \alpha_{14}\eta^2\xi + \alpha_{15}\zeta^2\xi + \alpha_{16}\zeta^2\eta$$
$$+ \alpha_{17}\xi\eta\zeta + \alpha_{18}\xi^2\eta\zeta + \alpha_{19}\eta^2\zeta\xi + \alpha_{20}\zeta^2\xi\eta$$

$$v = \alpha_{21} + \cdots + \alpha_{40}\zeta^2\xi\eta \tag{8.32}$$

$$w = \alpha_{41} + \cdots + \alpha_{60}\zeta^2\xi\eta$$

The breakdown of the corresponding strain modes are included in the Appendix A.

HYBRID ELEMENT

The procedure for the 20-node solid hybrid element development is similar to 8-node solid hybrid element. The stress modes are given in the Appendix A. In the final resulting assumed stress modes, Table A4, the "nonsense" modes include all cubic stress terms. This is consistent with the linear 8-node solid element where all quadratic terms are the "nonsense" modes. Furthermore, this is mathematically consistent since with quadratic displacement assumption, cubic stress modes does not contribute to general convergence of the element. Recall that both the stress and the displacement approximations must be improved properly and simultaneously. Since the accuracy of stresses from the displacements converge, at best, in a quadratic order (Optimal Gauss Points[17]), the cubic terms are only used for suppressing the zero-energy deformation modes.

9. NUMERICAL EXAMPLES

The element nomenclature is given in the Appendix B for quick reference. In order to numerically support the discussion in the previous sections, various samples of stress assumptions have been implemented. However, bear in mind that most of the numerical examples given are carried out to provide a foundation for the inductive process used in the previous sections.

All calculations for the numerical examples are done under double precision using Digital Vax 11/780 computer. The Gaussian quadrature order used for the numerical integration correspond to exact integration for each element type.

9.1 CANTILEVER BEAM USING SINGLE 4-NODE PLANE STRESS ELEMENT

Refer to the Figure 9.1 for the problem description and geometry. The cantilever beam problem has been chosen to depict the bending behavior. Since the purpose for this example is to illustrate the nature of the interaction of the stress modes, only single element mesh is needed. The Poisson's ratio has been set to zero to isolate the modes. The analytical solution is based upon the Bernoulli beam theory. The tip deflection and the maximum normal stress, σ_x , for the five different stress assumption is given in the Table 9.1.

TABLE 9.1. Cantilever beam using Single 4-node element.

ELEMENT	δ_{TIP}	$\sigma_{x_{MAX}}$
RP4A 5 β's	.015	3000
RP4B 5 β's	.0012	0
RP4C 7 β's	.0011	226.3
RP4D 9 β's	.0011	222.2
RP4E 5 β's	.0012	0
DP4 (π_p)	.0011	222.2
Analytical	.015	3000

The non-zero β's for each stress assumptions for the cantilever beam bending are listed below.

$$
\text{RP4A} \quad \begin{cases} \sigma_x = \beta_1 + \beta_4 y \\ \sigma_y = 0 \\ \sigma_{xy} = 0 \end{cases}
$$

$$
\text{RP4B} \quad \begin{cases} \sigma_x = 0 \\ \sigma_y = 0 \\ \sigma_{xy} = \beta_3 + \beta_4 x \end{cases}
$$

$$
\text{RP4C} \quad \begin{cases} \sigma_x = \beta_1 + \beta_2 y \\ \sigma_y = \beta_3 + \beta_7 y \\ \sigma_{xy} = \beta_5 + \beta_7 x \end{cases}
$$

$$
\text{RP4D} \quad \begin{cases} \sigma_x = \beta_1 + \beta_3 y \\ \sigma_y = 0 \\ \sigma_{xy} = \beta_7 + \beta_8 x \end{cases}
$$

$$
\text{RP4E} \quad \begin{cases} \sigma_x = 0 \\ \sigma_y = \beta_2 + \beta_5 y \\ \sigma_{xy} = \beta_3 - \beta_5 x \end{cases}
$$

Note that only in the Element RP4A the pure bending behavior is exactly modeled. Thus even in a complex mesh model, the transmitted bending load to each element is successfully modeled by the Element RP4A. In any complex loading problem the bending load will be present for many elements.

The reason for the choice of other stress assumptions are as follows:

RP4B - 5β case with zero-energy deformation mode suppressed.

RP4C - Complete linear stress assumption with equilibrium condition imposed.

RP4D - Complete linear stress assumption.

RP4E - Alternate 5β case with equilibrium satisfied

As indicated by the results, if the corresponding stress modes are available, the interaction between the stress and strain modes will reintroduce the artificial coupling. By using the minimum required number of β's, 5 in this case, and choosing the stress modes in full recognition of the strain modes, above interaction can be avoided.

The nature of the stiffness matrices for a square element can be summarized by the examination of the trace.

TABLE 9.2. Trace of the stiffness matrix.

ELEMENT	Trace = Σ Eigenvalues
RP4A	$.3634 \times 10^{8}$
RP4B	.3223
RP4C	.3727
RP4D	.3956
RP4E	.3152
DP4 (π_p)	.4615

The Element RP4E is most flexible element in sum, yet this flexibility does not extend to the bending behavior.

9.2 CANTILEVER BEAM USING SINGLE 8-NODE PLANE STRESS ELEMENT

Identical problem shown in the Figure 9.1 is solved using single 8-node plane stress element. Recall that during the process of the derivation of the hybrid 8-node plane element, the strain modes from the displacement modes, Equation (8.15), has been shown to contain the bending modes, α_4 and α_{12}. Thus any stress assumption with bending modes must give exact solution. The tip deflection results are given in the Table 9.3.

TABLE 9.3. Tip deflection - Cantilever Beam Problem.

ELEMENT	δ_{TIP}
DP8	.0137
RP8A	.015
RP8B	.015
RP8C	.015
RP8D	.015
RP8E	.015
RP8F	.015
Analytical	.015

The assumed displacement element, DP8, did not give the exact solution due to the interaction of α_4 and α_{13} term in the Equation (8.15). As a point of interest, the trace of the stiffness matrix from the Elements RP8E and RP8F is identical.

9.3 CURVED CANTILEVER BEAM USING 8-NODE PLANE STRESS ELEMENT

The curved cantilever beam problem, Figure 9.2, has been motivated by Spilker,Maskeri, and Kania[16]. In the article, to achieve invariance under coordinate rotation the stress modes are expanded to full cubic. In order to further reduce the number of β 's, the compatibility condition is imposed on the stress. In Appendix B, this element is named RP8D. The Elements DP8, RP8A, RP8B, and RP8C are used for comparison.

The tip deflection results are shown in the Figure 9.3. The analytical solution has been obtained from Timoshenko and Goodier[18]. Note that this solution is approximate and thus the percent error only has an approximate meaning.

The stress results for the five element mesh are plotted on the Figure 9.4. The results are obtained at various angles for r=11.58. Specifically, these points correspond to the optimal stress points. Since the stress distributions obtained from the Elements RP8A, RP8B, and RP8C are close, only the RP8A stress distribution is shown.

Overall results indicate that the Hybrid formulation converges much faster then the assumed displacement formulation in the curved beam analysis. However, between the Hybrid elements there is no consistant way to evaluate

which element has the best result. To eliminate the occillation of the Element RP8A stress distribution two additional analyis should be made.

1) Use local coordinate for RP8A, RP8B, RP8C Elements.
2) Develop an element using the natural coordinate system for the stress modes.

9.4 CANTILEVER BEAM USING 8-NODE SOLID ELEMENT

The cantilevered beam problem, Figure 9.5, is solved using several mesh arrangements, Figure 9.6. A moment, Load Case I, and a shear, Load Case II, loadings are considered. The analytical solution is based upon the Bernoulli beam theory. The tip deflection results are given in the Tables 9.4 and 9.5.

In a rectangular solid mesh configuration, the tip deflection results demonstrate that the Elements RUS8A and RUS8B contains the pure bending modes induced by the moment couple in the Load Case I. As expected, the results from the Elements RUS8D and RUS8E are similar to the result from the assumed displacement element DS8. This is a further evidence that inclusion of unnecessary β's simply reduces the hybrid element behavior similar to the assumed displacement element.

In order to assess the rate of degredation of accuracy as the elements are skewed, the cantilevered beam problem is repeated by steadily increasing the distortion. The result from the distortion sensitivity analysis of the hybrid element, RUS8A, is plotted on the Figure 9.7. As shown, the Element RUS8A has a high degredation rate initially and then effectively reduces to zero after b/a = 2. An interesting point to consider is that the value of the tip deflection beyond b/a = 2 is approximately the same as the result obtained from the assumed displacement

TABLE 9.4. Tip Deflection

LOAD CASE I

ELEMENT	MESH1	MESH2	MESH3	MESH4	MESH5
DS8	9.00	27.78	20.27	23.52	18.81
RUS8A	100	100	51.1	46.0	25.8
RUS8B	100	100	51.1	43.5	25.8
RUS8D	9.26	30.2	22.5	23.0	16.6
RUS8E	9.26	30.2	22.5	23.3	16.7
Analytical	100	100	100	100	100

LOAD CASE II

ELEMENT	MESH1	MESH2	MESH3	MESH4	MESH5
DS8	9.26	28.50	22.81	24.08	20.77
RUS8A	77.5	96.0	58.9	55.2	40.1
RUS8B	77.5	96.0	58.9	53.3	40.1
RUS8D	9.44	30.8	23.8	25.4	20.8
RUS8E	9.44	30.8	23.8	25.7	20.9
Analytical	100	100	100	100	100

element, DS8. Basically, the distortion reintroduces the artificial coupling into the stress modes. This observation provides a clue to develop a more effective element with less sensitivity to distortion. The tip deflection result for b/a = 99 is 34.9 which further supports that the accuracy of the hybrid element will be equal or greater then the assumed displacement element no matter how large the distortion becomes for the cantilevered beam problem.

Backtracking for a moment, re-examine the Table 9.4 and 9.5 comparing the Elements RUS8A and RUS8B. Recall that these two elements employ similar assumed stress modes. Only difference being that one uses the xyz coordinates and the other the natural coordinates. The comparison of these elements indicate further modification is necessary to achieve distortion insensitive element then just expressing the stress modes in the natural coordinate system. Above remark seems reasonable since the mapping a linear mode from xyz coordinate to the natural coordinate system yields also a linear mode. As a point for future research, the mechanics of distortion should be studied in view of the coupling between the stress modes.

In any structural problems, a reference coordinate system must be defined to locate each point in the volumetric space. Thus next step of analysis studies the solution response of the cantilever beam problem under

concentrated tip load as the reference coordinates are rotated. Since the stress assumption for the Elements RUS8A and RUS8B are not a complete polynomial, the invariance condition is not automatically satisfied. Before presenting the results, note that an alternate way to establish the reference coordinate invariance is to use a local coordinate system for each element.

The results from the rotation of the reference frame is shown in the Figure 9.8. The Element RUS8A using the Cartesian coordinate system for the stress modes contains zero-energy deformation modes at $\theta = 45^{o}$. This is verified by eigenvalue analysis of the stiffness matrix generated at this angle. Furthermore, as the angle approaches the value of 45^{o} the element becomes more and more flexible till it becomes unstable at $\theta = 45^{o}$. However, by the use of the natural coordinate system, Element RUS8B, eliminates this unstable mode. Notice that the variation of the result remains negligible for $\theta < 30^{o}$.

Before the reader becomes too astounded by above results, several comforting observations are in order. In most engineering problems, the reference coordinate chosen coincide with the physical structural geometry which eliminates the possibility of the complete structural instability. To clarify, due to the boundary conditions and the assembly with stable elements, the total structure will be stable even when part of the mesh is parallel with

45^{o} line. Another strategy to eliminate the possibility of the unstable mode is partially distorting the element in the same plane of the expected angle θ . Following result demonstrates this numerically.

TABLE 9.5. Tip deflection, Load Case II at $\phi = 45^{o}$.

ELEMENT	MESH2	MESH3	MESH4
RUS8A	$-.599 \times 10^{13}$	$-.240 \times 10^{5}$	132
RUS8B	159	143	129

The angle ϕ lies in the x-y plane, Figure 9.5. Since the Mesh 4 is distorted in the x-y plane, the unstable mode is partially dampened. Above analysis also holds for the reduced integration technique. Same approach can be used to employ elements with zero-energy deformation modes.

As a final note, for the quadratic elements, since the stress assumption is complete to the linear order, no instability will arise for the bending problem. Overall, the remedy to introduce invariance with respect to the reference frame should be made by using the local coordinate system. The problem of arbitrary reference coordinate system should not enter into the element development. Combat coordinates with coordinates.

9.5 CIRCULAR HOLE IN AN INFINITE STRIP USING 8-NODE SOLID ELEMENT

The model for the circular hole in an infinite strip is shown in the Figure 9.9. The Figure 9.10 provide a plane view of the four configurations of mesh using 8-node solid elements. Although, due to the curved geometry of the hole, higher order element should be used, this problem nicely demonstrates the limitations of the hybrid elements developed for general purpose applications. Furthermore, this problem establishes the groundwork for the discussion of the special purpose elements presented in the next section.

The result from the displacement convergence study is given in Figure 9.11. The stress distribution along $x = 0$ for the four mesh configurations are provided in Figures 9.12 to 9.15. The elements used in the analysis are the Elements DS8 and RUS8A. Recall that RUS8A can model pure bending exactly as demonstrated in the subsection 9.4. Since the results from the Element RUS8B with stress assumption in the natural coordinate system are very close to the results from the Element RUS8A, these results are omitted.

In the overall sense the difference between the results from Element DS8 and RUS8A are not overly dramatic. In the development of the 8-node solid elements, the assumed stress modes clearly show that the

advantage of the hybrid 8-node over the assumed displacement 8-node is the bending behavior. In any other type of mode excitation, the convergence of the 8-node solids using either element will be similar. However, note that this characteristic is purposely imposed in order to construct a general purpose element.

In the stress distribution obtained, the results from the assumed displacement element are actually little more accurate then the result from the hybrid element. The only way this can be explained is that the artificially coupled terms inhence the accuracy for the class of problems exemplified by the circular hole problem. From a logical extension to the above conclusion, introducing more descriptive modes will increase the accuracy for the corresponding class of problems, i.e. special purpose. Further discussion is reserved for the next section.

9.6 HOLLOW SPHERE UNDER TEMPERATURE DISTRIBUTION USING 20-NODE SOLID ELEMENT

The problem chosen to evaluate the 20-node solid elements is the hollow sphere under temperature distribution, Figure 9.16. Six element mesh is adequate to study the relaxation and symmetry condition on the cubic terms. Six diffenent stress assumptions are used for direct comparison. Element used in this analysis are listed below with comment for their choice.

ASSUMED DISPLACEMENT ELEMENT

DS20

HYBRID ELEMENTS

RS20A - Equilibrium relaxed for
all cubic stress modes.
Symmetry Maintained.

RS20B - Equilibrium relaxed for only $\sigma_x = x^3$, $\sigma_y = y^3$, and $\sigma_z = z^3$ term.
Symmetry Maintained.

RS20C - Equilibrium imposed in unsymmetric fashion.

RS20D - Equilibrium relaxed for both quadratic and cubic stress modes.
Symmetry Maintained.

RS20E - Alternate stress modes used to complete the stress assumption, 57 β's.
Equilibrium relaxed for all cubic stress modes.
Symmetry Maintained.

RS20F - Also an alternate form, 54 β's.
Equilibrium relaxed for all cubic stress modes.
Symmetry Maintained.

The analytical solution for the hollow sphere problem is obtained from Timoshenko and Goodier[18]. A comparison of the radial displacement distribution obtained by Elements DS20 and RS20A is shown in Figure 9.17. The results are both very accurate when compared with the analytical solution. Again for the tangental stress distribution result, Figure 9.18, both elements provide accurate solutions. This is expected since the rate of curvature change is slow for the tangental stress distribution. Thus the excitation of the higher order stress modes are correspondingly small.

The radial stress distribution provide high enough rate of curvature change to excite the higher order stress modes in order to distinguish each element performance. The Figure 9.19 compares the radial stress distributions obtained from the assumed displacement element, DS20, and

the hybrid element, RS20A. In general, a significant disparity of results, exemplified in Figure 9.19, between $\overline{\Pi}_P$ and $\overline{\Pi}_H$ element will be observed for any problem with stress distribution that has a high rate of curvature change. In another words, when the quadratic stress modes are excited disparity between the two formulation will arise. Above remark is a simple extension of bending problem, linear mode excitation, using 8-node solid element.

The radial stress distribution comparison between hybrid elements with various other stress assumptions are shown in Figures 9.20 to 9.23. The results indicate that the equilibrium can be relaxed for all cubic stress modes and the symmetry condition should be maintained. Also, the elements RS20A, RS20E, and RS20F gave almost identical stress distributions. Overall, the hollow sphere problem numerically supports the discussions on the previous sections.

9.7 CANTILEVERED BEAM USING 20-NODE SOLID ELEMENTS

In a recent article by Spilker and Singh[19], a hybrid element with complete cubic assumed stress distribution satisfying both equilibrium and compatibility conditions is presented. This element is named RS20G (refer to Appendix B). An example given is a cantilevered beam problem with distributed end shear loading. The normal and shear stress distribution results are given in Figures 9.24 and 9.25, respectively. The results from all three elements, DS20, RS20A, and RS20G, are comparable as expected from previous beam bending analysis.

The purpose for constructing the Element RS20G, by Spilker and Singh, is to implement element invariance with respect to the reference coordinate. The invariance is accomplished by expanding the stress into full cubic distribution. The stress compatibility condition had to be used to reduce the number of β's to 69. This is compared to 54 β's used for the Element RS20A.

Under a close examination, several severe limitations on the Element RS20G restrict its applicability. First, the element is limited to isotropic material only. Also, excessive computational cost prohibit practical application. Uncoupled stress formulation cannot be used to reduce cost since 51 constraints are necessary to reduce full cubic, 120 β's, to 69 β's. A lesson learned from this example is to use local coordinate system to achieve element invariance.

9.8 HU-WASHIZU ELEMENT EVALUATION

In order to numerically compare the difference in the solution between π_R and π_{HW} when the stress-strain relation is relaxed, two previous problems, given in the subsections 9.6 and 9.7, are solved using similar P matrix. The elements used are 20-node solid elements RS20A and HS20A (Appendix B).

For the cantilevered beam problem, the tip deflection results are given in Table 9.6.

TABLE 9.6. Tip deflection of cantilevered beam.

# of Elements in the mesh	π_P , DS20	π_R, RS20A	π_{HW}, HS20A
1	$-.956\times10^{-2}$	-1.05×10^{-2}	-1.05×10^{-2}
2	-1.08	-1.09	-1.09
4	-1.10	-1.11	-1.11

$\delta_{analytical} = -1.132\times10^{-2}$ (Transverse shear included)

Also the shear stress results between RS20A and HS20A are identical up to 3 digits. Figure 9.26 demonstrates this graphically. The reason the results between RS20A and HS20A are similar is that the cantilevered beam problem has a linear distribution in the normal stress and a constant distribution in the shear stress. In comparison of the stress assumptions for these two elements, Appendix

B, showes that for the constant and linear terms, the equivalence conditions are identically satisfied.

The previous discussion on the Hu-Washizu formulation asserted that the stress-strain relation can only be relaxed for the cubic "nonsense" stress modes. To illustrate the consequence when the stress-strain relation is also relaxed for the quadratic modes, the hollow sphere problem is solved using Element HS20A. Recall that the condition required to satisfy the stress-strain relation constrains the $\underset{\sim}{P}_i$'s to be equal. The Figure 9.27 clearly demonstrates the difference between the two formulations. Since the stress-strain relation for the quadratic terms for Element HS20A are not satisfied, the result is poor.

9.9 CPU TIME FOR STIFFNESS MATRIX GENERATION OF 8-NODE SOLID ELEMENTS

To justify the use of the hybrid elements for practical industrial application, normalized CPU time for stiffness matrix generation of 8-node solid elements are provided in Table 9.7.

TABLE 9.7. Normalized CPU time for stiffness matrix generation of 8-node solid elements.

DS8 - Assumed Displacement Method	1
RS8A - Original Hybrid Stress Method	1.62
RUS8A - Uncoupled Stress Method	0.96
RUS8C - Uncoupled Stress Method	0.60

Note that all three hybrid elements, RS8A, RUS8A, and RUS8C, provide exact pure bending behavior. Thus by using the flexibility allowed in the uncoupled stress method, the economic roadblock on the hybrid elements can be easily bypassed.

10. SPECIAL PURPOSE ELEMENTS

The special purpose elements, as differentiated from the general purpose elements, are tailored for a restricted class of problems. By restriction, the convergence using the special purpose elements can be significantly increased. The aim of the present discussion is to direct future research in the special purpose elements.

In the previous sections, much emphasis is placed on the examination of both displacement and stress modes in conjunction. The resulting combinations that satisfy the governing equations establish the accuracy of each element. If the exact mode is included in the assumed modes, only a single element is necessary to obtain the exact solution. If otherwise, the convergence depends on the ability of a linear combination of modes to approximate the solution.

Inevitably, the next generation of elements will involve a joint effort of theoretical solid mechanics and finite element strategy. Expanding, as Wilson attempted to purposely insert bending modes, the modes obtained from analytical means will be implemented into the assumed modes. Observe that the displacement and stress modes obtained analytically for a sepecific problem satisfy the governing equations a priori. Furthermore, for a similar class of problems, this mode will be highly excited.

Overall, above technique simulates the Eigenmode expansion and series expansion used for many years to solve structural problems for the finite element method.

The desirability is established and thus the next question is the feasibility. To begin with, the use of the hybrid formulation provides a convenient method to implement any desired modes. By examining, step by step, the construction of hybrid element, the only roadblock present is the numerical integration of the elementary functions such as the trigonometric and exponential functions. A brute force solution is integrating each term analytically. A tremendous amount of necessary algebra should be done using an algebraic manipulator. Other solutions will be found as the research evolve in the development of special purpose elements.

11. CONCLUSION

The key to unlocking the mystery of the Hybrid stress formulation is to understand the interaction of the assumed displacement and stress distribution. Using the isoparametric method as the basis for the assumed displacement, a consistent stress distribution can be obtained. In practical engineering applications, each element is employed to cover a "finite" domain. Therefore, the mathematical proofs on convergence, derived on the assumption of the limiting process, have only restricted practicality. The bridge to fill the gap between mathematical abstraction and practical reality of finite element method is the application of the physics involved in continuum mechanics. In this context, all of the painstaking development of analytical solution can be applied in the finite element method. Recognize that the finite element method is a numerical method operating on the parameters provided through the assumed variable distributions.

In the discussion of general purpose elements, the Statement of Equivalence convey that if the assumed displacement, obtained through isoparametric formulation, is complete to order P, then the Hybrid and the assumed displacement element stress accuracy is equivalent to order (P-1). The actual superiority of the hybrid element will be visible for the problems requiring the stress

modes represented in the order P. This is demonstrated by constant stress problem verses cantilever beam problem for 8-node solid element (P=1).

In sum, the most attractive attribute of the hybrid stress formulation has not been yet fully exploited. The flexibility to easily include assumed modes obtained through analytical methods differentiates hybrid elements from the assumed displacement elements. Always remember that flexibility is an attribute when applied with understanding.

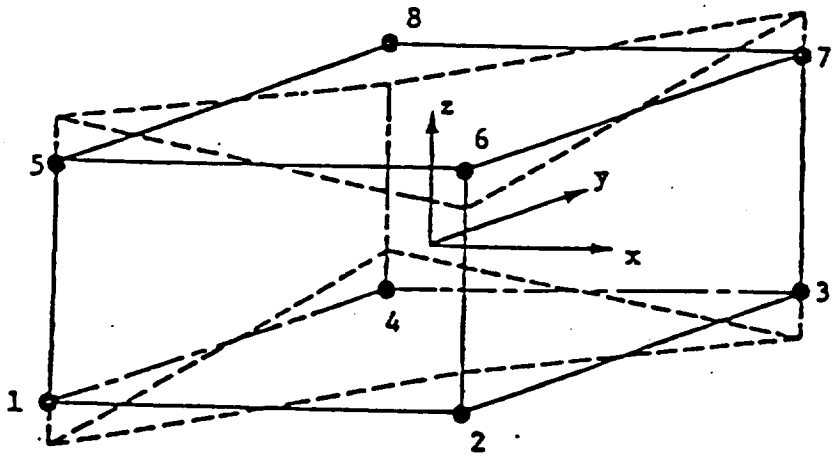

FIGURE 6.1 Possible deflection mode for 8-node solid requiring a "nonsense" stress term (in this case $\sigma_z = xy$) to prevent such a zero-energy deformation mode [15].

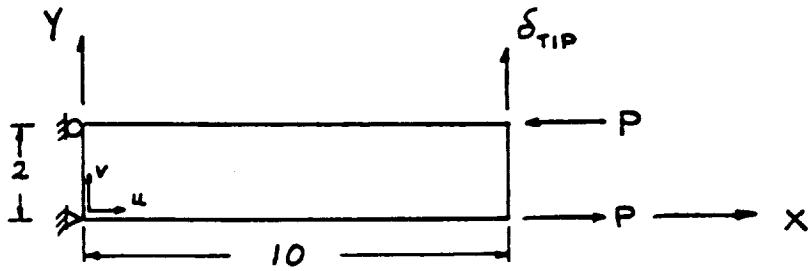

u=0

u=v=0

P = 1000

E = 10^7

ν = 0

FIGURE 9.1 Cantilever beam using single 4-node plane stress element.

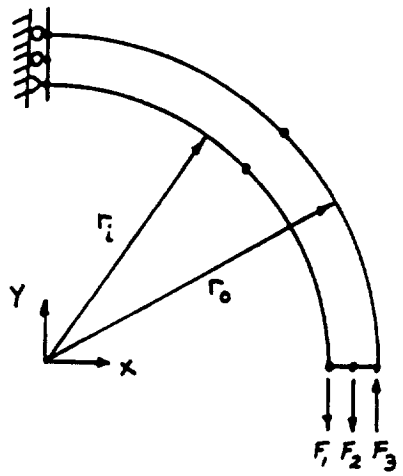

$E = 10^7$ $\qquad$ $r_o = 12$

$\nu = .3$ $\qquad$ $r_i = 10$

$F_1 = 270.3$

$F_2 = 56.3$ $\qquad$ Total Moment = 600

$F_3 = 326.6$

MESH 1 = 16 DOF (1 element)

MESH 2 = 26 (2 elements)

MESH 3 = 36 (3 elements)

MESH 4 = 46 (4 elements)

MESH 5 = 56 (5 elements)

FIGURE 9.2 Curved cantilevered beam using 8-node plane stress elements.

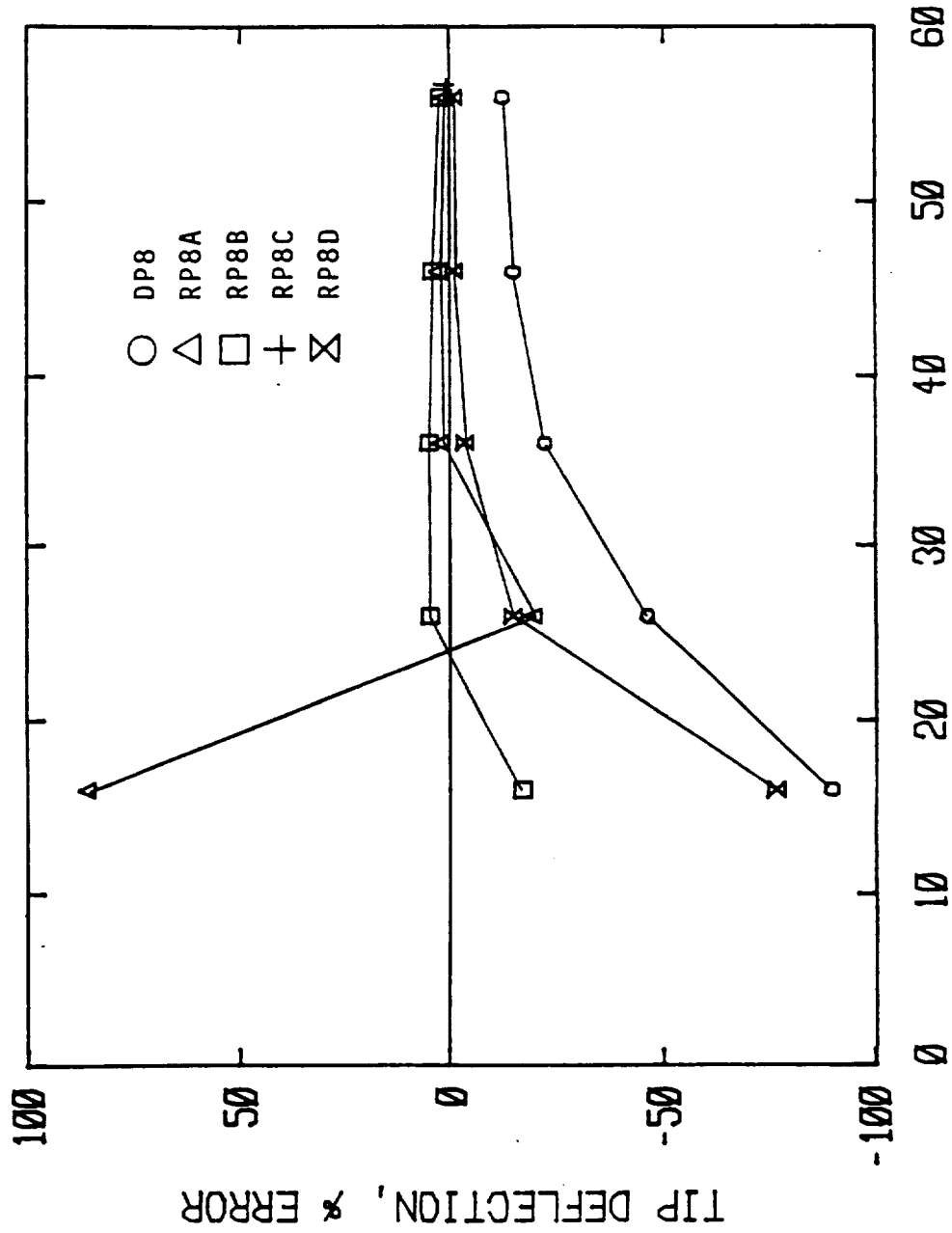

FIGURE 9.3 Tip deflection for curved beam.

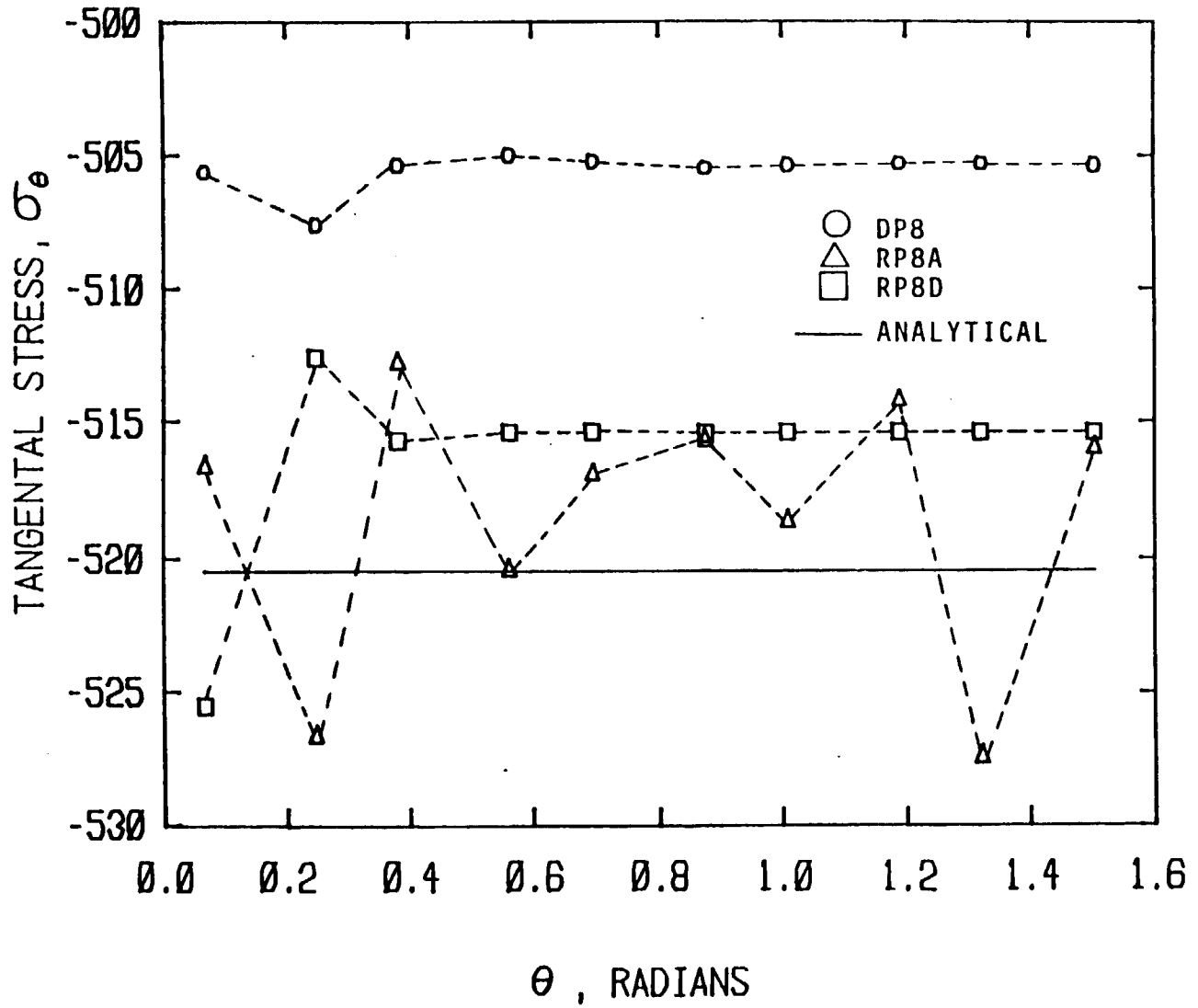

FIGURE 9.4 Tangental stress at optimal stress points, r=11.34, for 5 element mesh curved beam.

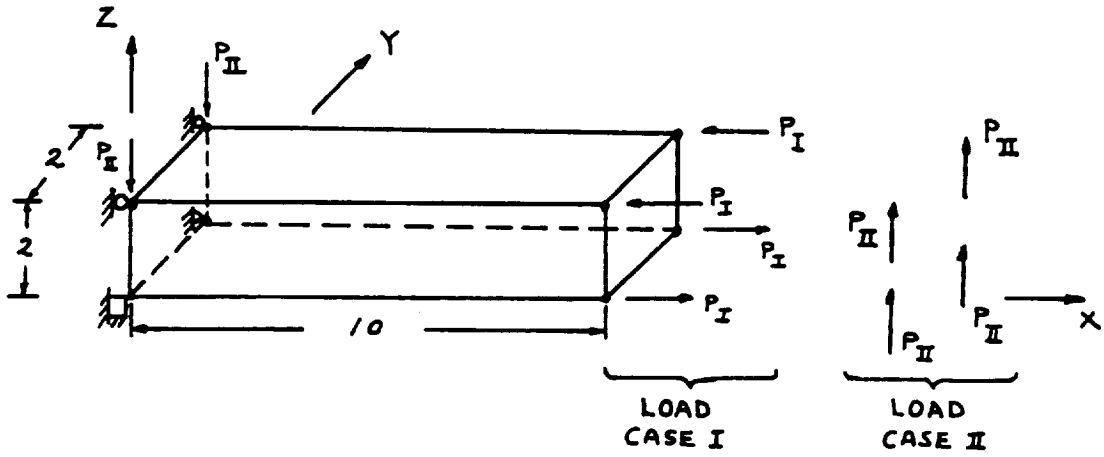

$P_I = 1000$

$P_{II} = 150$

u=0

u=w=0

u=v=w=0

E = 1500

$\nu = 0.25$

FIGURE 9.5 Cantilever beam using 8-node solid elements.
(Single element mesh - MESH 1)

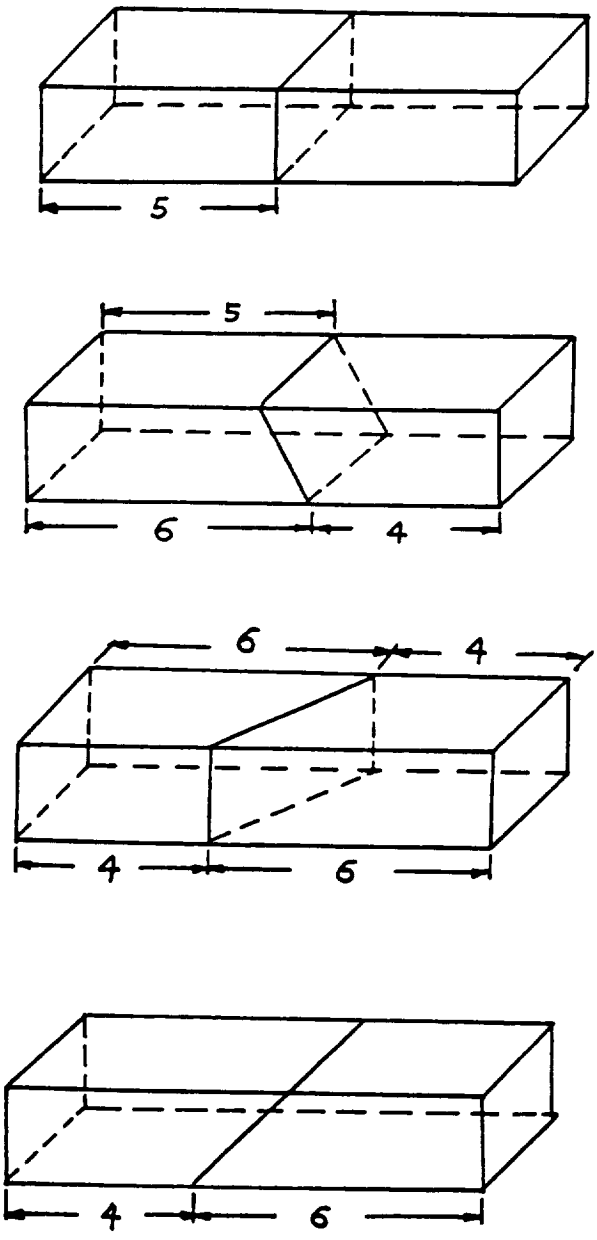

FIGURE 9.6 Two element mesh arrangements.

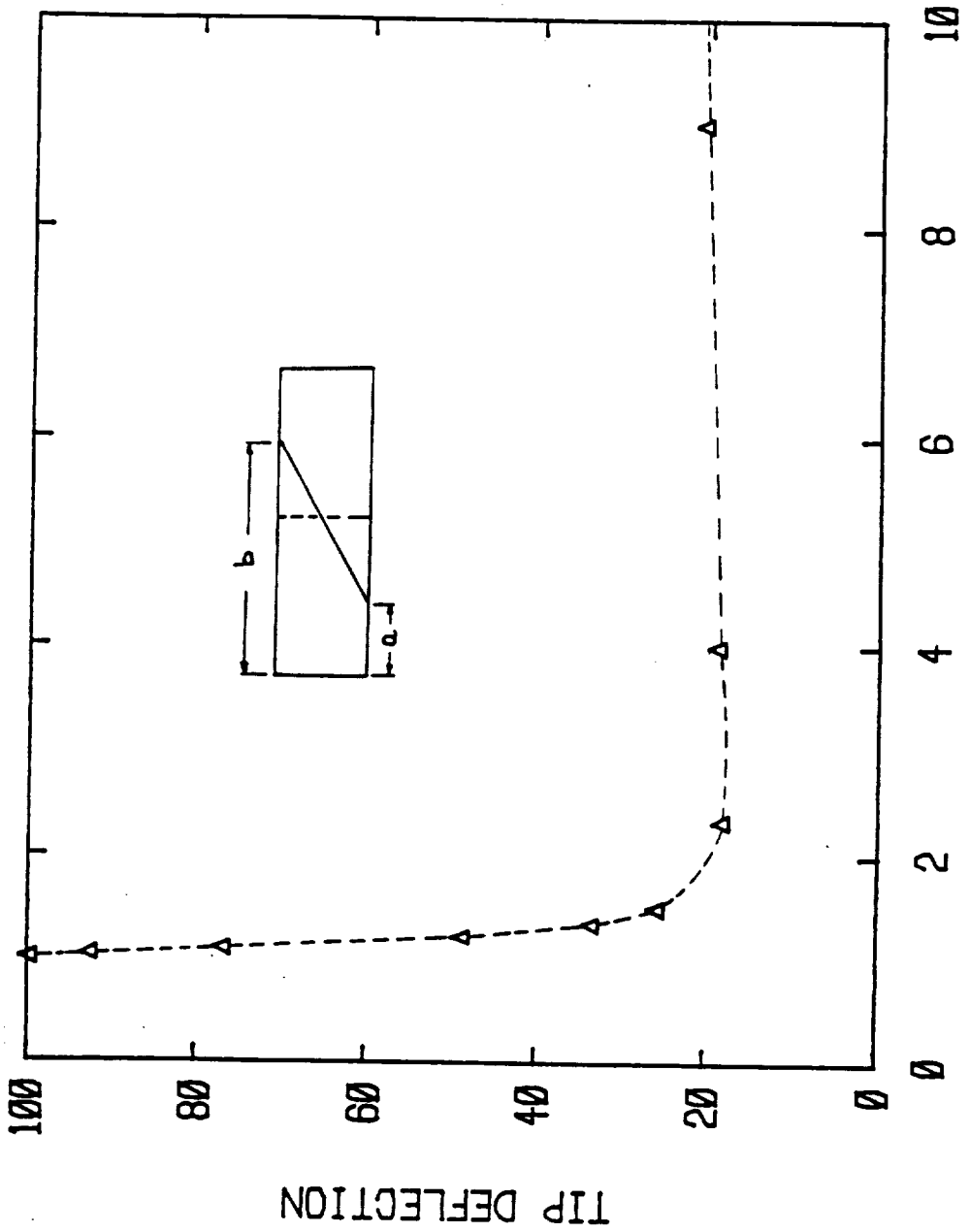

FIGURE 9.7 Distortion sensitivity of ELEMENT RUSBA.

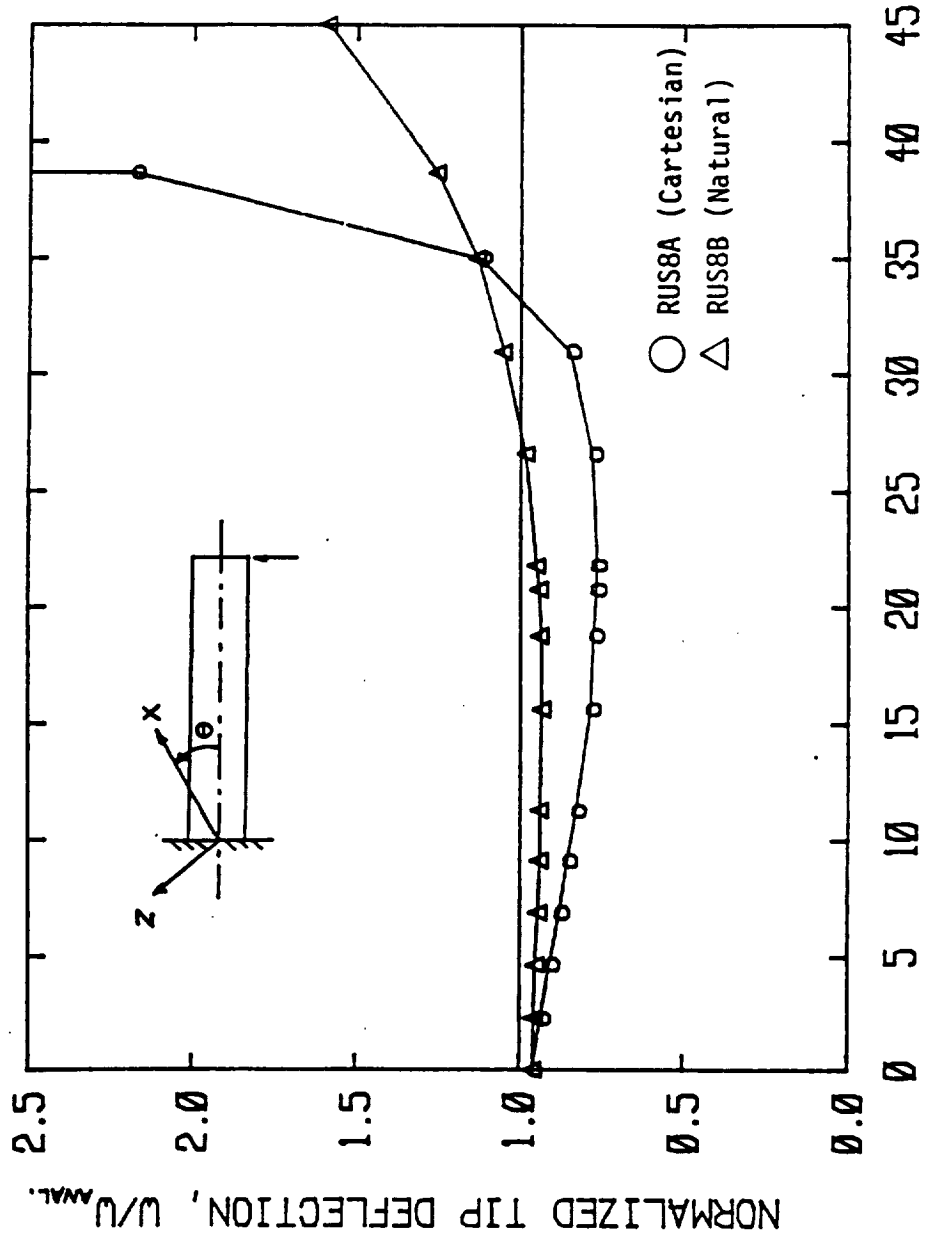

FIGURE 9.8 Deflection of cantilever beam under concentrated tip load as the reference coordinates are rotated.

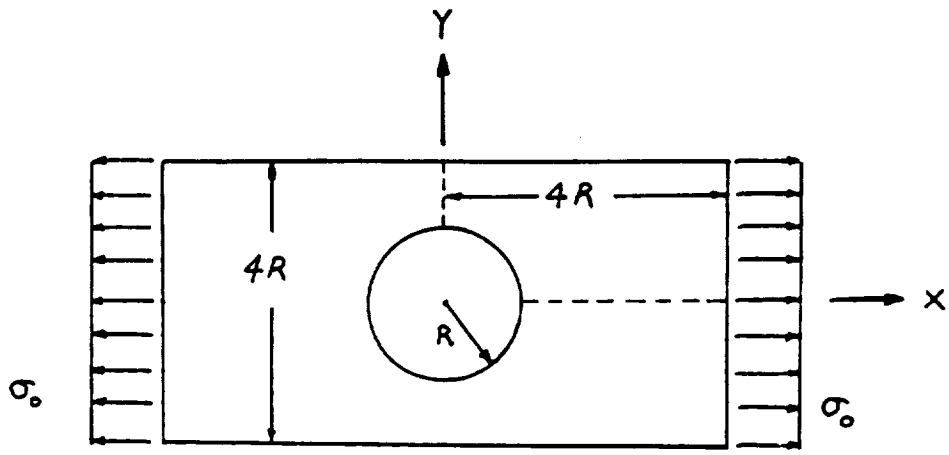

R = 1

σ_o = 1000

FIGURE 9.9 Circular hole in an infinite strip.

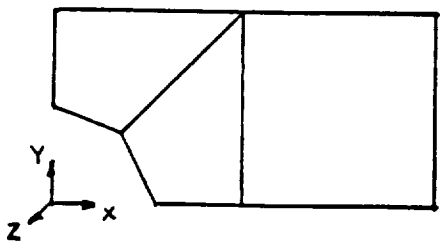

MESH 1

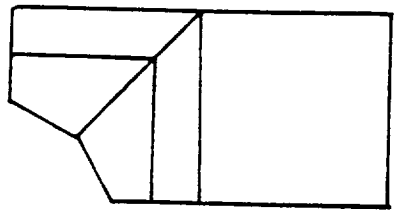

MESH 2

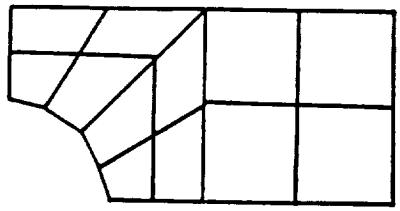

MESH 3

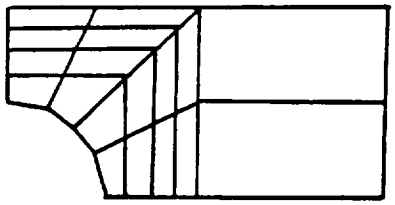

MESH 4

FIGURE 9.10 Plane view of the mesh configurations.

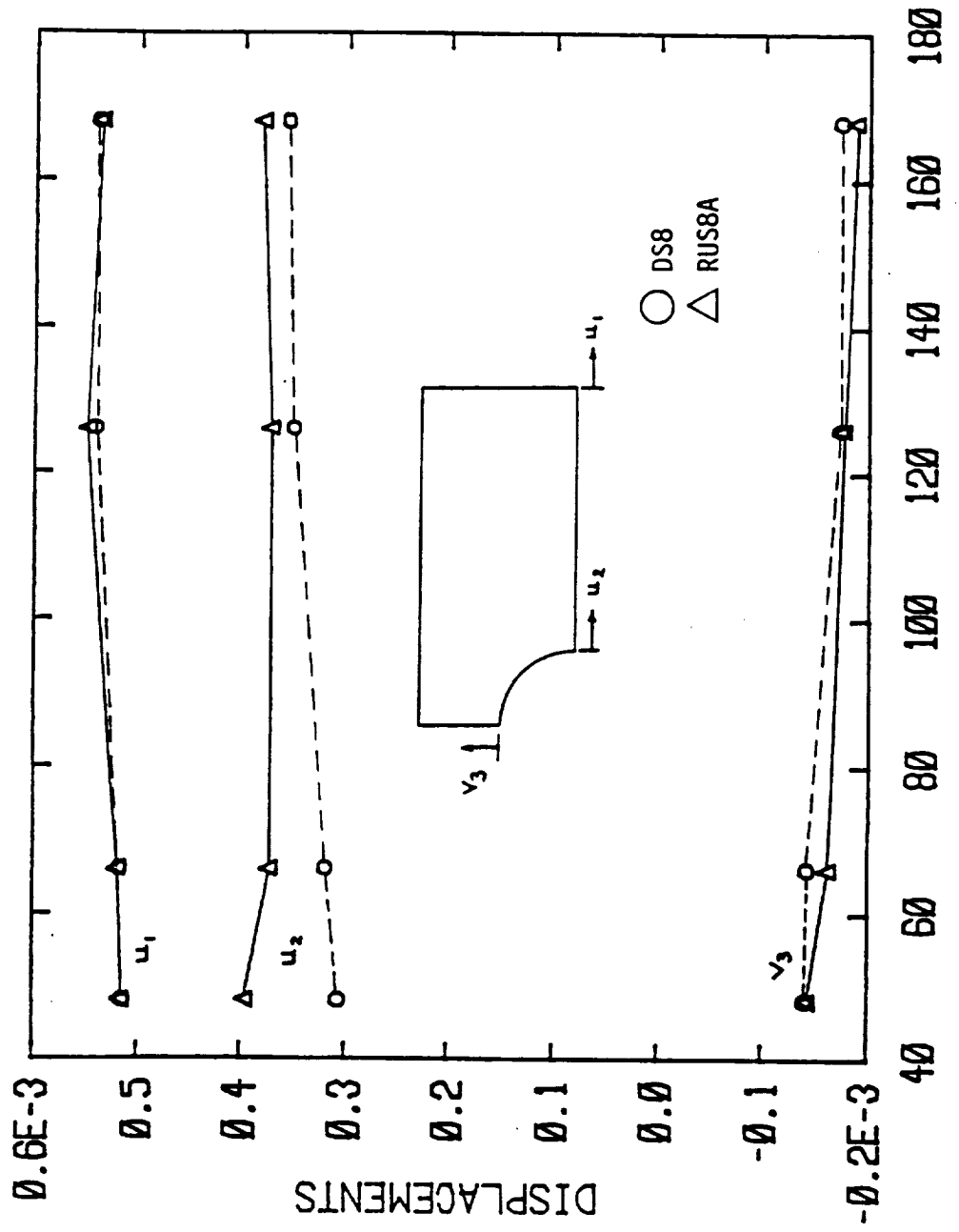

FIGURE 9.11 Displacement convergence results.

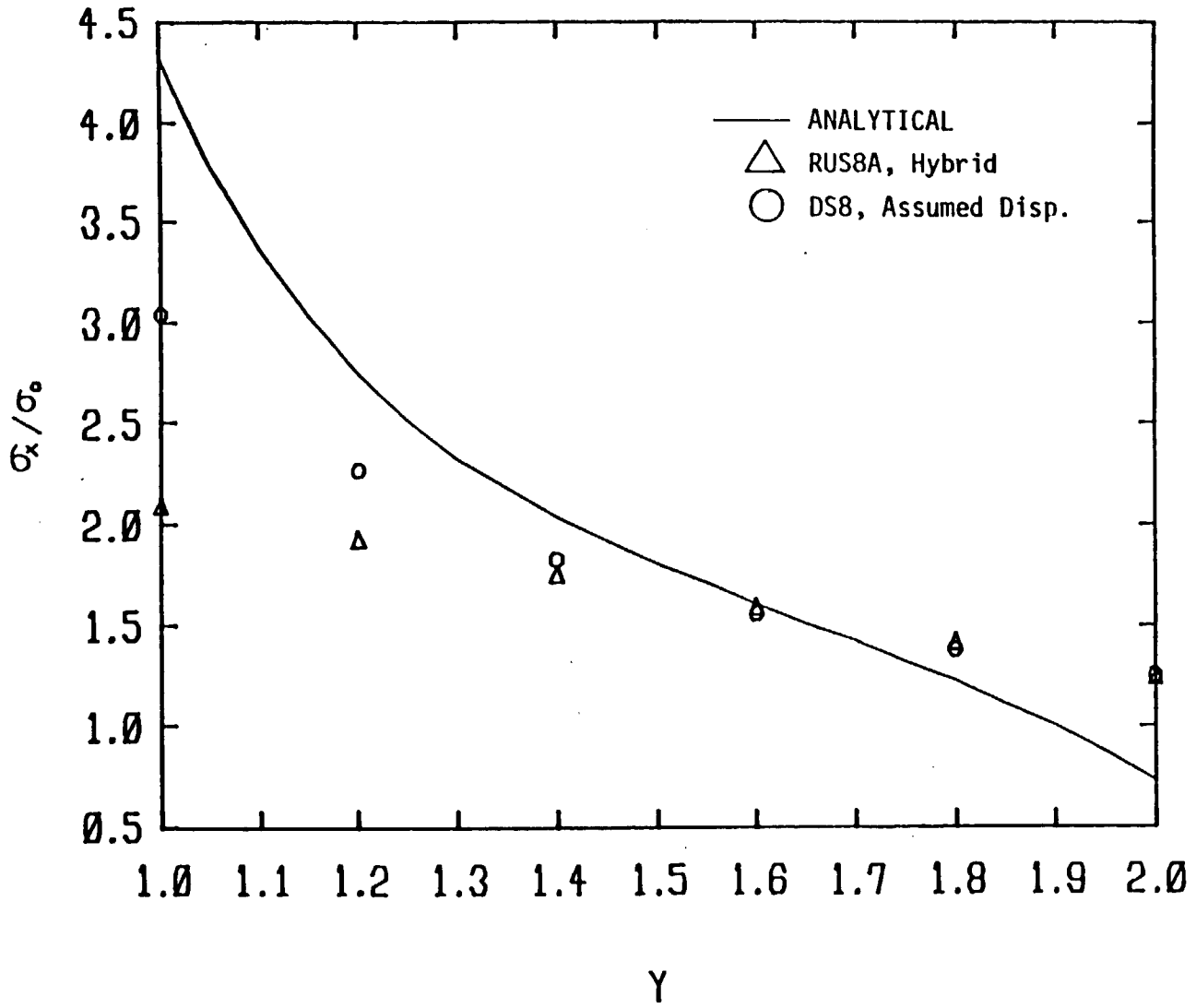

FIGURE 9.12 Stress distribution along x=0, MESH 1.

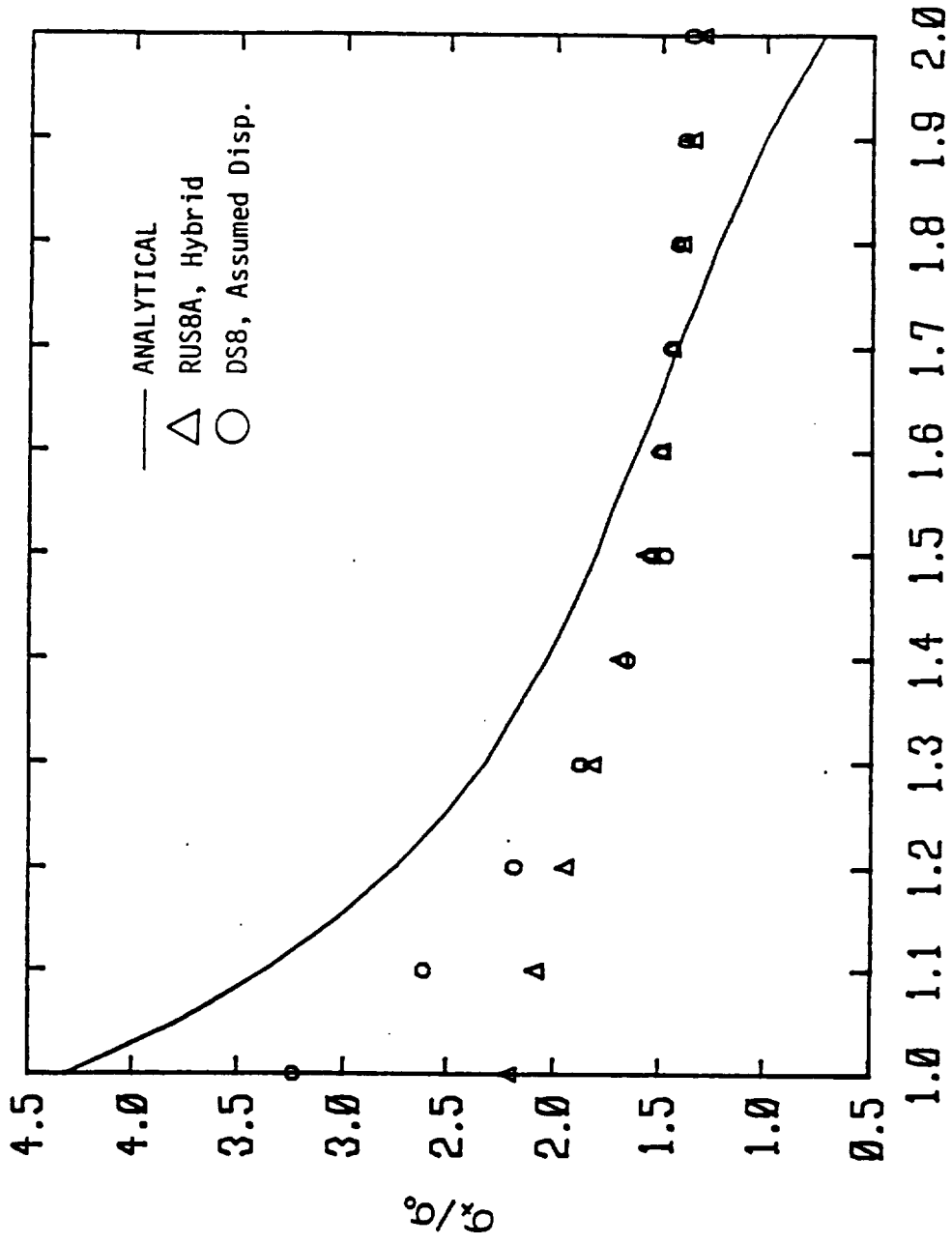

FIGURE 9.13 Stress distribution along x=0, MESH 2.

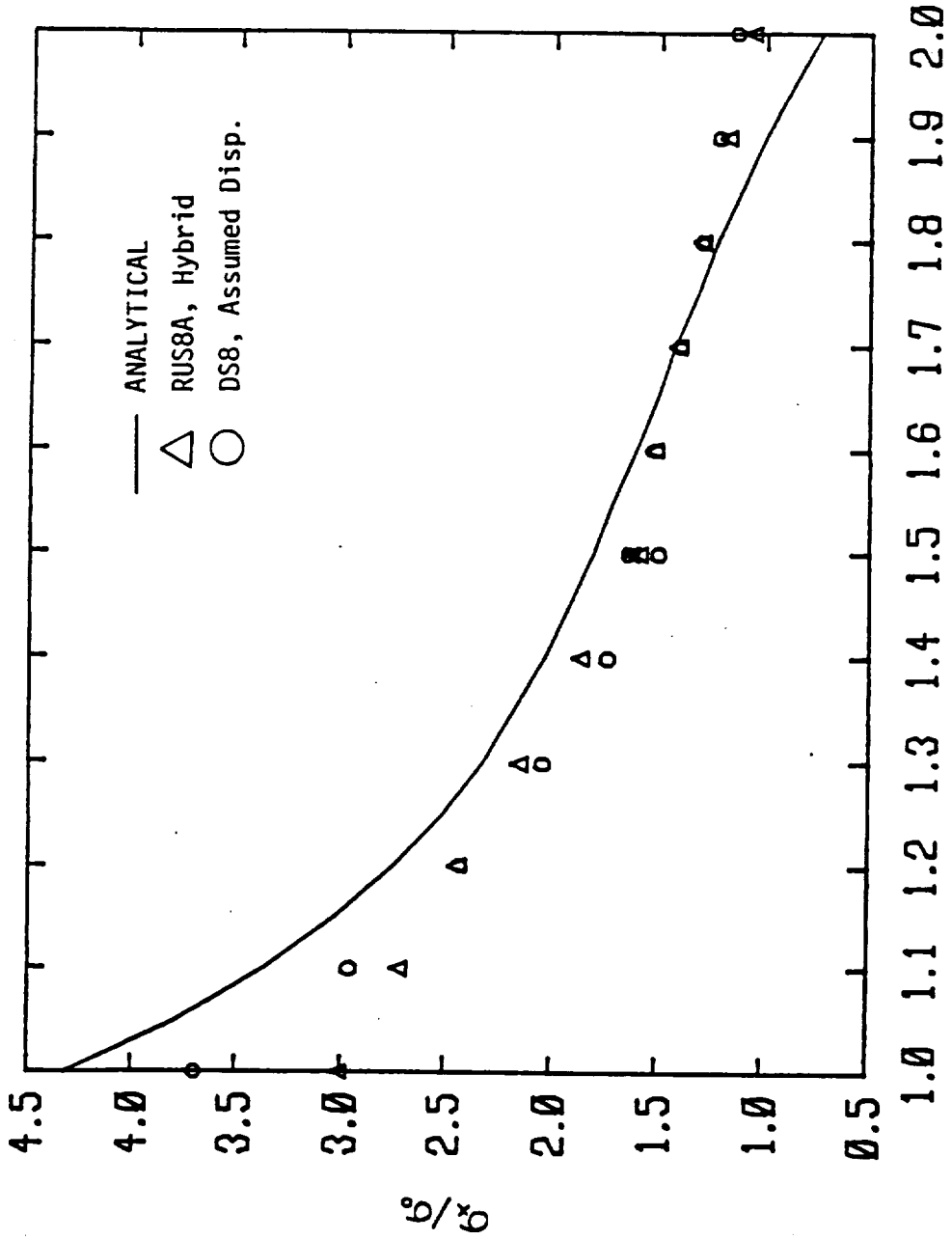

FIGURE 9.14 Stress distribution along x=0, MESH 3.

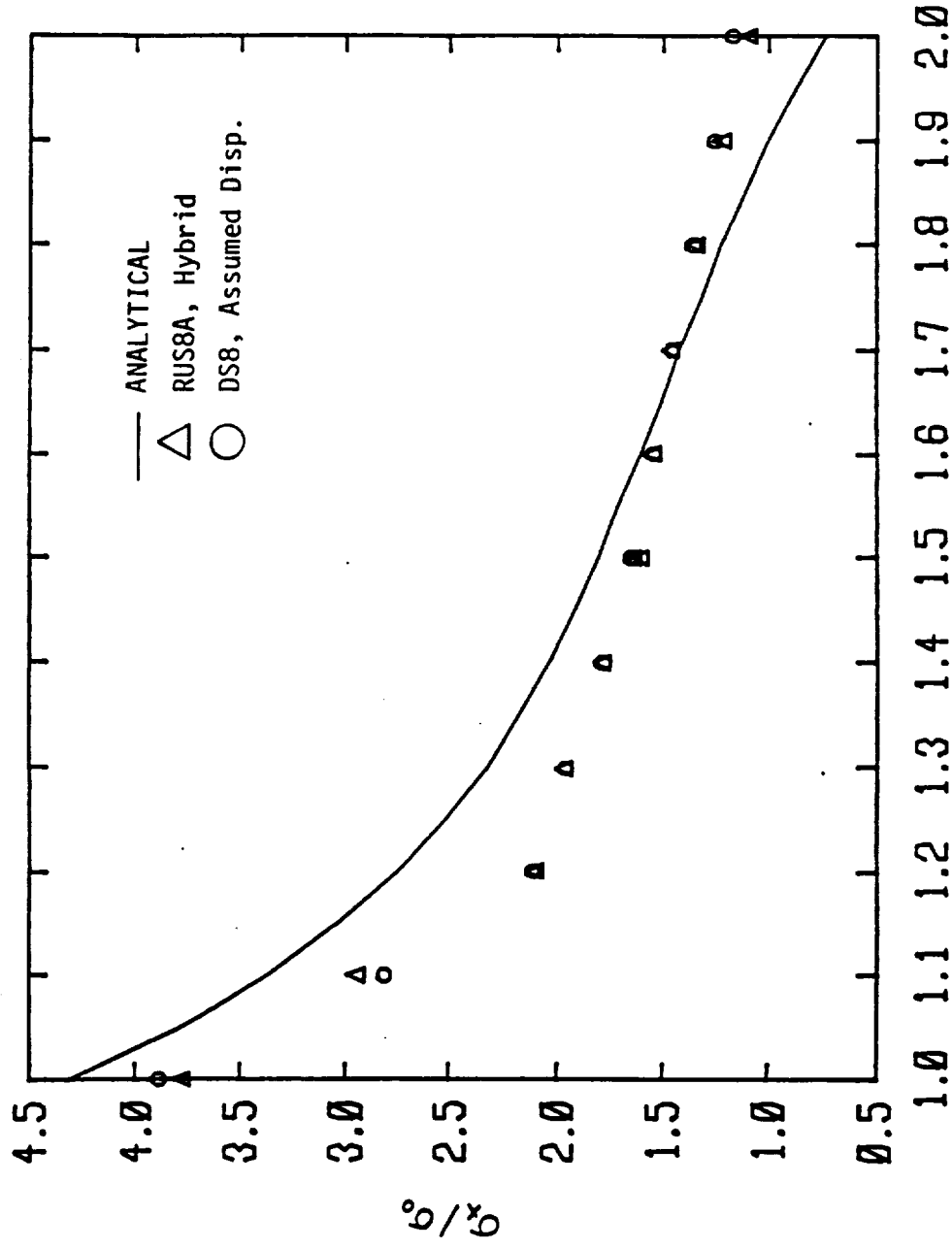

FIGURE 9.15 Stress distribution along x=0, MESH 4.

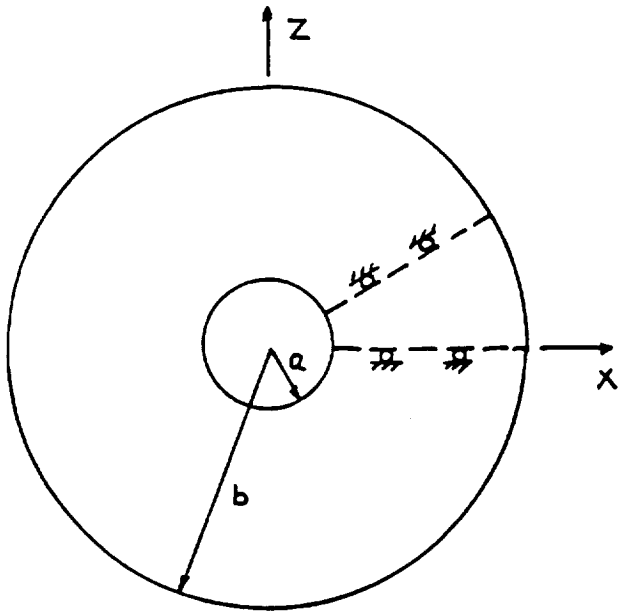

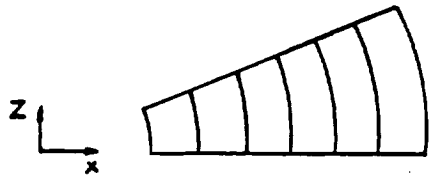

6-ELEMENT MESH

TEMPERATURE DISTRIBUTION

$$T = \frac{T_o\, a}{b-a}(b/R-1)$$

$a = 2$ cm.
$b = 8$ cm.
$T_o = 100^\circ$ C
$\alpha = 1.22\times10^{-5}/^\circ$C
$\nu = .3$
$E = 2.1\times10^{7}$ Nt/cm.^{2}

FIGURE 9.16 Hollow sphere under temperature distribution using 20-node solid elements.

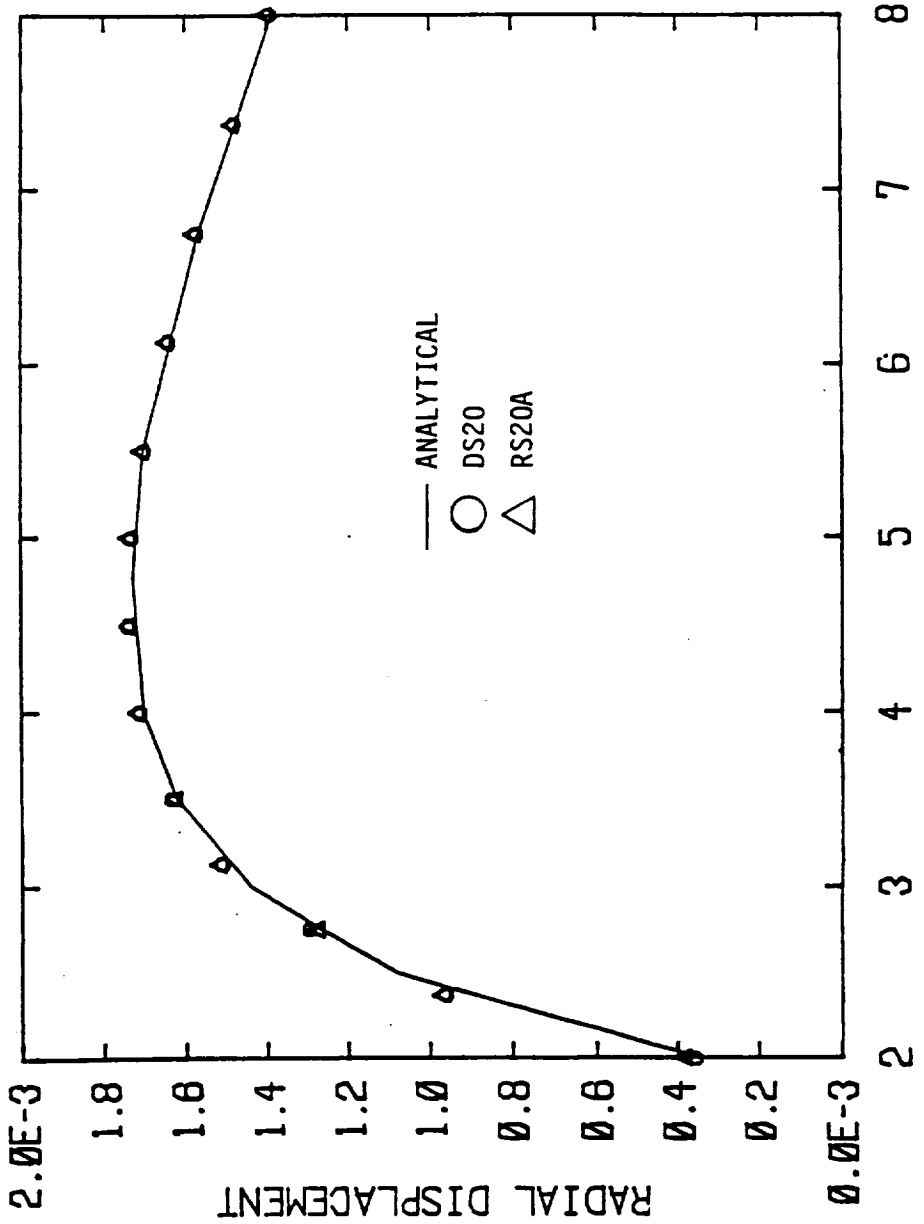

FIGURE 9.17 Radial displacement distribution along the x-axis.

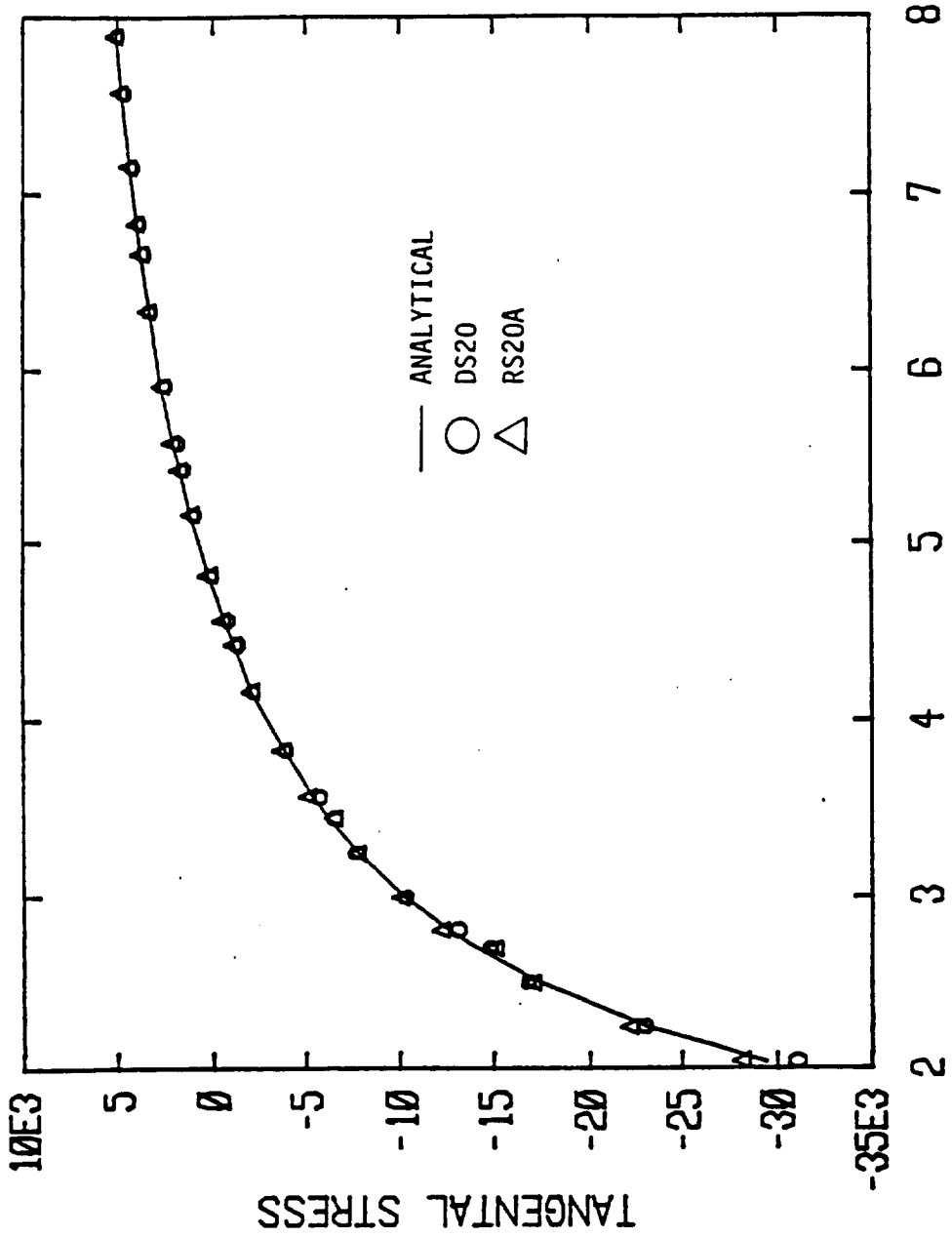

FIGURE 9.18 Tangental stress distribution.

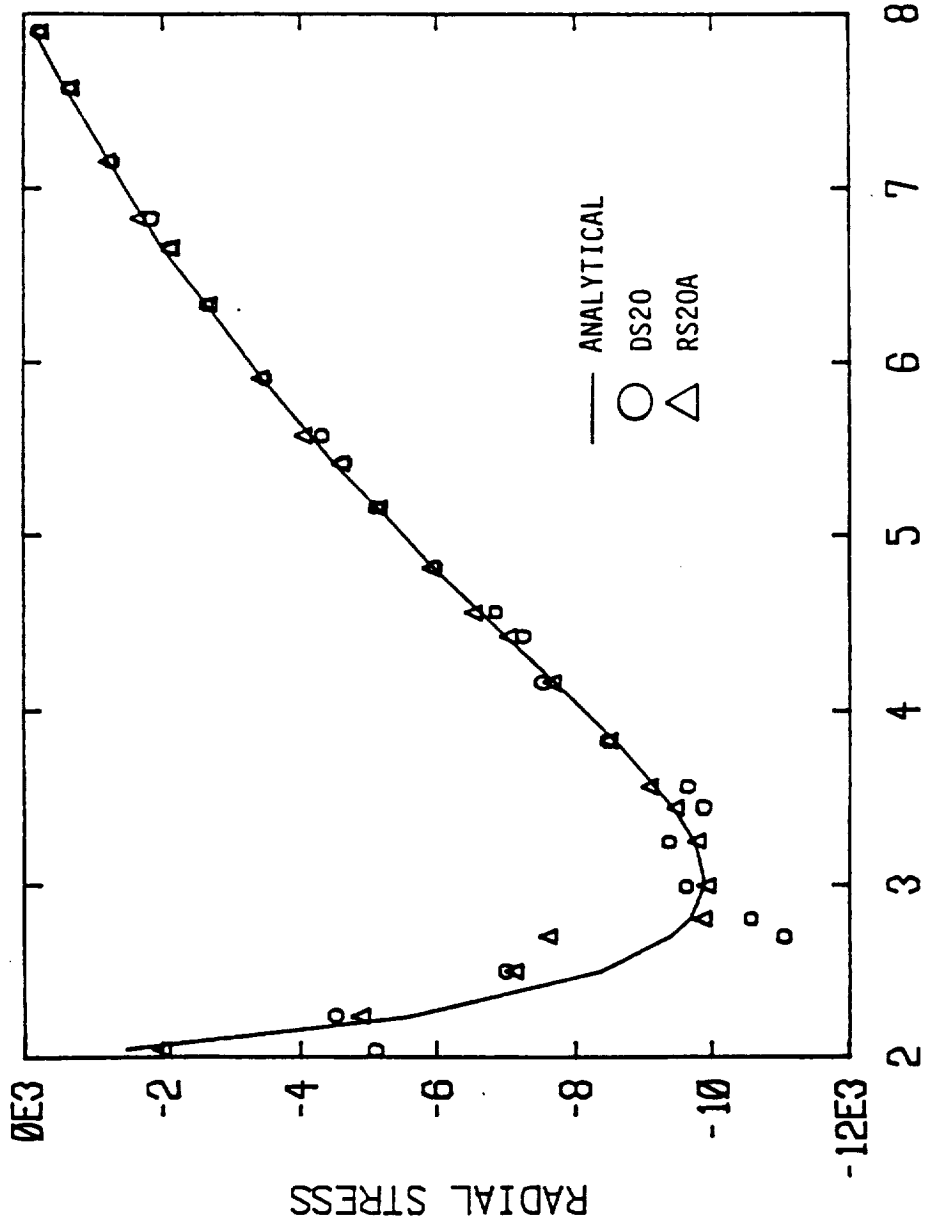

FIGURE 9.19 Radial stress distribution.

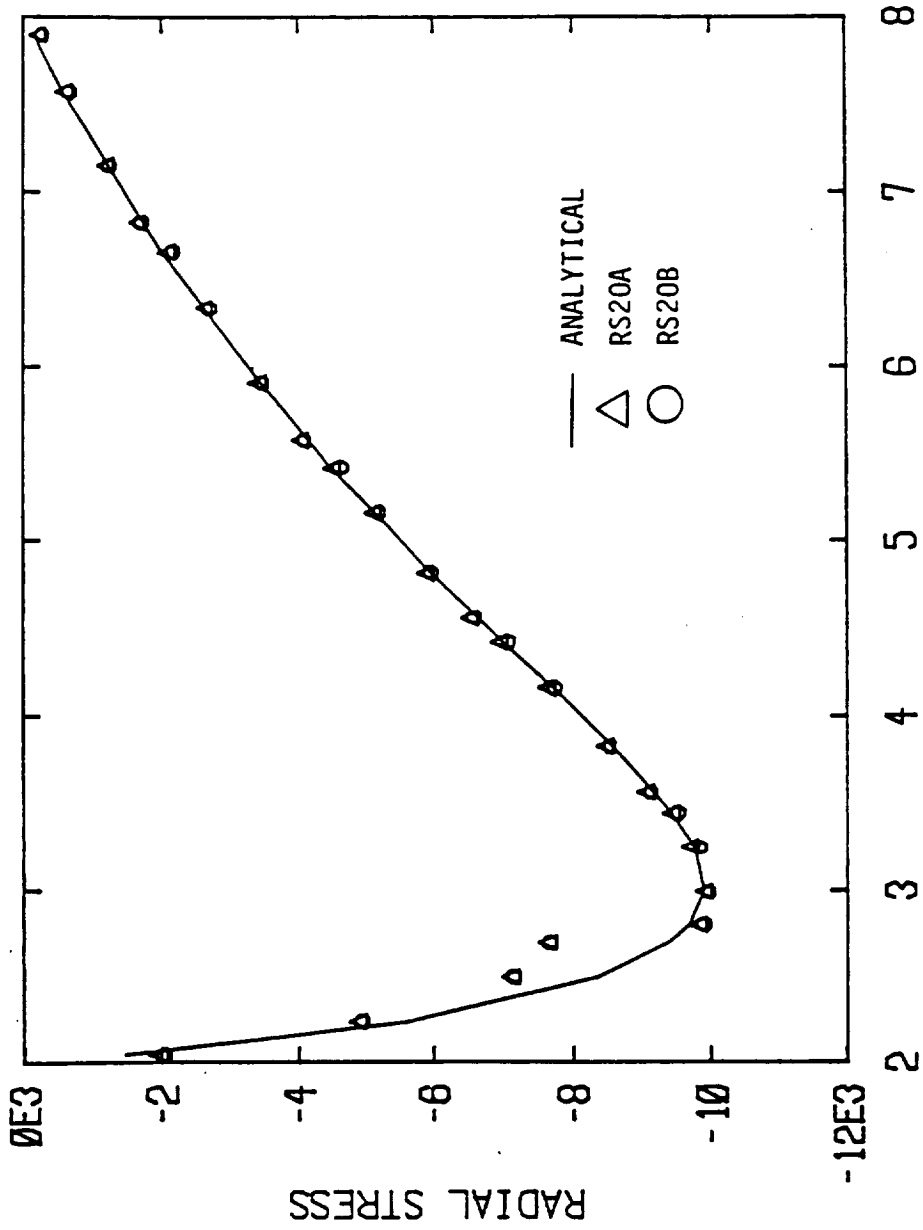

FIGURE 9.20 Radial stress distribution.

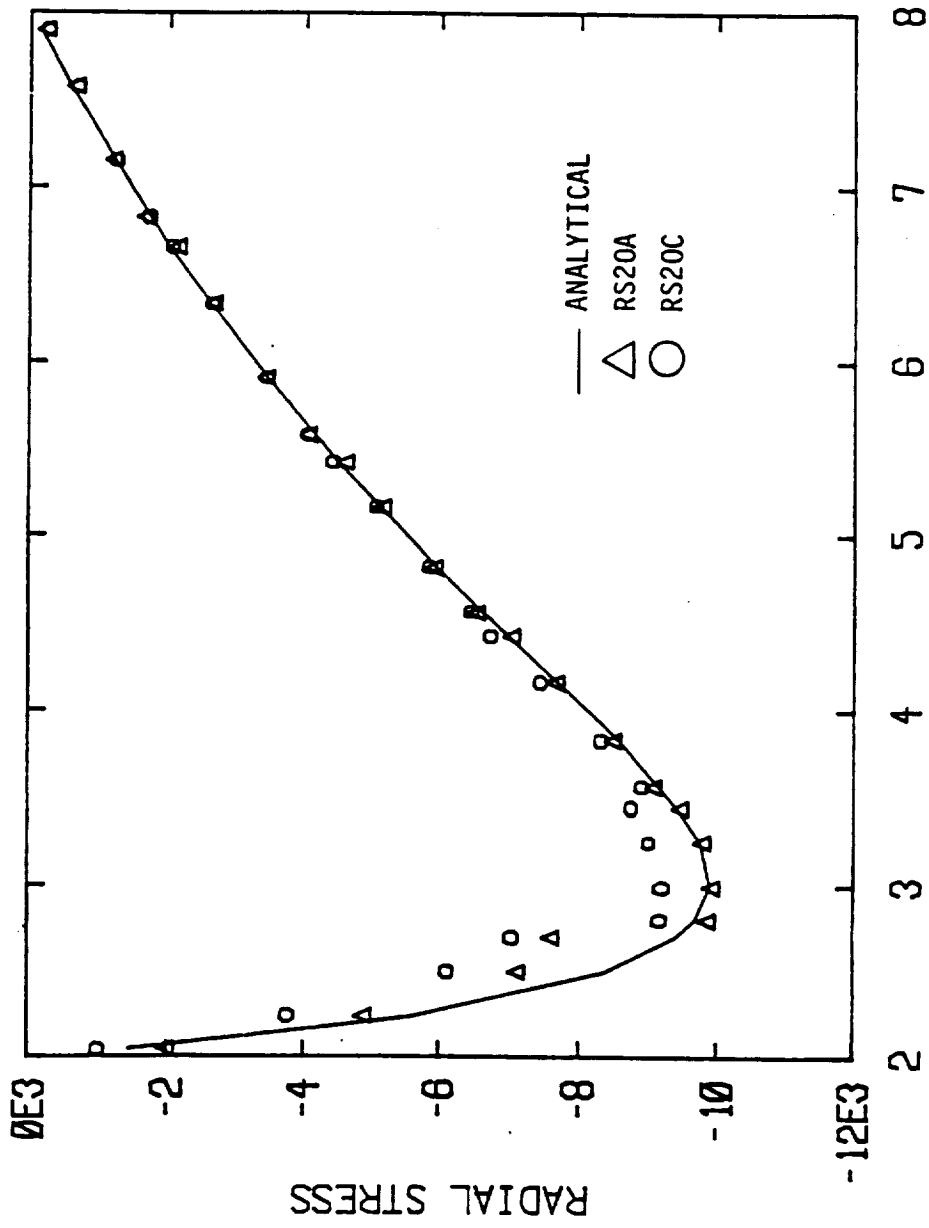

FIGURE 9.21 Radial stress distribution.

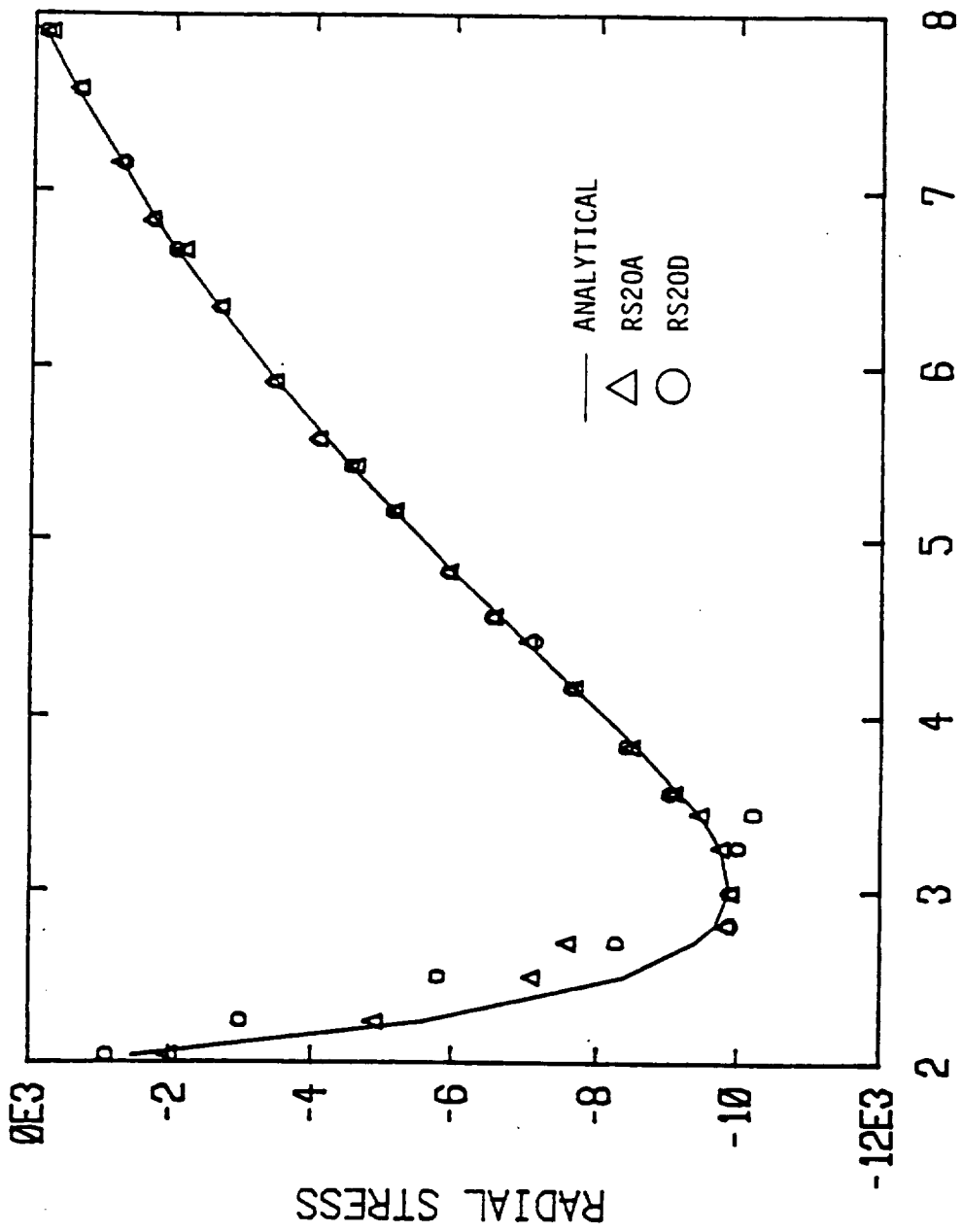

FIGURE 9.22 Radial stress distribution.

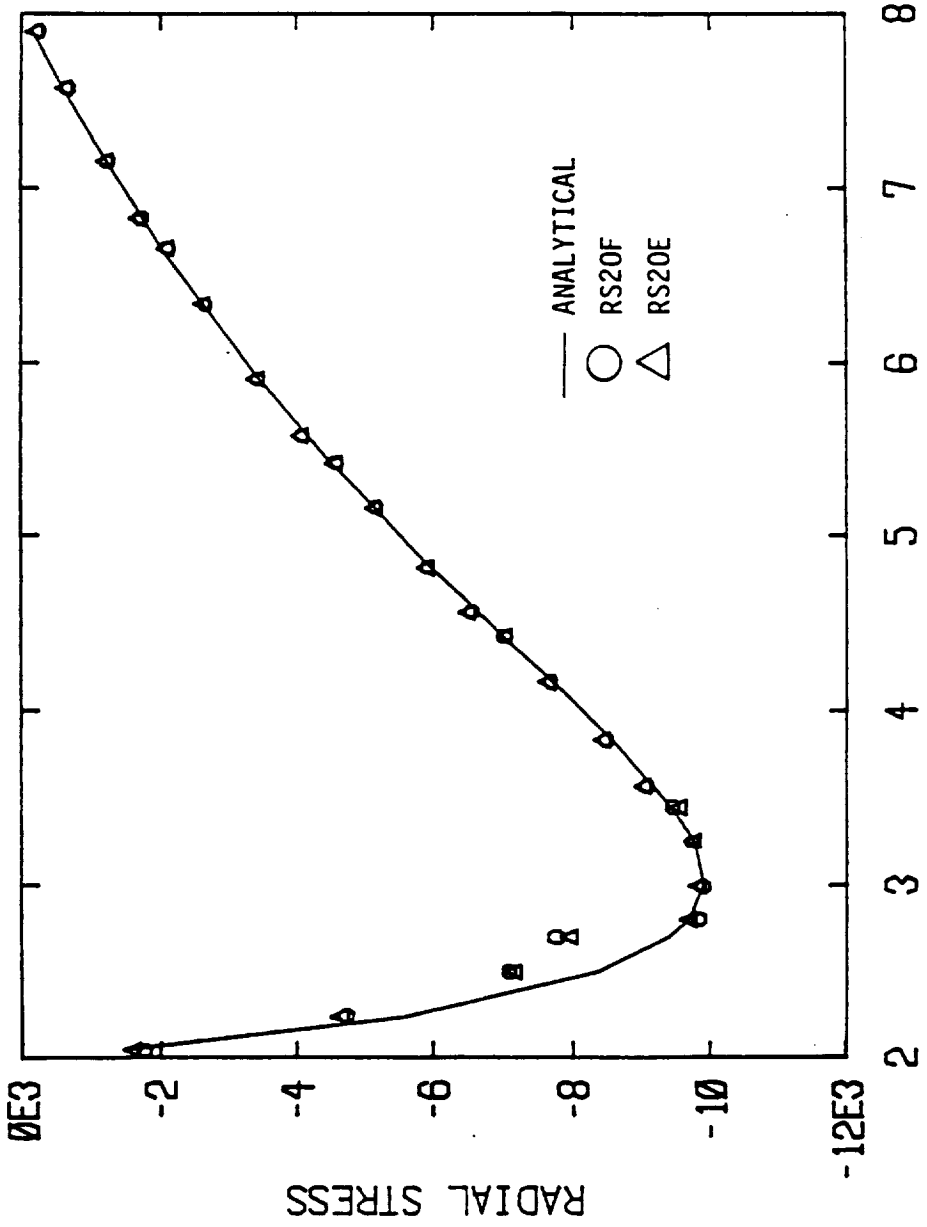

FIGURE 9.23 Radial stress distribution.

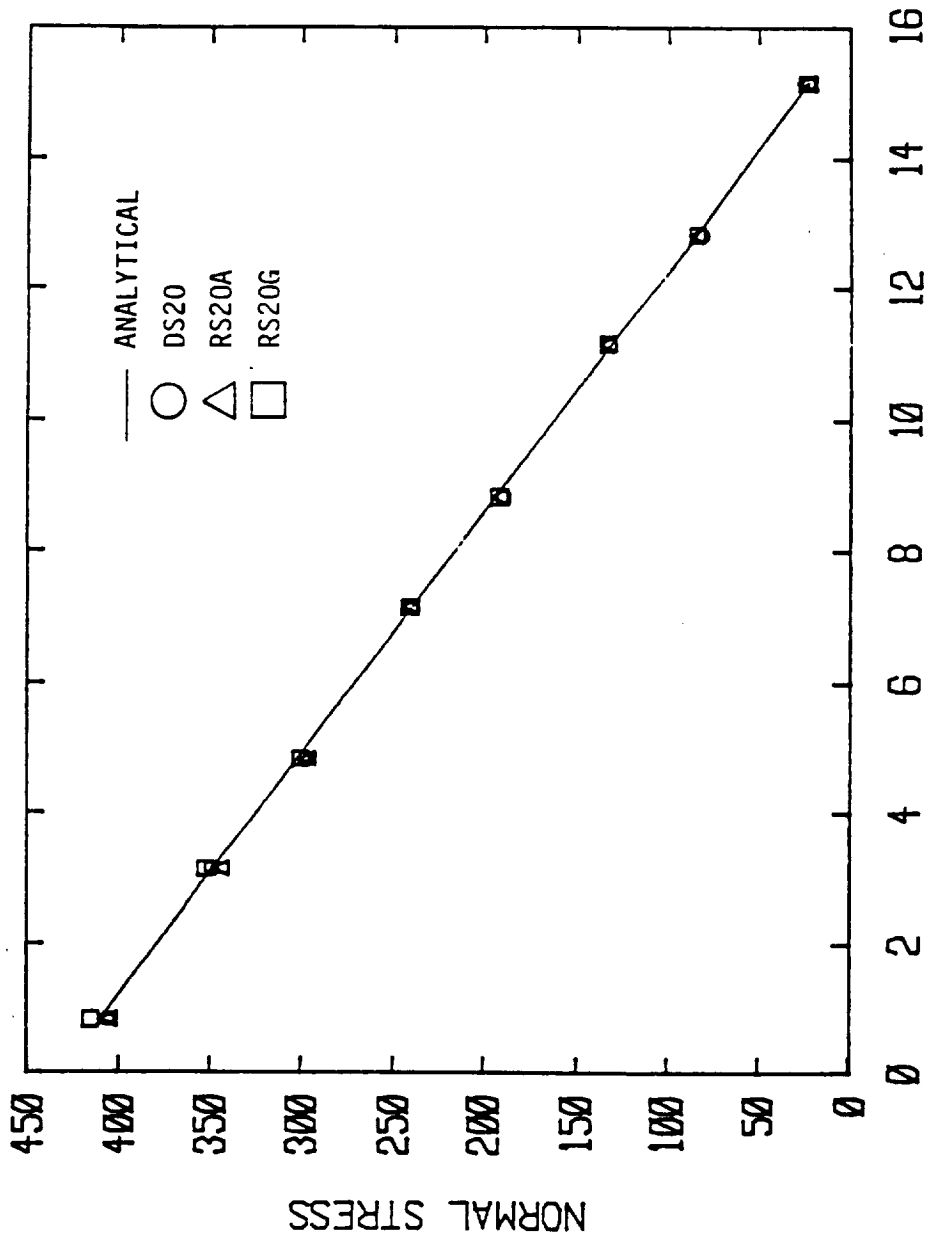

FIGURE 9.24 Cantilevered beam using 20-node solid elements.

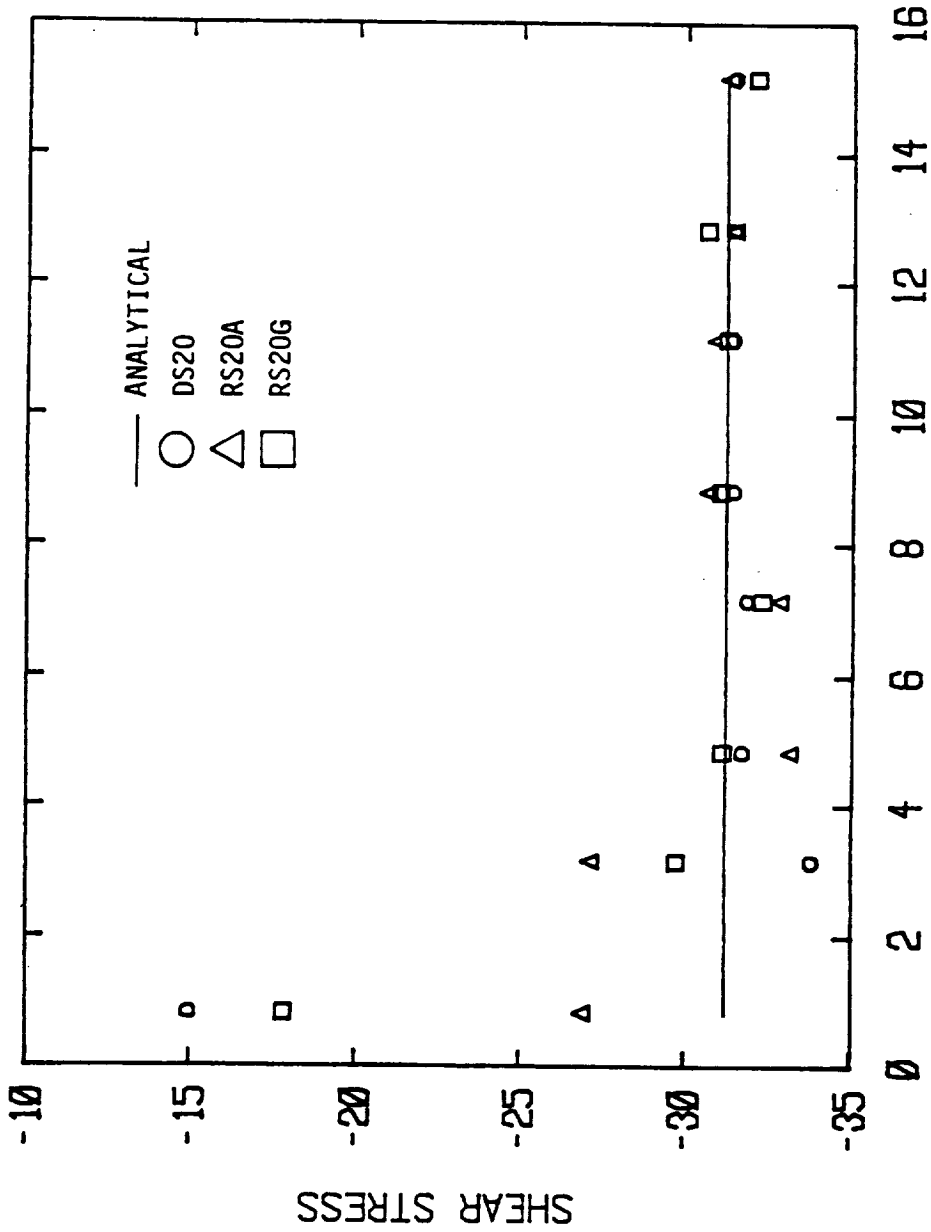

FIGURE 9.25 Cantilevered beam using 20-node solid elements.

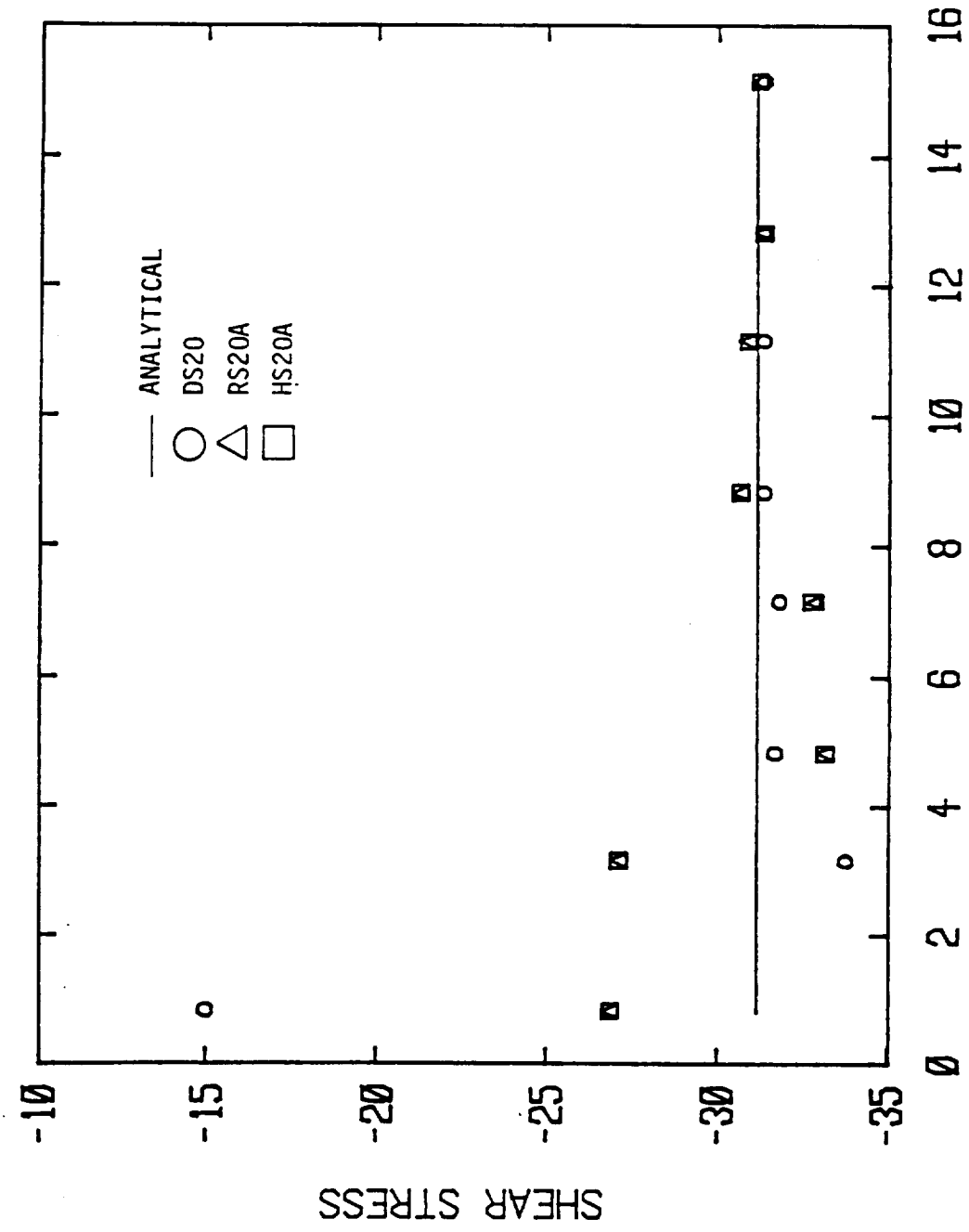

FIGURE 9.26 Cantilevered beam using 20-node solid elements.

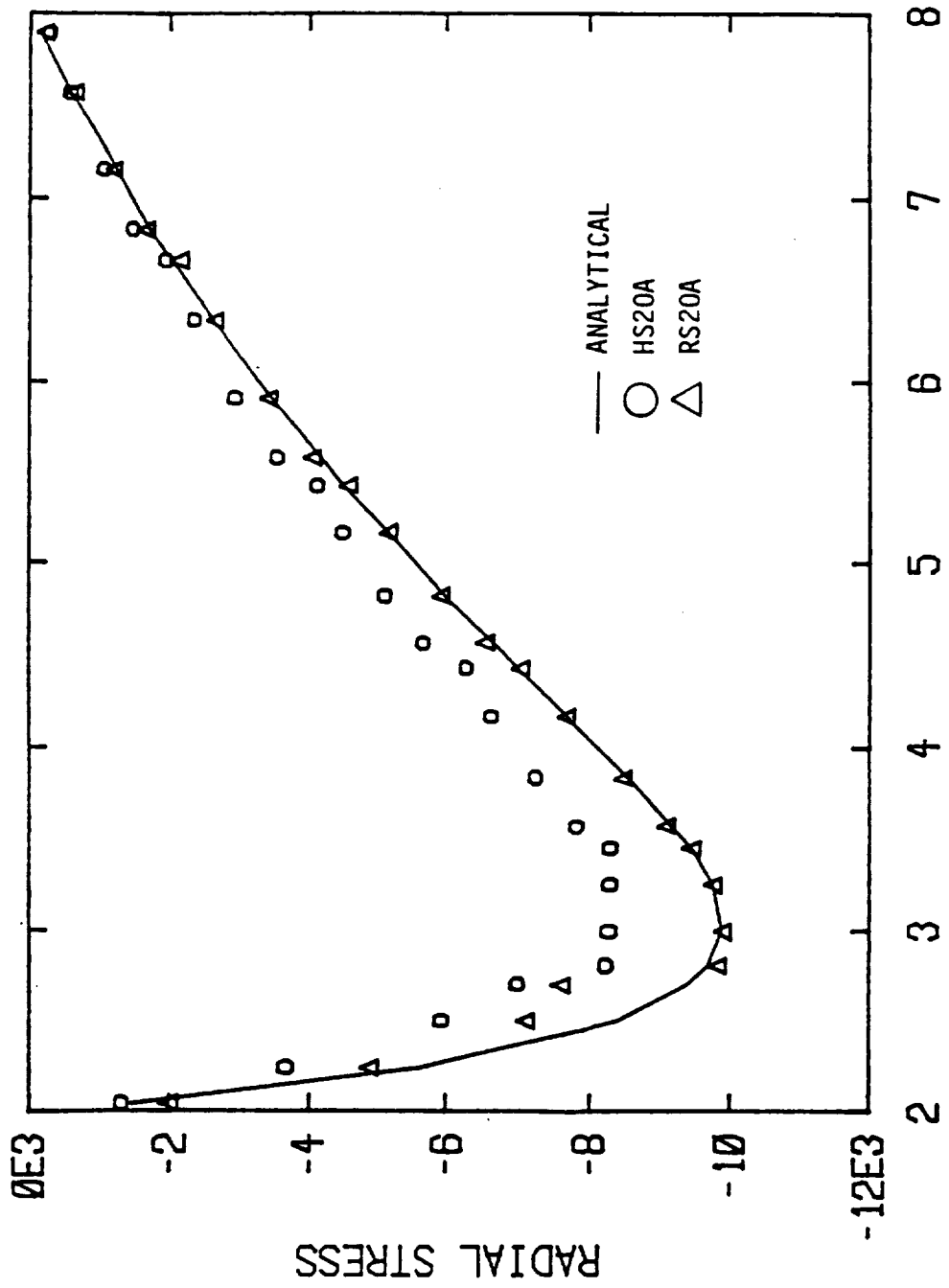

FIGURE 9.27 Hollow sphere under temperature distribution.

APPENDIX A

TABLE A1. Strain modes from assumed displacement modes.

ε_x	α_2	$\alpha_5 y$	$\alpha_7 z$	$2\alpha_8 x$	$2\alpha_{11} xy$	$2\alpha_{12} xz$	$\alpha_{14} y^2$
ε_y	α_{23}						
ε_z	α_{44}						
γ_{xy}	$\alpha_3 + \alpha_{22}$	$\alpha_5 x$			$\alpha_{11} x^2$		$2\alpha_{14} yx$
γ_{yz}	$\alpha_{24} + \alpha_{43}$						
γ_{xz}	$\alpha_4 + \alpha_{42}$		$\alpha_7 x$			$\alpha_{12} x^2$	

$\alpha_{15} z^2$	$\alpha_{17} yz$	$2\alpha_{18} xyz$	$\alpha_{19} y^2 z$	$\alpha_{20} z^2 y$			
					$\alpha_{25} x$	$\alpha_{26} z$	$2\alpha_{29} y$
	$\alpha_{17} xz$	$\alpha_{18} x^2 z$	$2\alpha_{19} xyz$	$\alpha_{20} z^2 x$	$\alpha_{25} y$		
						$\alpha_{26} y$	
$2\alpha_{15} xz$	$\alpha_{17} xy$	$\alpha_{18} x^2 y$	$\alpha_{19} y^2 x$	$2\alpha_{20} xyz$			

$\alpha_{31} x^2$	$2\alpha_{33} yz$	$2\alpha_{34} yx$	$\alpha_{36} z^2$	$\alpha_{37} xz$	$\alpha_{38} x^2 z$	$2\alpha_{39} xyz$	$\alpha_{40} z^2 x$
$2\alpha_{31} xy$		$\alpha_{34} y^2$		$\alpha_{37} yz$	$2\alpha_{38} xyz$	$\alpha_{39} y^2 z$	$\alpha_{40} z^2 y$
	$\alpha_{33} y^2$		$2\alpha_{36} yz$	$\alpha_{37} xy$	$\alpha_{38} x^2 y$	$\alpha_{39} y^2 x$	$2\alpha_{40} xyz$

$\alpha_{46} y$	$\alpha_{47} x$	$2\alpha_{50} z$	$\alpha_{52} x^2$	$\alpha_{53} y^2$	$2\alpha_{55} xz$	$2\alpha_{56} yz$	$\alpha_{57} xy$
$\alpha_{46} z$				$2\alpha_{53} yz$		$\alpha_{56} z^2$	$\alpha_{57} xz$
	$\alpha_{47} z$		$2\alpha_{52} xz$		$\alpha_{55} z^2$		$\alpha_{57} yz$

TABLE A1. Continued.

ε_x							
ε_y							
ε_z	$\alpha_{58} x^2 y$	$\alpha_{59} y^2 x$	$2\alpha_{60} xyz$				
γ_{xy}				$\alpha_6 z$	$2\alpha_9 y$	$2\alpha_{13} yz$	$\alpha_{16} z^2$
γ_{yz}	$\alpha_{58} x^2 z$	$2\alpha_{59} xyz$	$\alpha_{60} z^2 x$				
γ_{xz}	$2\alpha_{58} xyz$	$\alpha_{59} y^2 z$	$\alpha_{60} z^2 y$	$\alpha_6 y$		$\alpha_{13} y^2$	$2\alpha_{16} yz$

$\alpha_{27} z$	$2\alpha_{28} x$	$2\alpha_{32} xz$	$\alpha_{35} z^2$				
$\alpha_{27} x$		$\alpha_{32} x^2$	$2\alpha_{35} xz$	$2\alpha_{30} z$	$\alpha_{45} x$	$2\alpha_{49} y$	$\alpha_{51} x^2$
					$\alpha_{45} y$		$2\alpha_{51} xy$

$2\alpha_{54} yx$							
$\alpha_{54} y^2$	$2\alpha_{10} z$	$2\alpha_{48} x$					

TABLE A2. After elimination of the Artificial Coupling.

	σ_x	σ_y	σ_z	σ_{xy}	σ_{yz}	σ_{zx}
CONST.	β_1	β_2	β_3	β_4	β_5	β_6
X	β_7	β_8	β_9	β_{10}	β_{11}	β_{12}
Y	β_{13}	β_{14}	β_{15}	β_{16}	β_{17}	β_{18}
Z	β_{19}	β_{20}	β_{21}	β_{22}	β_{23}	β_{24}
XY	β_{25}	β_{26}	β_{27}	β_{28}	β_{29}	β_{30}
YZ	β_{31}	β_{32}	β_{33}	β_{34}	β_{35}	β_{36}
XZ	β_{37}	β_{38}	β_{39}	β_{40}	β_{41}	β_{42}
X^2		β_{43}	β_{44}	β_{45}	β_{46}	β_{47}
Y^2	β_{48}		β_{49}	β_{50}	β_{51}	β_{52}
Z^2	β_{53}	β_{54}		β_{55}	β_{56}	β_{57}
XYZ	β_{58}	β_{59}	β_{60}	β_{61}	β_{62}	β_{63}
XY^2			β_{70}		β_{71}	β_{72}
X^2Y			β_{64}		β_{65}	β_{66}
YZ^2	β_{79}			β_{80}		β_{81}
Y^2Z	β_{73}			β_{74}		β_{75}
XZ^2		β_{76}		β_{77}	β_{78}	
X^2Z		β_{67}		β_{68}	β_{69}	
X^3						
Y^3						
Z^3						

TABLE A3. Equilibrium applied.

	σ_x	σ_y	σ_z	σ_{xy}	σ_{yz}	σ_{zx}
CONST.	β_1	β_2	β_3	β_4	β_5	β_6
X	β_7	β_8	β_9	β_{10}	β_{11}	β_{12}
Y	β_{13}	β_{14}	β_{15}	β_{16}	β_{17}	β_{18}
Z	β_{19}	β_{20}	$-\beta_{12}-\beta_{17}$	β_{21}	$-\beta_{10}-\beta_{14}$	$-\beta_7-\beta_{16}$
XY	β_{22}	β_{23}	β_{24}		β_{25}	β_{26}
YZ	β_{27}	β_{28}	β_{29}	β_{30}		β_{31}
XZ	β_{32}	β_{33}	β_{34}	β_{35}	β_{36}	
X^2		β_{37}	β_{38}	$-\frac{\beta_{33}}{2}-\frac{\beta_{36}}{2}$	β_{39}	$-\frac{\beta_{35}}{2}-\frac{\beta_{34}}{2}$
Y^2	β_{40}		β_{41}	$-\frac{\beta_{32}}{2}-\frac{\beta_{31}}{2}$	$-\frac{\beta_{30}}{2}-\frac{\beta_{29}}{2}$	β_{42}
Z^2	β_{43}	β_{44}		β_{45}	$-\frac{\beta_{28}}{2}-\frac{\beta_{35}}{2}$	$-\frac{\beta_{30}}{2}-\frac{\beta_{32}}{2}$
XYZ	β_{46}	β_{47}	β_{48}			
XY^2			β_{53}		$-\frac{\beta_{48}}{2}-\beta_{50}$	
X^2Y			β_{49}			β_{50}
YZ^2	β_{57}					$-\frac{\beta_{46}}{2}-\beta_{55}$
Y^2Z	β_{54}			β_{55}		
XZ^2		β_{56}			$-\frac{\beta_{47}}{2}-\beta_{52}$	
X^2Z		β_{51}		β_{52}		
X^3						
Y^3						
Z^3						

When the Table A4 is compared to the Table A1, the stress modes β_{50}, β_{52}, and β_{55} are not present. Thus these modes are due to the process of decoupling the stress modes. Furthermore, the presence of β_{39}, β_{42}, and β_{45} are redundant and should be removed. In the final form of the stress assumption, Table A4, the equilibrium condition is relaxed for the cubic terms. Also for convenience, the numbering scheme has been changed. The x^3, y^3, and z^3 terms are chosen to eliminate the additional zero-energy deformation modes.

TABLE A4. Final form with equilibrium for cubic terms relaxed.

	σ_x	σ_y	σ_z	σ_{xy}	σ_{yz}	σ_{zx}
CONST.	β_1	β_2	β_3	β_4	β_5	β_6
X	$-\beta_{14}-\beta_{21}$	β_9	β_{11}	β_{13}	β_{16}	β_{19}
Y	β_7	$-\beta_{13}-\beta_{18}$	β_{12}	β_{14}	β_{17}	β_{20}
Z	β_8	β_{10}	$-\beta_{17}-\beta_{19}$	β_{15}	β_{18}	β_{21}
XY	β_{22}	β_{27}	β_{32}		β_{39}	β_{41}
YZ	β_{23}	β_{28}	β_{33}	β_{37}		β_{42}
XZ	β_{24}	β_{29}	β_{34}	β_{38}	β_{40}	
X^2		β_{30}	β_{35}	$-\frac{\beta_{27}}{2}-\frac{\beta_{40}}{2}$		$-\frac{\beta_{34}}{2}-\frac{\beta_{39}}{2}$
Y^2	β_{25}		β_{36}	$-\frac{\beta_{23}}{2}-\frac{\beta_{42}}{2}$	$-\frac{\beta_{33}}{2}-\frac{\beta_{41}}{2}$	
Z^2	β_{26}	β_{31}			$-\frac{\beta_{28}}{2}-\frac{\beta_{38}}{2}$	$-\frac{\beta_{24}}{2}-\frac{\beta_{37}}{2}$
XYZ	β_{49}	β_{50}	β_{51}			
XY^2			β_{47}			
X^2Y			β_{48}			
YZ^2	β_{43}					
Y^2Z	β_{44}					
XZ^2		β_{45}				
X^2Z		β_{46}				
X^3	β_{52}					
Y^3		β_{53}				
Z^3			β_{54}			

APPENDIX B. ELEMENT NOMENCLATURE

--- ASSUMED DISPLACEMENT FORMULATION ---

D - Assumed Displacement

P - Plane Stress

S - Solid

- Number of Nodes

DP4 - 4-Node Plane Stress Element

DP8 - 8-Node Plane Stress Element

DS8 - 8-Node Solid Element

DS20 - 20-Node Solid Element

--- HYBRID FORMULATION ---

R - π_R

H - π_{HW}

U - Uncouple (Blank for Coupled)

P - Plane Stress

S - Solid

- Number of Nodes

A,B,C,... Assumed Stress Version

4-Node Plane Stress Elements

RP4A — 5 β's

$$\sigma_x = \beta_1 + \beta_4 y$$
$$\sigma_y = \beta_2 + \beta_5 x$$
$$\sigma_{xy} = \beta_3$$

(8.12)

RP4B — 5 β's

$$\sigma_x = \beta_1$$
$$\sigma_y = \beta_2$$
$$\sigma_{xy} = \beta_3 + \beta_4 x + \beta_5 y$$

RP4C — 7 β's

$$\sigma_x = \beta_1 + \beta_2 y + \beta_6 x$$
$$\sigma_y = \beta_3 + \beta_4 x + \beta_7 y$$
$$\sigma_{xy} = \beta_5 - \beta_7 x - \beta_6 y$$

RP4D — 9 β's

$$\sigma_x = \beta_1 + \beta_2 x + \beta_3 y$$
$$\sigma_y = \beta_4 + \beta_5 x + \beta_6 y$$
$$\sigma_{xy} = \beta_7 + \beta_8 x + \beta_9 y$$

RP4E — 5 β's

$$\sigma_x = \beta_1 + \beta_4 x$$
$$\sigma_y = \beta_2 + \beta_5 y$$
$$\sigma_{xy} = \beta_3 - \beta_4 y - \beta_5 x$$

	σ_x	σ_y	σ_{xy}
CONST.	β_1	β_6	β_{11}
X	β_{12}	β_7	$-\beta_{13}$
Y	β_2	β_{13}	$-\beta_{12}$
XY	β_4	β_{10}	
X^2		β_9	$-\frac{1}{2}\beta_{10}$
Y^2	β_5		$-\frac{1}{2}\beta_4$
XY^2	β_3		
X^2Y		β_8	
X^3			$(-\frac{1}{3}\beta_8)$
Y^3			$(-\frac{1}{3}\beta_3)$

8-Node Plane Stress Elements

RP8A - Delete circled terms. (Equation 8.22)

RP8B - All terms included.

	σ_x	σ_y	σ_{xy}
CONST.	β_1	β_6	β_{11}
X	β_{12}	β_7	$-\beta_{13}$
Y	β_2	β_{13}	$-\beta_{12}$
XY	β_4	β_{10}	
X^2		β_9	$-\frac{1}{2}\beta_{10}$
Y^2	β_5		$-\frac{1}{2}\beta_4$
XY^2			
X^2Y			
X^3	β_3		
Y^3		β_8	

RP8C - Alternate version of RP8A.

	σ_x	σ_y	σ_{xy}
CONST.	β_1	β_3	β_5
X	β_6	β_4	$-\beta_7$
Y	β_2	β_7	$-\beta_6$
XY	$2\beta_9$	$2\beta_{11}$	$-2\beta_{10}$
X^2	β_{10}	$-\beta_8-2\beta_{10}$	$-\beta_{11}$
Y^2	β_8	β_{10}	$-\beta_9$
XY^2	$3\beta_{14}$	$3\beta_{12}$	$-3\beta_{13}$
X^2Y	$3\beta_{13}$	$3\beta_{15}$	$-3\beta_{12}$
X^3	β_{12}	$-2\beta_{12}-\beta_4$	$-\beta_{15}$
Y^3	$-2\beta_{13}-\beta_{15}$	β_{13}	$-\beta_{14}$

RP8D - Complete Cubic Equilibrium and Compatibility imposed (Ref. [16])

	σ_x	σ_y	σ_{xy}
CONST.	β_1	β_6	β_{11}
X	β_2	β_7	β_{12}
Y	β_3	β_8	β_{13}
XY	β_4	β_9	
X^2		β_{10}	
Y^2	β_5		
XY^2			
X^2Y			
X^3			
Y^3			

RP8E - Stress assumption to only suppress kinematic modes without regards to equilibrium.

RP8F - Complete quadratic, ignores equilibrium.

	σ_X	σ_Y	σ_{XY}
CONST.	β_1	β_7	β_{13}
X	β_2	β_8	β_{14}
Y	β_3	β_9	β_{15}
XY	β_4	β_{10}	β_{16}
X^2	β_5	β_{11}	β_{17}
Y^2	β_6	β_{12}	β_{18}
XY^2			
X^2Y			
X^3			
Y^3			

8-Node Solid Hybrid Elements

* Equilibrium condition is fully satisfied unless otherwise indicated.

RS8A

$$\begin{aligned}
\sigma_x &= \beta_1 + \beta_7 y + \beta_{10} z + \beta_{16} yz \\
\sigma_y &= \beta_2 + \beta_8 x + \beta_{11} z + \beta_{17} xz \\
\sigma_z &= \beta_3 + \beta_9 x + \beta_{12} y + \beta_{18} xy \\
\sigma_{xy} &= \beta_4 + \beta_{13} z \\
\sigma_{yz} &= \beta_5 + \beta_{14} x \\
\sigma_{xz} &= \beta_6 + \beta_{15} y
\end{aligned} \qquad (8.24)$$

RUS8A - 9 Constraints on β's from Equilibrium Condition.

$$\begin{aligned}
\sigma_x &= \beta_1 + \beta_2 x + \beta_3 y + \beta_4 z + \beta_5 xy + \beta_6 yz + \beta_7 xz \\
\sigma_y &= \beta_8 + \beta_9 x + \beta_{10} y + \beta_{11} z + \beta_{12} xy + \beta_{13} yz + \beta_{14} xz \\
\sigma_z &= \beta_{15} + \beta_{16} x + \beta_{17} y + \beta_{18} z + \beta_{19} xy + \beta_{20} yz + \beta_{21} xz \\
\sigma_{xy} &= \beta_{22} + \beta_{23} z \\
\sigma_{yz} &= \beta_{24} + \beta_{25} x \\
\sigma_{xz} &= \beta_{26} + \beta_{27} y
\end{aligned} \qquad (8.25)$$

* Note that RS8A and RUS8A are equivalent element with different programming algorythm introduced in the uncoupled stress formulation.

RUS8B - 9 Constraints.

$$\begin{aligned}
\sigma_x &= \beta_1 + \beta_2\xi + \beta_3\eta + \beta_4\zeta + \beta_5\xi\eta + \beta_6\eta\zeta + \beta_7\xi\zeta \\
\sigma_y &= \beta_8 + \beta_9\xi + \beta_{10}\eta + \beta_{11}\zeta + \beta_{12}\xi\eta + \beta_{13}\eta\zeta + \beta_{14}\xi\zeta \\
\sigma_z &= \beta_{15} + \beta_{16}\xi + \beta_{17}\eta + \beta_{18}\zeta + \beta_{19}\xi\eta + \beta_{20}\eta\zeta + \beta_{21}\xi\zeta \\
\sigma_{xy} &= \beta_{22} + \beta_{23}\zeta \\
\sigma_{yz} &= \beta_{24} + \beta_{25}\xi \\
\sigma_{xz} &= \beta_{26} + \beta_{27}\eta
\end{aligned} \qquad (8.26)$$

*RUS8B is equivalent to RUS8A for rectangular elements.

RUS8C - 3 Constraints.

$$\begin{aligned}
\sigma_x &= \beta_1 + \beta_2\xi + \beta_3\eta + \beta_4\zeta + \beta_5(\xi\eta + \eta\zeta + \xi\zeta) \\
\sigma_y &= \beta_6 + \beta_7\xi + \beta_8\eta + \beta_9\zeta + \beta_{10}(\xi\eta + \eta\zeta + \xi\zeta) \\
\sigma_z &= \beta_{11} + \beta_{12}\xi + \beta_{13}\eta + \beta_{14}\zeta + \beta_{15}(\xi\eta + \eta\zeta + \xi\zeta) \\
\sigma_{xy} &= \beta_{16} + \beta_{17}\zeta \\
\sigma_{yz} &= \beta_{18} + \beta_{19}\xi \\
\sigma_{xz} &= \beta_{20} + \beta_{21}\eta
\end{aligned} \qquad (8.28)$$

*RUS8C - Equilibrium relaxed for quadratic terms.

RUS8D - 9 Constraints.

$$\sigma_x = \beta_1 + \beta_2 x + \beta_3 y + \beta_4 z$$
$$\sigma_y = \beta_5 + \beta_6 x + \beta_7 y + \beta_8 z$$
$$\sigma_z = \beta_9 + \beta_{10} x + \beta_{11} y + \beta_{12} z$$

$$\sigma_{xy} = \beta_{13} + \beta_{14} x + \beta_{15} y + \beta_{16} z + \beta_{17} yz + \beta_{18} xz + \beta_{19} x^2 + \beta_{20} y^2$$
$$\sigma_{yz} = \beta_{21} + \beta_{22} x + \beta_{23} y + \beta_{24} z + \beta_{25} xz + \beta_{26} xy + \beta_{27} y^2 + \beta_{28} z^2$$
$$\sigma_{xz} = \beta_{29} + \beta_{30} x + \beta_{31} y + \beta_{32} z + \beta_{33} xy + \beta_{34} yz + \beta_{35} z^2 + \beta_{36} x^2$$

RUS8E - 9 Constraints.

$$\sigma_x = \beta_1 + \beta_2 x + \beta_3 y + \beta_4 z + \beta_5 xy + \beta_6 yz + \beta_7 xz$$
$$\sigma_y = \beta_8 + \beta_9 x + \beta_{10} y + \beta_{11} z + \beta_{12} xy + \beta_{13} yz + \beta_{14} xz$$
$$\sigma_z = \beta_{15} + \beta_{16} x + \beta_{17} y + \beta_{18} z + \beta_{19} xy + \beta_{20} yz + \beta_{21} xz$$

$$\sigma_{xy} = \beta_{22} + \beta_{23} x + \beta_{24} y + \beta_{25} z$$
$$\sigma_{yz} = \beta_{26} + \beta_{27} x + \beta_{28} y + \beta_{29} z$$
$$\sigma_{xz} = \beta_{30} + \beta_{31} x + \beta_{32} y + \beta_{33} z$$

20-Node Solid Hybrid Elements

	σ_x	σ_y	σ_z	σ_{xy}	σ_{yz}	σ_{zx}
CONST.	β_1	β_2	β_3	β_4	β_5	β_6
X	$-\beta_{14}-\beta_{21}$	β_9	β_{11}	β_{13}	β_{16}	β_{19}
Y	β_7	$-\beta_{13}-\beta_{18}$	β_{12}	β_{14}	β_{17}	β_{20}
Z	β_8	β_{10}	$-\beta_{17}-\beta_{19}$	β_{15}	β_{18}	β_{21}
XY	β_{22}	β_{27}	β_{32}		β_{39}	β_{41}
YZ	β_{23}	β_{28}	β_{33}	β_{37}		β_{42}
XZ	β_{24}	β_{29}	β_{34}	β_{38}	β_{40}	
X^2		β_{30}	β_{35}	$\left\langle -\frac{\beta_{37}}{2}-\frac{\beta_{40}}{2}\right\rangle$		$\left\langle -\frac{\beta_{23}}{2}-\frac{\beta_{39}}{2}\right\rangle$
Y^2	β_{25}		β_{36}	$\left\langle -\frac{\beta_{22}}{2}-\frac{\beta_{42}}{2}\right\rangle$	$\left\langle -\frac{\beta_{33}}{2}-\frac{\beta_{41}}{2}\right\rangle$	
Z^2	β_{26}	β_{31}			$\left\langle -\frac{\beta_{28}}{2}-\frac{\beta_{38}}{2}\right\rangle$	$\left\langle -\frac{\beta_{24}}{2}-\frac{\beta_{37}}{2}\right\rangle$
XYZ	β_{49}	β_{50}	β_{51}			
XY^2		$3\beta_{52}$	β_{47}			
X^2Y			β_{48}	$-3\beta_{52}$		$\left[-\frac{\beta_{51}}{2}\right]$
YZ^2	β_{43}		$3\beta_{53}$			
Y^2Z	β_{44}			$\left[-\frac{\beta_{49}}{2}\right]$	$-3\beta_{53}$	
XZ^2		β_{45}			$\left[-\frac{\beta_{50}}{2}\right]$	$-3\beta_{54}$
X^2Z	$3\beta_{54}$	β_{46}		DELETE:	⬭ + [ ]	RS20A
X^3	β_{52}				⬭	RS20B
Y^3		β_{53}			none	RS20C
Z^3			β_{54}		⬭ + [ ] + ⟨⟩	RS20D

	σ_X	σ_Y	σ_Z	σ_{XY}	σ_{YZ}	σ_{ZX}
CONST.	β_1	β_2	β_3	β_4	β_5	β_6
X	$-\beta_{14}-\beta_{21}$	β_9	β_{11}	β_{13}	β_{16}	β_{19}
Y	β_7	$-\beta_{13}-\beta_{18}$	β_{12}	β_{14}	β_{17}	β_{20}
Z	β_8	β_{10}	$-\beta_{17}-\beta_{19}$	β_{15}	β_{18}	β_{21}
XY	β_{22}	β_{27}	β_{32}		β_{39}	β_{41}
YZ	β_{23}	β_{28}	β_{33}	β_{37}		β_{42}
XZ	β_{24}	β_{29}	β_{34}	β_{38}	β_{40}	
X^2		β_{30}	β_{35}	$-\frac{\beta_{27}}{2}-\frac{\beta_{30}}{2}$		$-\frac{\beta_{34}}{2}-\frac{\beta_{39}}{2}$
Y^2	β_{25}		β_{36}	$-\frac{\beta_{22}}{2}-\frac{\beta_{42}}{2}$	$-\frac{\beta_{33}}{2}-\frac{\beta_{41}}{2}$	
Z^2	β_{26}	β_{31}			$-\frac{\beta_{28}}{2}-\frac{\beta_{38}}{2}$	$-\frac{\beta_{24}}{2}-\frac{\beta_{37}}{2}$
XYZ	β_{49}	β_{50}	β_{51}			
XY^2	β_{52}		β_{47}			
X^2Y		β_{53}	β_{48}			
YZ^2	β_{43}	β_{56}				
Y^2Z	β_{44}		β_{54}			
XZ^2	β_{55}	β_{45}				
X^2Z		β_{46}	β_{57}			
X^3				DELETE:		
Y^3					none	RS20E
Z^3						RS20F

RS20G (Ref. [19])

$$\sigma_{xx} = \beta_1 + \beta_2 x + \beta_3 y + \beta_4 z + 1/2(y^2 - x^2)\beta_{22} + 1/2\lambda[-y^2 - \lambda x^2 + (1+\lambda)z^2]\beta_{23}$$
$$+ 1/2\lambda(1-\lambda)[-(1+\lambda^2)y^2 + (1-\lambda^2)z^2]\beta_{24} + 1/(1-\lambda)[y^2 - (1-\lambda)z^2]\beta_{25}$$
$$+ 1/\lambda[y^2 - z^2]\beta_{26} + 1/\lambda(1-\lambda^2)[(1+\lambda^3)y^2 - (1-\lambda^2)z^2]\beta_{27} + \beta_{28}xy + \beta_{29}xz + \beta_{30}yz$$
$$+ \beta_{53}[-x^3/3 + (1+\lambda)y^2x] + \beta_{61}[-x^3/3 + (\lambda+1)y^2x] + \beta_{43}[y^3 - 3z^2y]$$
$$+ \beta_{44}\left[z^3 + 3y^2z\frac{(\lambda^2 - \lambda + 1)}{\lambda - 1}\right] + \beta_{56}[-2xyz] + \beta_{63}[-2xyz] + \beta_{59}/2[-x^2y + z^2y]$$
$$+ \beta_{55}[-x^2y + z^2y] + \beta_{52}/2[-x^2z + y^2z] + \beta_{62}\left[-x^2z - y^2z\frac{(\lambda^2+1)}{\lambda - 1}\right] + \beta_{46}[-3\lambda y^2x]$$
$$+ \beta_{49}[-3\lambda y^2x] + \beta_{45}[-y^2x + z^2x] + \beta_{51}\left[y^2z\frac{\lambda}{\lambda - 1}\right] + \beta_{47}[3\lambda y^2z]$$
$$+ \beta_{69}[-\lambda y^2z] + \beta_{48}\left[-\left(\frac{\lambda}{\lambda - 1}\right)z^2y\right] + \beta_{50}\left[-\left(\frac{3\lambda}{\lambda - 1}\right)z^2y\right] + \beta_{67}\left[\left(\frac{2\lambda}{\lambda - 1}\right)z^2y\right]$$

$$\sigma_{yy} = \beta_5 + \beta_6 x + \beta_7 y + \beta_8 z + 1/2(x^2 - y^2)\beta_{22} + \frac{x^2}{2}\beta_{23} + \frac{1}{2(1-\lambda)}[2x^2 - (1-\lambda)y^2]\beta_{24}$$
$$+ \frac{1}{(1-\lambda)}[-x^2 + (1-\lambda)z^2]\beta_{25} - \beta_{26}x^2 - \frac{1}{(1-\lambda)}x^2\beta_{27} + \beta_{31}xy + \beta_{32}xz$$
$$+ \beta_{33}yz + \beta_{46}[x^3 - 3z^2x] + \beta_{55}\left[-\frac{y^3}{3} + (\lambda+1)x^2y\right] + \beta_{67}\left[-\frac{y^3}{3} + (\lambda+1)x^2y\right]$$
$$+ \beta_{47}[z^3 - 3x^2z] + \beta_{54}[-2xyz] + \beta_{68}[-2xyz] + \beta_{43}[-3\lambda x^2y] + \beta_{50}[-3\lambda x^2y]$$
$$+ \beta_{48}[-x^2y + z^2y] + \beta_{51}\left[-\left(\frac{\lambda}{\lambda - 1}\right)x^2z\right] + \beta_{44}\left[-\left(\frac{3\lambda}{\lambda - 1}\right)x^2z\right] + \beta_{69}[x^2z - y^2z]$$
$$+ \beta_{52}/2[x^2z - y^2z] + \beta_{62}\left[\left(\frac{2\lambda}{\lambda - 1}\right)x^2z\right] + \beta_{65}/2[-y^2x + z^2x] + \beta_{53}[-y^2x + z^2x]$$
$$+ \beta_{45}\left[-\left(\frac{\lambda}{\lambda - 1}\right)z^2x\right] + \beta_{49}\left[-\left(\frac{3\lambda}{\lambda - 1}\right)z^2x\right] + \beta_{61}\left[\left(\frac{2\lambda}{\lambda - 1}\right)z^2x\right]$$

$$\sigma_{zz} = \beta_9 + \beta_{10}x + \beta_{11}y + \beta_{12}z + \beta_{26}x^2 + \beta_{27}y^2 - 1/2(\beta_{23} + \beta_{24})z^2 + \beta_{34}xy$$
$$+ \beta_{35}xz + \beta_{36}yz + \beta_{49}\left[x^3 + y^2x\frac{3(\lambda^2 - \lambda + 1)}{\lambda - 1}\right] + \beta_{50}\left[y^3 + x^2y\frac{3(\lambda^2 - \lambda + 1)}{\lambda - 1}\right]$$
$$+ \beta_{62}\left[-\frac{z^3}{3} + (\lambda+1)y^2z\right] + \beta_{69}\left[-\frac{z^3}{3} + (\lambda+1)y^2z\right] + \beta_{60}[-2xyz]$$
$$+ \beta_{66}[-2xyz] + \beta_{48}\left[\left(\frac{\lambda}{\lambda - 1}\right)x^2y\right] + \beta_{43}[3\lambda x^2y] + \beta_{55}[-\lambda x^2y]$$

$$+\beta_{67}\left[-x^2y\left(\frac{\lambda^2+1}{\lambda-1}\right)-z^2y\right]+\frac{\beta_{59}}{2}[x^2y-z^2y]+\beta_{51}[x^2z-y^2z]+\beta_{45}\left[\left(\frac{\lambda}{\lambda-1}\right)y^2x\right]$$

$$+\beta_{46}[3\lambda y^2x]+\beta_{53}[-\lambda y^2x]+\beta_{61}\left[-\frac{\lambda^2+1}{\lambda-1}y^2x-z^2x\right]+\frac{\beta_{65}}{2}[y^2x-z^2x]$$

$$+\beta_{44}[-3\lambda y^2z]+\beta_{47}[-3\lambda y^2z]$$

$$\sigma_{xy}=\beta_{13}+\beta_{14}x-(\beta_2+\beta_{18})y+\beta_{15}z+(x^2-z^2)\beta_{37}+(y^2-z^2)\beta_{38}$$

$$-\frac{\lambda}{2}(\beta_{28}+\beta_{31}+\beta_{34})z^2+\beta_{22}xy-(\beta_{33}+2\beta_{39})xz-(\beta_{29}+2\beta_{40})yz$$

$$+\beta_{48}\left[-\frac{x^3}{3(\lambda-1)}-z^2x\right]+\beta_{50}\left[-\frac{\lambda}{(\lambda-1)}x^3\right]+\beta_{55}\left[-\frac{x^3}{3}+y^2x\right]+\beta_{64}[x^3-3z^2x]$$

$$+\beta_{67}\left[\frac{2}{3}\frac{\lambda}{(\lambda-1)}x^3\right]+\beta_{45}\left[-\frac{1}{3(\lambda-1)}y^3-z^2y\right]+\beta_{49}\left[-\left(\frac{\lambda}{\lambda-1}\right)y^3\right]$$

$$+\beta_{53}\left[-\frac{y^3}{3}+x^2y\right]+\beta_{58}[y^3-3z^2y]+\beta_{61}\left[\frac{2\lambda}{3(\lambda-1)}y^3\right]+\beta_{54}\left[\frac{\lambda-1}{3}z^3+x^2z\right]$$

$$+\beta_{56}\left[\frac{\lambda-1}{3}z^3+y^2z\right]+\beta_{60}\left[\frac{\lambda z^3}{3}\right]+\beta_{63}\left[\frac{\lambda z^3}{3}\right]+\beta_{66}\left[\frac{\lambda z^3}{3}\right]+\beta_{68}\left[\frac{\lambda z^3}{3}\right]+\beta_{52}(xyz)$$

$$\sigma_{yz}=\beta_{19}+\beta_{20}x+\beta_{21}y-(\beta_7+\beta_{14})z+(y^2-x^2)\beta_{42}+(z^2-x^2)\beta_{39}$$

$$-\frac{\lambda}{2}(\beta_{30}+\beta_{33}+\beta_{36})x^2-(\beta_{35}+2\beta_{41})xy-(\beta_{31}+2\beta_{37})xz+\beta_{24}yz$$

$$+\beta_{66}\left[\frac{(\lambda-1)x^3}{3}+y^2x\right]+\beta_{68}\left[\frac{\lambda-1}{3}x^3+z^2x\right]+\beta_{54}\left[\frac{\lambda x^3}{3}\right]+\beta_{56}\left[\frac{\lambda}{3}x^3\right]$$

$$+\beta_{60}\left[\frac{\lambda}{3}x^3\right]+\beta_{63}\left[\frac{\lambda}{3}x^3\right]+\beta_{51}\left[-\frac{y^3}{3(\lambda-1)}-x^2y\right]+\beta_{44}\left[-\frac{\lambda}{\lambda-1}y^3\right]+\beta_{69}\left[-\frac{y^3}{3}+z^2y\right]$$

$$+\beta_{57}[y^3-3x^2y]+\beta_{62}\left[\frac{2\lambda y^3}{3(\lambda-1)}\right]+\beta_{64}[z^3-3x^2z]+\beta_{65}[xyz]+\beta_{43}[3\lambda x^2z]$$

$$+\beta_{50}\left[\frac{3\lambda^2}{\lambda-1}x^2z\right]+\beta_{48}\left[\frac{\lambda x^2z}{\lambda-1}\right]+\beta_{55}[-\lambda x^2z]+\beta_{67}\left[-\frac{(\lambda^2+2\lambda-1)}{\lambda-1}x^2z+y^2z\right]$$

$$\sigma_{xz}=\beta_{16}-(\beta_{12}+\beta_{21})x+\beta_{17}y+\beta_{18}z+(x^2-y^2)\beta_{41}+(z^2-y^2)\beta_{40}$$

$$-\frac{\lambda}{2}(\beta_{29}+\beta_{32}+\beta_{35})y^2-(\beta_{36}+2\beta_{42})xy+\beta_{23}xz-(\beta_{28}+2\beta_{38})yz$$

$$+\beta_{57}[x^3-3y^2x]+\beta_{60}\left[\frac{(\lambda-1)y^3}{3}+x^2y\right]+\beta_{63}\left[\frac{(\lambda-1)y^3}{3}+z^2y\right]$$

$$+\beta_{54}\left[\frac{\lambda y^3}{3}\right]+\beta_{56}\left[\frac{\lambda y^3}{3}\right]+\beta_{66}\left[\frac{\lambda y^3}{3}\right]+\beta_{68}\left[\frac{\lambda}{3}y^3\right]+\beta_{58}[z^3-3y^2z]$$

	σ_X	σ_Y	σ_Z	σ_{XY}	σ_{YZ}	σ_{ZX}
CONST.	β_1	β_{14}	β_{27}	β_{40}	β_{48}	β_{56}
X	β_2	β_{15}	β_{28}	β_{41}	β_{49}	β_{57}
Y	β_3	β_{16}	β_{29}	β_{42}	β_{50}	β_{58}
Z	β_4	β_{17}	β_{30}	β_{43}	β_{51}	β_{59}
XY	β_5	β_{18}	β_{31}		β_{52}	β_{60}
YZ	β_6	β_{19}	β_{32}	β_{44}		β_{61}
XZ	β_7	β_{20}	β_{33}	β_{45}	β_{53}	
X^2		β_{21}	β_{34}	β_{46}		β_{62}
Y^2	β_8		β_{35}	β_{47}	β_{54}	
Z^2	β_9	β_{22}			β_{55}	β_{63}
XYZ	β_{10}	β_{23}	β_{36}			
XY^2			β_{37}			
X^2Y			β_{38}			
YZ^2	β_{11}					
Y^2Z	β_{12}					
XZ^2		β_{24}				
X^2Z		β_{25}				
X^3	β_{13}					
Y^3		β_{26}			HS20A	
Z^3			β_{39}			

REFERENCES

1. B. Irons and S. Ahmad, Techniques of Finite Elements, Wiley, New York, 1980.

2. K-J Bathe, Finite Element Procedures In Engineering Analysis, Prentice-Hall, Inc., Englewood Cliffs, New Jersey, 1982.

3. L.E. Malvern, Introduction to the Mechanics of a Continuous Medium, Prentice-Hall, Inc., Englewood Cliffs, N.J., 1969.

4. T.H.H. Pian and P. Tong, "Basis of Finite Element Methods for Solid Continua", Int. J. Num. Meth. Engng., 1, 3-28, 1969.

5. T.H.H. Pian and D.P. Chen, "Alternative Ways for Formulation of Hybrid Stress Elements", To be published in Int. J. Num. Meth. Engng..

6. G. Strang and G.J. Fix, An Analysis of the Finite Element Method, Prentice-Hall, Englewood Cliffs, N.J., 1973.

7. P. Tong and T.H.H. Pian, "A Variational Principle and the Convergence of a Finite-Element Method Based on Assumed Stress Distribution", Int. J. Num. Meth. Engng., 5, 463-472, 1969.

8. I. Babuska and B. Szabo, "On the Rates of Convergence of the Finite Element Method", Int. J. Num. Meth. Engng., 18, 323-341, 1982.

9. Fenves, Perrone, Robinson, and Schnobrich, Edts., Numerical and Computer Methods in Structural Mechanics, Academic Press, New York, 1973.

10. T.H.H. Pian and D.P. Chen, "Zero Energy Deformation Modes in Assumed Stress Finite Elements", To be published.

11. B.M. Irons, An Assumed-Stress Version of the Wilson 8-Node Isoparametric Brick, Computer Report CNME/CR/56, Univ. College of Swansea, 1972.

12. T.H.H. Pian, "Derivation of Element Stiffness Matrices by Assumed Stress Distribution", AIAA J., 2, 1333-1336, 1964.

13. K.J. Bathe and S. Bolourchi, "A Geometric and Material Nonlinear Plate and Shell Element", J. Computers and Structures, 11, 23-48, 1980.

14. T.H.H. Pian, D. Chen, and D. Kang, "A New Formulation of Hybrid/Mixed Finite Element", To be published in Computers and Structures.

15. M. Loikkanen, Hybrid Finite Elements with Shape Function Subroutine, PhD Thesis, Univ. of Calgary, 1981.

16. R.L. Spilker, S.M. Maskeri, and E. Kania, "Plane Isoparametric Hybrid Stress Elements: Invariance and Optimal Sampling", Int. J. Num. Meth. Engng., 17, 1469-1496, 1981.

17. J. Barlow, "Optimal Stress Locations in Finite Element Models", Int. J. Num. Meth. Engng., 10, 243-251, 1976.

18. S.P. Timoshenko and J.N. Goodier, Theory of Elasticity, 3rd Edn., McGraw-Hill, New York, 1970.

19. R.L. Spilker and S.P. Singh, "Three-Dimensional Hybrid-Stress Isoparametric Quadratic Displacement Elements", Int. J. Num. Meth. Engng., 18, 445-465, 1982.

20. C.T. Yang, R. Rubinstein, and S.N. Atluri, "On Some Fundamental Studies into the Stability of Hybrid/Mixed Finite Element Methods for Navier-Stokes Equations in Solid/Fluid Mechanics", Report No. GIT-CACM-SNA-82-20, 1982.

21. A.K. Noor and J.M. Peters, "Mixed Models and Reduced/Selective Integration Displacement Models for Vibration Analysis of Shells", To be published in Hybrid and Mixed Finite Element Methods, Edts: Atluri, et. al., Wiley, Chichester, England.

22. O.C. Zienkiewicz, R.L. Taylor, and J.M. Too, "Reduced Integration Technique in General Analysis of Plates and Shells", Int. J. Num. Meth. Engng., 3, 275-290, 1971.

23. E.D.L. Pugh, E. Hinton, and O.C. Zienkiewicz, "A Study of Quadrilateral Plate Bending Elements with 'Reduced' Integration", Int. J. Num. Meth. Engng., 12, 1059-1079, 1978.

24. T.J.R. Hughes, M. Cohen, and M. Haroun, "Reduced and Selective Integration Techniques in the Finite Element Analysis of Plates", Nuclear Engng and Design, 46, 203-222, 1978.

25. N. Bicanic and E. Hinton, "Spurious Modes in Two-Dimensional Isoparametric Elements", Int. J. Num. Meth. Engng., 14, 1545-1557, 1979.

26. T.J.R. Hughes, "Generalization of Selective Integration Procedures to Anisotropic and Nonlinear Media", Int. J. Num. Meth. Engng., 15, 1413-1418, 1980.

27. D.S. Malkus and T.J.R. Hughes, "Mixed Finite Element Methods - Reduced and Selective Integration Techniques: A Unification of Concepts", Comp. Meth. App. Mech. and Engng., 15, 63-81, 1978.

28. R.L. Spilker and N.I. Munir, "The Hybrid-Stress Model for Thin Plates", Int. J. Num. Meth. Engng., 15, 1239-1260, 1980.

29. R.L. Spilker and N.I. Munir, "A Serendipity Cubic-Displacement Hybrid-Stress Element for Thin and Moderately Thick Plates", Int. J. Num. Meth. Engng., 15, 1269-1278, 1980.

30. B.M. Irons, "Quadrature Rules for Brick Based Finite Elements", Int. J. Num. Meth. Engng., 3, 293-294, 1971.

REPORT DOCUMENTATION PAGE

Form Approved
OMB No. 0704-0188

1. AGENCY USE ONLY (*Leave blank*)	2. REPORT DATE	3. REPORT TYPE AND DATES COVERED
	November 1991	Final Contractor Report

4. TITLE AND SUBTITLE

C° Continuity Elements by Hybrid Stress Method

5. FUNDING NUMBERS

WU-505-36-5B
G-NAG3-33

6. AUTHOR(S)

David Sung-Soo Kang

7. PERFORMING ORGANIZATION NAME(S) AND ADDRESS(ES)

Massachusetts Institute of Technology
Department of Aeronautics and Astronautics
Cambridge, Massachusetts 02139

8. PERFORMING ORGANIZATION REPORT NUMBER

None

9. SPONSORING/MONITORING AGENCY NAMES(S) AND ADDRESS(ES)

National Aeronautics and Space Administration
Lewis Research Center
Cleveland, Ohio 44135-3191

10. SPONSORING/MONITORING AGENCY REPORT NUMBER

NASA CR-189040

11. SUPPLEMENTARY NOTES

Project Manager, C.C. Chamis, Structures Division, NASA Lewis Research Center, (216) 433-3252. Report was submitted as a thesis in partial fulfillment of the requirements for the degree of Master of Science to the Massachusett: Institute of Technology in September 1982.

12a. DISTRIBUTION/AVAILABILITY STATEMENT

Unclassified - Unlimited
Subject Category 39

12b. DISTRIBUTION CODE

13. ABSTRACT (*Maximum 200 words*)

An intensive study of the assumed variable distribution necessary for the Assumed Displacement Formulation, the Hellinger-Reissner Formulation, and the Hu-Washizu Formulation is made in a unified manner. With emphasis on physical explanation, a systematic method for the Hybrid Stress element construction is outlined. The numerical examples employ four and eight node plane stress elements and eight and twenty node solid elements. Computation cost study indicates that the hybrid stress element derived using recently developed Uncoupled Stress Formulation is comparable in CPU time to the Assumed Displacement element. Overall, main emphasis is placed on providing a broader understanding of the Hybrid Stress Formulation.

14. SUBJECT TERMS

Finite elements; Displacements energy principles; Computational algorithm; Sample cases

15. NUMBER OF PAGES

138

16. PRICE CODE

A07

17. SECURITY CLASSIFICATION OF REPORT	18. SECURITY CLASSIFICATION OF THIS PAGE	19. SECURITY CLASSIFICATION OF ABSTRACT	20. LIMITATION OF ABSTRAC
Unclassified	Unclassified	Unclassified	